



NTNU – Trondheim
Norwegian University of
Science and Technology

Virtual Synchronous Machine-based Power Control in Active Rectifiers for Micro Grids

Aravinda Perera

Master of Science in Electric Power Engineering

Submission date: July 2012

Supervisor: Tore Marvin Undeland, ELKRAFT

Co-supervisor: Roy Nilsen, Wärtsilä Norway AS
Salvatore D'arco, SINTEF

Norwegian University of Science and Technology
Department of Electric Power Engineering

Virtual Synchronous Machine-based
Power Control in Active Rectifiers for
Micro Grids

PROBLEM DESCRIPTION

The concept of micro grid interfaced with an active rectifier is an emerging technology for smart integration of dc distributed generation units to the ac grid where active rectifier plays the role of inverting dc to ac with appropriate control strategies.

Having the operation of a synchronous generator in a micro grid introduces several advantages in terms of stability and reliability in the power system due the inherent damping and inertia properties of the machine. These advantages motivate the question if an active rectifier of a micro grid can imitate the behaviour of those inherent properties, can such stability and reliability be emulated in a micro grid.

With the above intention, under the scope of the master thesis, firstly, a research should be carried on the state-of-the-art for uninterruptible power supplies (UPS) to mainly identify the active rectifier control strategies. Secondly, the concept of virtual synchronous machine (VSM) has to be further extended with the pre-studies from the fall project to observe the effects of virtual inertia and damping properties.

Incorporating the above studies and simulations based on UPS and VSM, a model of an active rectifier should be developed making the choices from available control strategies. The model should be operable alone and in parallel with several active rectifiers in a micro grid both in grid-tied and island modes. Also the active rectifier model needs to emulate the inertia, damping and power sharing properties.

Assignment given: Trondheim 01.02.2012

Supervisor: Prof. Tore Marvin Undeland, Department of Electric Power Engineering, NTNU

ABSTRACT

This dissertation presents an analytical study on *virtual synchronous machine-based power control in active rectifiers for micro grids* supported by prototype modelling, simulation results and discussions.

Popularity and demand of the distributed energy resources and renewable energy sources are increasing due to their economic and environmental friendliness. Concept of micro grid with an active rectifier (AR) interface has been found to be promising for smart integration of such distributed generation units.

Having the presence of a synchronous generator (SG) in a micro grid introduces several advantages in terms of stability and reliability in the power system. This is mainly owed to the inertia, damping and load sharing properties of SG. This in return, gives rise to the question if an AR of a micro grid can imitate the behaviour of a synchronous generator, can the stability and reliability introduced by SG be replicated in a micro grid.

A research on the state-of-the-art for uninterruptible power supplies (UPS) has been carried out to identify the implementation and the control strategies of redundancy and parallel operation as UPS has been an established technology over the last decades. The theoretical study on virtual synchronous machine (VSM) concept in the fall, 2011, has been extended in developing a model with classical inner current control and outer voltage control loops based on the synchronous reference frame.

The complete active rectifier model has been able to emulate the inertia, damping and load sharing properties of a SG and redundancy and expandability of parallel UPS systems. It must be emphasized that due to the flexibility of the virtual machine parameters and the absence of magnetic saturation and eddy current losses, a much improved performance have been achieved with a VSM compared to a synchronous generator.

Simulations have been carried out for single and parallel operation of active rectifiers in island and grid-tied modes with satisfactory stability, damping and power sharing features.

Key words – Active rectifier, virtual synchronous machine, micro grid, uninterruptible power supply, load sharing, redundancy, island mode, grid-tied mode, synchronous reference frame

PREFACE

In partial fulfillment of the Master of Science Degree in electrical power engineering in Norwegian University of Science and Technology (NTNU), this master thesis has been carried out in the spring 2012.

It has been a remarkable period of intensive studies which exposed me to a several profoundly interesting and novel research fields. If there had been a term known as 'learning density', it would be the highest in this span of study in my entire academic life from the kindergarten.

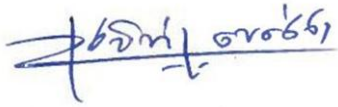
The thesis title was proposed and partly sponsored by the Department of Ship Power Future Systems of Wärtsilä Norway AS. I express my sincere gratitude to Dr. Roy Nilsen of Wärtsilä Norway AS for providing guidance and supervision from the very beginning. I am also immensely grateful to the co-supervisor of the thesis, Dr. Salvatore D'Arco for his kind and generous support who deserves much credit of the work. Thankfulness is extended to Dr. Jon Are Suul, Dr. Trond Troftevaag and Sverre Gjerde whom I have bumped on for quick fixes and different viewpoints.

The script of my destiny has been quite fascinating when Professor Tore Undeland became my supervisor in Norway when his co-authored book on Power Electronics had been revered during my Bachelor Studies back in Sri Lanka. I am indebted for all his advice and words of encouragement during the difficult times of studies.

At this point of marking an end, probably temporary, to my academic life in Norway, I state my gratefulness to all my classmates who made my stay memorable. I shall also remember my girlfriend with great love, Raneshi Perera, who selflessly let me to pursue my dreams a many thousand miles apart. Last but never the least, I am thankful to almighty God for enormous blessings throughout to conquer many feats in the last couple of years.

In conclusion, it has been a journey of delight and enlightenment with the thesis where I discovered a thousand and one methods how *not* to do many things as Thomas Edison did in

the course of inventing the light bulb. With the intention of looking forward to the next life challenge, I wish you happy reading of this dissertation!

A handwritten signature in blue ink, appearing to be 'Aravinda Perera', written in a cursive style.

Aravinda Perera

Trondheim, 02.07.2012

CONTENTS

| | |
|---|-------------|
| PROBLEM DESCRIPTION..... | iii |
| ABSTRACT | v |
| PREFACE..... | vii |
| CONTENTS..... | ix |
| LIST OF FIGURES | xiii |
| LIST OF TABLES | xvii |
| NOMENCLATURE AND ABBREVIATIONS | xix |
| 1 Introduction | 1 |
| 1.1 Background & Motivation | 1 |
| 1.2 System Overview, Objective & Applications | 3 |
| 1.3 Scope of the Thesis & Sequence of Work | 7 |
| 1.4 Outline of the Thesis | 8 |
| 1.5 Summary of Chapter | 9 |
| 2 State-of-the-Art for Active Rectifiers..... | 11 |
| 2.1 State-of-the-Art for Active Rectifiers | 11 |
| 2.2 Communication & Communication-less topologies | 12 |
| 2.3 Summary of Chapter | 12 |
| 3 Uninterruptible Power Supply | 15 |
| 3.1 Introduction to UPS..... | 15 |
| 3.2 UPS Classification and Configurations..... | 16 |
| 3.2.1 Classification | 16 |
| 3.2.2 Redundancy | 17 |
| 3.3 Paralleling UPS..... | 18 |

| | | |
|----------|--|-----------|
| 3.3.1 | Active Load Sharing..... | 18 |
| 3.3.2 | Droop Control Methods..... | 19 |
| 3.4 | Battery Management | 20 |
| 3.5 | Harmonic Filtering..... | 20 |
| 3.5.1 | Theoretical Review..... | 20 |
| 3.5.2 | Effects of Harmonics | 21 |
| 3.6 | Summary of Chapter | 21 |
| 4 | Virtual Synchronous Machine Concept & Control Strategies | 23 |
| 4.1 | Synchronous Generator Operation | 23 |
| 4.1.1 | Inertia in the Synchronous Generator due to the Rotating Masses..... | 25 |
| 4.1.2 | Damping effect due to the damper windings in the rotor | 25 |
| 4.1.3 | Droop Characteristics of a Synchronous Generator in Load Sharing | 27 |
| 4.2 | Virtual Synchronous Machine | 28 |
| 4.2.1 | Virtual Inertia | 29 |
| 4.2.2 | Virtual Damping | 30 |
| 4.2.3 | Virtual Impedance..... | 30 |
| 4.3 | Summary of Chapter | 33 |
| 5 | Active Rectifier Control Strategies | 35 |
| 5.1 | Single Control Loop vs. Multiple Control Loop | 36 |
| 5.2 | Stationary Reference Frame Control vs. Synchronous Reference Frame Control.... | 38 |
| 5.3 | Control Loops | 42 |
| 5.3.1 | Inner Current Control Loop..... | 42 |
| 5.3.2 | Outer Voltage Control Loop..... | 42 |
| 5.4 | Controllers..... | 43 |
| 5.4.1 | Linear PI Controller | 43 |
| 5.4.2 | PR Controller | 43 |
| 5.4.3 | Hysteresis Controller..... | 44 |
| 5.5 | Decoupling Control of d and q Components..... | 44 |
| 5.5.1 | Decoupling Control of PI Current Controller | 45 |
| 5.5.2 | Decoupling Control of PI Voltage Controller | 47 |

| | | |
|----------|---|-----------|
| 5.6 | P-Q vs. VSI Control..... | 49 |
| 5.7 | Droop Control..... | 50 |
| 5.8 | Phase-Locked Loop..... | 50 |
| 5.9 | Summary of Chapter | 51 |
| 6 | Modeling of Active Rectifier | 53 |
| 6.1 | Proposed Active Rectifier Model | 53 |
| 6.2 | Phase-Locked Loop (PLL)..... | 54 |
| 6.3 | Inner Current Control Loop | 56 |
| 6.4 | Outer Voltage Control Loop | 58 |
| 6.5 | Virtual Synchronous Machine Model..... | 60 |
| 6.6 | Active Rectifier Simulation Model..... | 62 |
| 6.7 | Summary of Chapter | 65 |
| 7 | Simulation Results & Discussion | 67 |
| 7.1 | Single Active Rectifier Simulation | 68 |
| 7.1.1 | Grid-tied Mode | 68 |
| 7.1.2 | Island Mode | 68 |
| 7.1.3 | Simulation for different cases..... | 70 |
| 7.2 | Parallel Active Rectifier Simulation | 75 |
| 7.2.1 | Grid-tied Mode | 77 |
| 7.2.2 | Island Mode | 78 |
| 7.2.3 | Simulation for different cases..... | 79 |
| 7.2.4 | Redundancy | 82 |
| 7.3 | Summary of Chapter | 83 |
| 8 | Conclusion | 85 |
| 8.1 | Conclusions..... | 85 |
| 8.2 | Further Work..... | 86 |
| 8.3 | Recommendations | 86 |
| 9 | References | 87 |
| | Appendix A: Definition of per-unit system | 93 |
| | Appendix B: Reference frame transformations..... | 94 |

Appendix C: Tuning of control loops 95

LIST OF FIGURES

| | |
|--|----|
| Figure 1-1: Grid structural transformation from vertical to mesh structure due to the distributed generation | 2 |
| Figure 1-2: System overview with (a) SG-SG (b) SG-AR (c) AR-AR..... | 5 |
| Figure 1-3: Total system overview with functionalities..... | 6 |
| Figure 3-1: Block diagram of a rotary UPS system | 16 |
| Figure 3-2: Block diagram for UPS control with virtual output impedance loop | 19 |
| Figure 3-3: Power cube with harmonic power | 21 |
| Figure 4-1: Schematic view of a 2-pole, single phase synchronous generator, Source: [34].. | 23 |
| Figure 4-2: Generation unit block diagram, Source: [9] | 24 |
| Figure 4-3: Rotor and power oscillations with damping included, Source: [9] | 27 |
| Figure 4-4: Speed-droop characteristics of a synchronous generator | 28 |
| Figure 4-5: Equivalent steady state circuit diagram of a salient pole synchronous generator | 30 |
| Figure 4-6: Basic power flow diagram between a generator and grid across line impedance | 31 |
| Figure 5-1: Grid Connected Three-Phase, Two-Level Active Rectifier with LC filter | 35 |
| Figure 5-2: Generic control loop configuration of active rectifier | 36 |
| Figure 5-3: Block diagram of single feedback loop..... | 36 |
| Figure 5-4: Detailed multiple control loop configuration of an active rectifier | 37 |
| Figure 5-5: Orientation of the natural abc-reference frame, stationary $\alpha\beta$ -reference frame and synchronously rotating dq-reference frame | 39 |
| Figure 5-6: Generic control architecture for SRF based control strategy | 41 |
| Figure 5-7: LCL filter of the grid side of the active rectifier | 45 |
| Figure 5-8: Feed-forward compensation in SRF for the PI current controller | 47 |
| Figure 5-9: Feed-forward compensation in SRF for the PI voltage controller..... | 48 |
| Figure 5-10: General structure of SRF PLL | 50 |
| Figure 6-1: Proposed total system architecture with virtual synchronous machine model ... | 53 |
| Figure 6-2: PLL (a) model mask (b) internal structure (c) simulation against a frequency step change in the grid | 55 |
| Figure 6-3: Frequency plot of PLL against a step change in grid frequency | 56 |
| Figure 6-4: Inner Current Controller (a) mask (b) internal structure | 57 |

| | |
|--|----|
| Figure 6-5: Inner current controller output d-q current plot against step changes in I_d and I_q reference currents at $t = 2$ and $t = 4$ respectively..... | 58 |
| Figure 6-6: Outer voltage controller (a) mask (b) internal structure | 59 |
| Figure 6-7: Outer voltage controller output d-q current plot against step changes in V_d and V_q reference currents at $t = 2$ and $t = 4$ respectively | 60 |
| Figure 6-8: Virtual synchronous machine model (a) mask (b) internal structure with mechanical dynamics..... | 61 |
| Figure 6-9: Integrated architecture of PLL, inner current controller, outer voltage controller and machine model | 63 |
| Figure 6-10: Active rectifier connected along with the LCL filter and controllable breaker to a local load and stiff grid..... | 64 |
| Figure 7-1: Active and reactive power plots of AR, grid and load in grid-tied mode. AR is connected to the grid at $t = 0.2$ s..... | 69 |
| Figure 7-2: Active and reactive power plots of AR, grid and load in grid-tied and island modes. AR is connected to the grid at $t = 0.2$ s, stiff grid is tripped at $t = 0.6$ s..... | 69 |
| Figure 7-3: Comparison of active and reactive powers when virtual inertia, $J = 0.5$ [SI] and $J = 50$ [SI] respectively..... | 70 |
| Figure 7-4: Active power steady state time variations against different virtual inertia values | 71 |
| Figure 7-5: Comparison of active and reactive powers when virtual damping, $D = 0.8e5$ [SI] and $D = 2e5$ [SI] respectively..... | 72 |
| Figure 7-6: Active power damping time variations against different virtual damping coefficient values..... | 73 |
| Figure 7-7: Active power plots against a step load change of 0.5 MW in grid-tied mode..... | 74 |
| Figure 7-8: Active power plots against a step load change of 0.5 MW in island mode | 74 |
| Figure 7-9: General simulation schematic with two active rectifiers connected in parallel with the stiff grid across their filters and impedances | 76 |
| Figure 7-10: Active and reactive power plots of AR 1, AR 2, grid and load in grid-tied mode | 77 |
| Figure 7-11: Frequency plots of AR1, AR2 and stiff grid in grid-tied mode..... | 77 |
| Figure 7-12: Active and reactive power plots of AR 1, AR 2, grid and load in island mode | 78 |
| Figure 7-13: Frequency plots of AR1, AR2 and grid in island mode | 78 |
| Figure 7-14: Active power plots of AR 1, AR 2, grid and load against a step load change of 3 MW in grid-tied mode..... | 80 |
| Figure 7-15: Frequency plots upon a step load change in grid-tied mode..... | 80 |
| Figure 7-16: Active power plots of AR 1, AR 2, grid and load against a step load change of 3 MW in island mode. Reference Powers: AR 1=AR 2=3 MW | 80 |
| Figure 7-17: Frequency plots of AR 1, AR 2 and grid mode against a step load in island | 81 |
| Figure 7-18: Paralleling of 3 ARs (a) in grid-tied mode (b) in island mode..... | 82 |

Figure 7-19: Active and reactive power plots of AR 1, AR 2, grid and load in island mode. AR 1 & AR 2 connected to the grid at $t = 0.2$. AR 1 tripped at $t = 0.6$82

LIST OF TABLES

| | |
|--|----|
| Table 1: UPS system configurations [21] | 18 |
| Table 2: Default values for LCL filter parameters | 62 |
| Table 3: Default values for active rectifier and system parameters..... | 68 |
| Table 4: Default parameters for each AR in parallel operation and system parameters..... | 75 |

NOMENCLATURE AND ABBREVIATIONS

Symbols:

| | |
|---------------|---|
| abc | Three phases in the natural reference frame |
| $\alpha\beta$ | Axes in the stationary $\alpha\beta$ -reference frame |
| dq | Axes in the synchronous reference frame |
| (s) | parameter in Laplace Domain |
| Eq. | Equation |
| J | Inertia |
| e·n | 10^n |

Subscripts:

| | |
|-------|------------------------------------|
| a,b,c | natural frame a,b,c phases |
| cap | capacitor |
| con | converter |
| D | variables of Damping related |
| e | variables of electrical quantities |
| filt | Filter |
| g | quantities related to generator |
| m | variables of mechanical quantities |
| syn | synchronous |

Superscripts:

| | |
|-----|---------------------|
| ° | Degrees |
| * | reference parameter |
| est | Estimated |

Abbreviations:

| | |
|-------|--|
| ac | Alternative current |
| dc | Direct current |
| DG | Distributed Generation |
| DSP | Digital Signal Processor |
| MG | Micro Grid |
| PI | Proportional-Integral (controller) |
| AR | Active Rectifier |
| AVR | Automatic Voltage Regulator |
| DSOGI | Dual Second Order Generalized Integrator |
| MTBF | Mean Time Before Failure |
| PLL | Phase-Locked Loop |
| PR | Proportional-Resonant (controller) |
| pu | per unit |
| PWM | Pulse Width Modulation |
| rms | root-mean-square |
| SG | Synchronous Generator |
| SI | International System of Units |
| SPS | Standby Power Supply |
| SPWM | Sinusoidal Pulse Width Modulation |
| SRF | Synchronous Reference Frame |
| UPS | Uninterruptible Power Supply |
| VCO | Voltage Controlled Oscillator |
| VOI | Virtual Output Impedance |
| VSI | Voltage Source Inverter |

1 Introduction

1.1 Background & Motivation

At present, the electrical power systems and networks around the globe are undergoing a timely change triggered by the economic and environmental [1] reasons supplemented with the rapid advancements in the field of power electronics. Renewable energy sources as such as wind energy and solar energy play a pivotal role in this transformation due their increasing popularity. It is evident from the fact that the European Union has issued the directives to achieve a 20% target from the overall share of energy from the renewable sources by 2020 [2].

Renewable energy sources and distributed energy resources have given risen to the requirement of distributed generation. Distributed generation has been the catalyst in the transition of the conventional vertical grid structure towards a much more meshed and amorphous grid structure as described in [3] and as illustrated in Figure 1-1.

The concept of micro-grid is found to be the most promising approach for the smart integration of such distributed generation units (or micro sources) to the main grid or for islanded autonomous operation [4] due to its enormous technical advantages outlined in [5] and [6] with respect to the distributed energy resources. Most of such micro sources could be interfaced with fast acting converters to harness the maximum effectiveness of the micro sources [7]. The converter could be a dc to ac power converter (inverter) in a case where the source is a dc generator like photovoltaic voltage panel or an energy storage unit like fuel cells or else back-to-back (ac-dc-ac) converter for example in wind power generation.

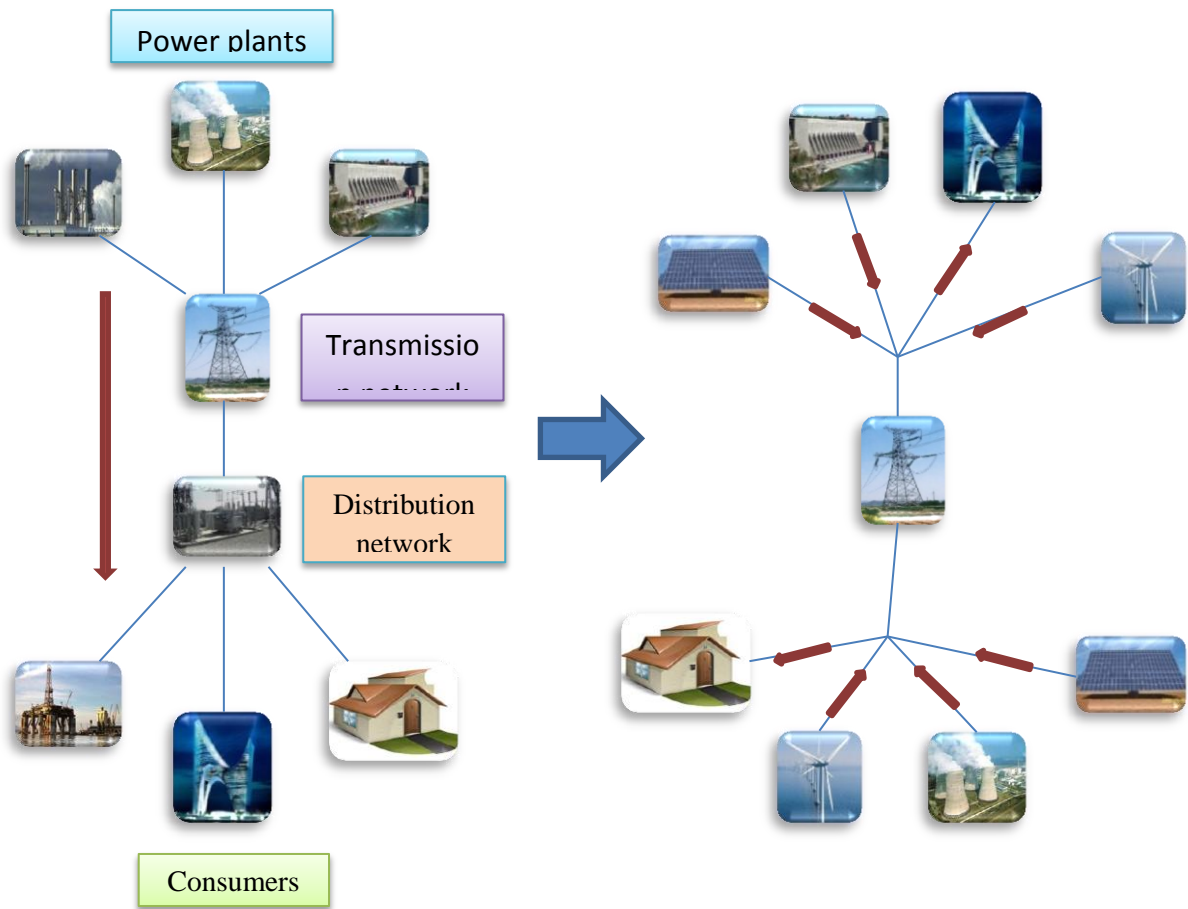


Figure 1-1: Grid structural transformation from vertical to mesh structure due to the distributed generation

When micro grids with micro sources interfaced with inverters are connected to the main grid, the micro sources will be in the grid-following mode [8] where the major responsibility of the system stability lies on the well-established main generators in the stiff grid. However, when the micro sources are required to operate in the island mode where the stiff grid network is no more connected to the micro grid, the challenge arises in the perspective of system stability and reliability.

While appreciating the inherent ability for system stability of a **synchronous generator (SG)** as described in [9], it also stimulates the question if the inverters of a micro grid can imitate the behaviour of a synchronous generator will the stability and reliability issues be overcome in a micro grid particularly in the island operation.

On the other hand, **uninterruptible power supplies (UPS)**, a well-proven technology over the past decades, share much similar philosophy and challenges in terms of power conditioning in a micro grid. In fact, apart from the supplementation of synthetic inertia response with back-up power supply, in a way, UPS attempts to mimic the synchronous generator behaviour with giving more focus on control strategies rather than **virtual synchronous machine (VSM)** implementation. Therefore, understanding the control strategies of UPS has been identified as a key component in realizing a robust, fast acting inverter to mimic a virtual synchronous machine.

Therefore, in summation, the motivation of the master thesis has been to imitate the damping and inertia properties of a synchronous generator and also replicate the modern control strategies of a UPS in an inverter such that the inverter acting in a micro grid will feature damping and inertia properties as well as redundancy and load sharing features of synchronous generator and UPS respectively.

It must be noted that, under the scope of the master thesis, the inverter with such VSM properties and control strategies will be known as an **active rectifier (AR)** throughout this dissertation.

1.2 System Overview, Objective & Applications

Objective of the specialization project can be easily comprehended by first analysing the system of interest given in the Figure 1-2

The system is comprised of synchronous generators and/or active rectifiers (AR) and a stiff grid as illustrated in the figure. Active rectifiers are sourced by the dc bus which could be powered by a battery bank or fuel cell. It must be noted that the source of the dc bus is not in the scope of the thesis therefore a constant dc voltage is reasonably assumed in the input side of the active rectifier.

The system can be broken into mainly two subsystems as follows;

1. Micro grid subsystem which is a mix of SG and/or AR and a local load
2. Stiff grid subsystem.

Micro grid contains the dc bus, active rectifier(s) and/or synchronous generator(s) and the local load. Synchronous generator within a micro grid is somewhat analogous to a stiff grid within the grid due to its much more robust electrical response upon a fault in the network and also for its line frequency forming nature.

The system operates at **690 V_{r.m.s}** line to line voltage at **60 Hz**. In a general view point, micro-grid plus stiff network may function in three operating cases with 2 modes as enlisted below;

1. SG-SG-Stiff Grid Case, Figure 1-2(a)
 - a. Grid connected mode
Both SGs are connected to the stiff network
 - b. Islanded mode
Stiff grid is disconnected from the micro grid, SGs are islanded
2. SG-AR-Stiff Grid Case, Figure 1-2(b)

Here one synchronous generator is replaced by one active rectifier

 - a. Grid connected mode
Micro grid is connected to the stiff grid
 - b. Islanded mode
Stiff grid is disconnected from the micro grid hence SG and AR are islanded
3. AR-AR-Stiff Grid Case, Figure 1-2(c)

Now instead of SGs, all sources in micro grid are ARs

 - a. Grid connected mode
Both ARs are connected to the stiff network
 - b. Islanded mode
Stiff grid is disconnected from the micro grid hence active rectifiers are islanded

Under the master thesis, case 3 is predominantly investigated.

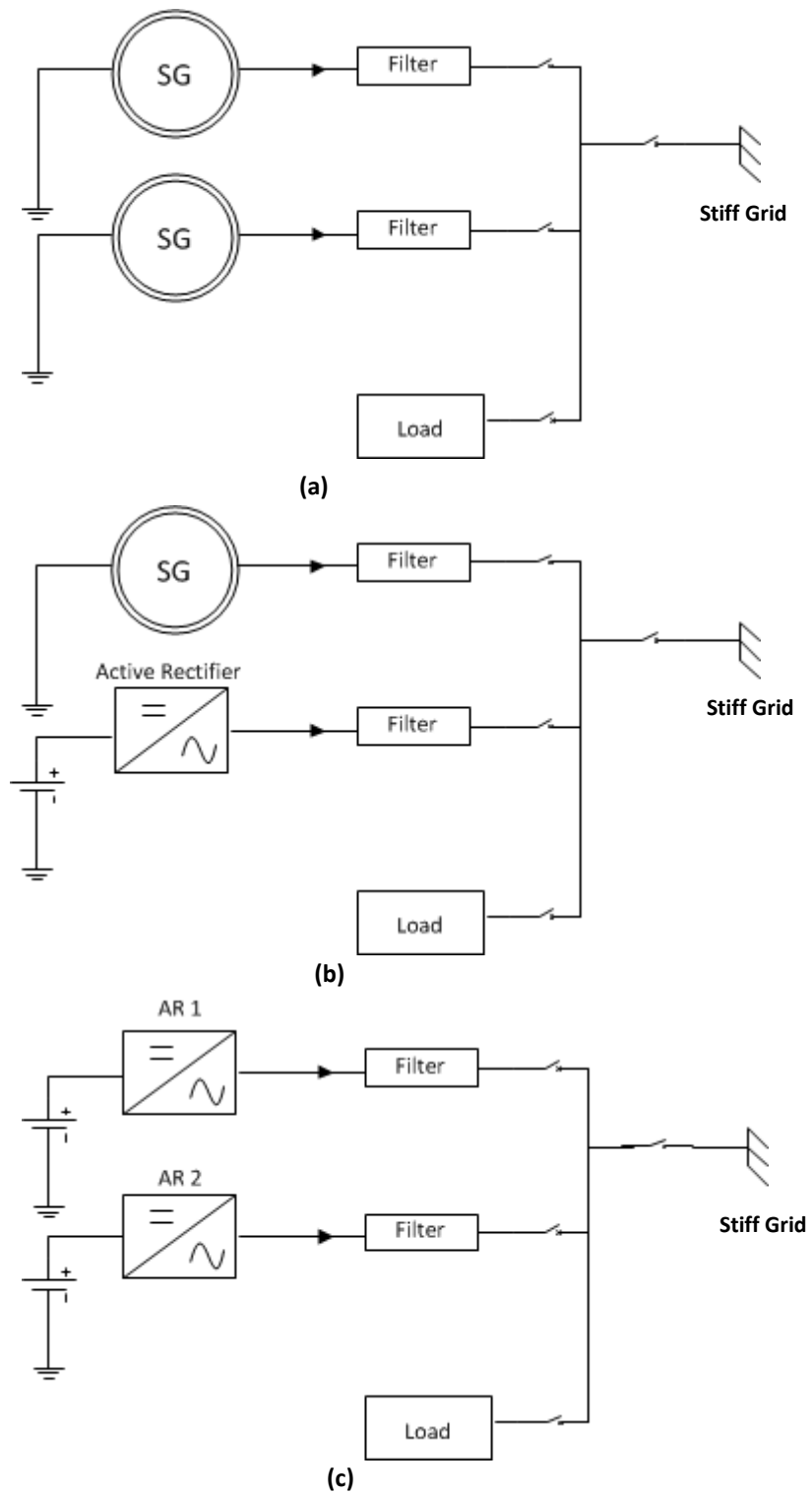


Figure 1-2: System overview with (a) SG-SG (b) SG-AR (c) AR-AR

Eventually, the total system with its functionality can be illustrated as in the Figure 1-3 below.

Therefore, the focus and objective of the project can be highlighted as follows.

The focus of the master thesis is the active rectifier units in the micro grid. The main objective of the project is to emulate virtual synchronous generator behaviour in the active rectifiers so that they will imitate a synchronous generator behaviour in both grid connected and islanded modes and thereby provide the inherent advantages (refer chapter 4) those are offered when actually a synchronous generator is connected instead to the micro grid. The control strategies of the active rectifiers will be mainly inspired by the UPS inverter control schemes (refer chapters 3 & 5).

Looking at the applications of the proposed solution in the master thesis, it is important to first look at what kind of micro grid which is interested in. Here, the micro grid could be a power network in an air craft, ship, an automobile or an offshore oil rig or even a small village.

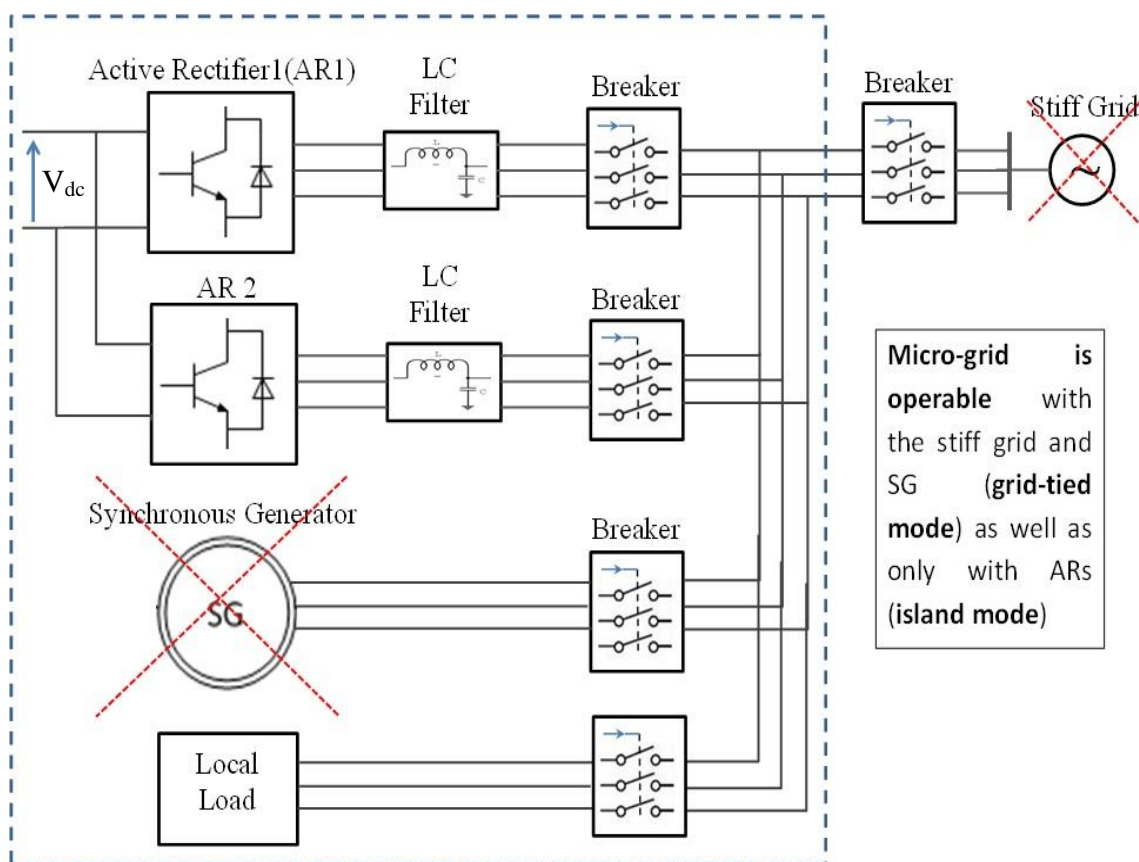


Figure 1-3: Total system overview with functionalities

In a time where rural electrification emerges with solar panels or localized wind turbines, the proposed solution of active rectifiers would be an ideal candidate to interconnect the intermittent renewable energy sources to form a stable and reliable micro grid.

Taking craft electrification into account, green energy has been the new competitive advantage in the upcoming transportation industry. Under this circumstance, many air/sea craft manufactures are now looking at power generation with minimal use of fossil fuels. This leads to the on-board power generation of both ac and dc systems. The proposed solution again provides a strong reinforcement to interconnect ac and dc micro sources into one micro grid.

1.3 Scope of the Thesis & Sequence of Work

Scope of the thesis can be enumerated as follows;

1. Theoretical study of state-of-the-art for UPS systems and their control strategies
2. Analysis of different control architectures and strategies of modelling the active rectifier
3. Modelling the active rectifier based on the optimal UPS and VSM control strategies to perform following features
 - a. Virtual inertia
 - b. Virtual damping
 - c. Redundancy
 - d. Load sharing
4. Simulation of the active rectifier in stand-alone and parallel cases in grid-tied and island modes

Sequence of Work:

1. Understanding the diesel generator, governor and AVR operation in a micro grid
2. Theoretical study on inertia, damping and load sharing of synchronous generators
3. Modelling & simulation of virtual synchronous machine model
4. Understanding the UPS features and control strategies
5. Modelling, tuning, optimizing and simulation of current & voltage control loops
6. Incorporating the classical control loop strategies along with VSM model to develop the VSM-based active rectifier
7. Simulation cases in stand-alone and in parallel on grid-tied and island modes

1.4 Outline of the Thesis

In the introduction chapter, a general introduction is presented highlighting the motivation, objective and application of the thesis. Also it contains the sequence of the thesis scope and sequence of work.

Chapter 2 investigates the state-of-the-art for the active rectifiers in micro grids in terms of hardware and control strategies. It touches the options of having communication channels between the modules for successful load sharing. The important areas of the literature review are presented in separate chapters 3, 4 and 5 for clarity and

Important studies of UPS are presented in the chapter 3. This chapter provides a total overview ranging from the classification to the harmonic but keeping the discussion within the scope of the thesis. The control strategies of the UPS systems are discussed in chapter 5 separately.

Chapter 4 is a review on synchronous generators and virtual synchronous machines. Most of this study was performed under the specialization project in the fall, 2011. The study analyses the physics behind the damping and inertia which are part of the core of the master thesis.

The various options of active rectifier control strategies and control architectures are analysed and compared in the chapter 5. At the end of each comparison, the choice of the strategy/option is outlined along with the basis of selection. It also provides important theoretical discussions on phase-locked loops (PLL).

Chapter 6 presents the modelling of different control modules based on the theoretical analysis in chapter 5. It provides simulation results to validate the model functionality and the theory behind its operation.

Chapter 7 unveils the important simulation results of the VSM-based power control in active rectifier in a micro grid in stand-alone as well as in parallel operation both on grid-tied and island modes.

Chapter 8 brings in the important conclusions of the thesis. Further work section outlines the areas to be given attention to and a recommendation section is included with personal opinions for an efficient model design

NOTE:

Throughout the thesis, important facts and conclusions have been emphasized in this format

1.5 Summary of Chapter

Introduction chapter presents the general introduction to the entire thesis while highlighting the core motivation of emulating synchronous generator behaviour for stability and reliability of the micro grid. Chapter further presents the application of the proposed solution and total system overview while demonstrating different cases through which system has to undergo. In addition, it contains the scope of the master thesis and how the entire project was carried out breaking into small work packages. Under the thesis outline, a brief summary of each chapter is presented.

2 State-of-the-Art for Active Rectifiers

2.1 State-of-the-Art for Active Rectifiers

Active rectifiers or power inverters have been an integral component of the power systems, power conditioning applications and motor drives technology since a many decades. Over the years, the art of inverter design has grown by leaps and bounds thanks to the ever advancing power electronic and semi-conductor technology.

The performance evaluation criteria for active rectifiers would be output voltage quality in relation to harmonic distortion, power circuitry complexity, and implementation cost [10]. The foremost attention has been given in the hardware design and optimization of active rectifiers. The hardware design candidates like multilevel inverters is now in the process of outclassing the classical two level inverters due to its inherent advantages of higher voltage capability, reduction of input and output harmonic content, lower switching losses, higher amplitude fundamental and lower dv/dt [11].

The advancement of control strategies of the active rectifiers has been the other corner stone for high performance. There had been many novel control strategies proposed over the last decade for current control, voltage control and power control out of which, the relevant ones are discussed in the chapter 5: Active Rectifier Control Strategies.

In general, the art of active rectifier design seemed to be highly influenced by the need for uninterruptible power supplies (UPS) for critical loads. Therefore, a complete chapter has been dedicated to discuss the UPS technologies. In the recent years, the synchronous generator behaviour has tremendously inspired the inverter technology. Especially with the emergence of renewable energy sources and distributed dc energy sources, the idea of synchronous generator behaviour emulation has found to be very promising and number of researches is being carried out.

I believe the future of the art of active rectifier control strategies would be highly revolutionized by the idea of virtual synchronous machine where the heavy rotating masses and bulky damper windings will be replaced by small micro controllers.

2.2 Communication & Communication-less topologies

One of the most obvious issues in a micro grid is whether to use a centralized or decentralized control structure for information of load sharing between the parallel active rectifiers. In the centralized control scheme, controller converter (or the master converter) will set the parameters to the rest of the slave converters whereas in return, the slave converters feedback the system information to the control converter. The communication can be carried out using a high frequency or low frequency communication channel. However, making the entire system depending on one control converter adds an extra element of risk to the system. Reliability of communication channels can be improved by utilizing the high frequency communication media like fibre optics which is then demanding in terms of infrastructure [12], [13], [14].

2nd option is using the classical droop control method for converter operation which is also known as virtual synchronous machine method. This approach will depend only on the local measurements and also will have no hierarchy for the converters. However, not having a frequency reference in the island mode will be an issue to be addressed.

Of course, it can be proposed to have a hybrid system of both communication and communication-less system breaking the converters into clusters depending on their proximity to each other.

2.3 Summary of Chapter

Hardware designs and control strategies of inverters have been ever advancing in terms of power quality, complexity of circuitry and cost of implementation. UPS and synchronous generator systems have vastly influenced the modern control strategies of active rectifiers.

Load sharing between the parallel active rectifiers in micro grids could be implemented using communication channels or wireless control strategies like droop control methods.

3 Uninterruptible Power Supply

3.1 Introduction to UPS

Under the pre-study on VSM concept in [15], it was understood that having synthetic inertia response is quintessential in emulating the synchronous generator behaviour in AR. As [16] explains, inverters can provide inertia response with well-defined control strategies to a certain degree however will be insufficient for fast frequency response. Having an energy storage system as a back-up supply in the AR side will emulate a synthetic inertia response in much favourable way. On the other hand, the studies on the state of the art of UPS systems provide innovative insights towards modelling and designing active rectifiers with VSM concept because the philosophies are much alike. Under this motivation, UPS systems were generally studied and some of the features were extracted in modelling the ARs for better performance.

UPS is a device that maintains a continuous supply of electric power to the connected equipment by supplying power from a separate source when the utility mains are not available [17]. In the perspective of the system of interest under the master thesis, the active rectifier is sourced by a dc source. [18], [19] and several other industrial datasheets outline several disturbance a power system can experience out of which brownouts, black outs, voltage spikes and ringing could be relevant for the system of interest. Also there is a portion of undesirable effects introduced by the harmonics due to non-linear devices as [20] describes which will be elaborated under the harmonic filtering section.

Looking at such different adverse effects and the possible remedies for avoidance and mitigation, four elements can be highlighted to evaluate the performance of a UPS as [21] specifies.

1. Reliability
2. Functionality
3. Maintainability
4. Fault tolerance

While constantly focussing on the above features, the report will mostly lace its discussion to distributed UPS systems which are operable in parallel based on [22].

3.2 UPS Classification and Configurations

3.2.1 Classification

UPS systems can be mainly classified as rotary and static based on [18], [23] and [24]. A classic example for rotary UPS systems would be fly wheels where the energy will be stored as mechanical inertia as illustrated in the figure below.

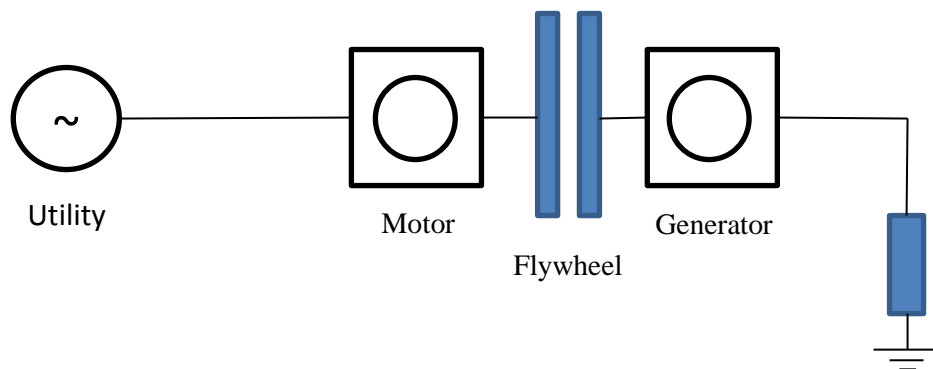


Figure 3-1: Block diagram of a rotary UPS system

However, under the system of interest, static UPS systems will be evaluated. Some sources further categorize the static UPS systems as follows;

1. Standby power Supply (SPS) also known as Offline UPS
 - a. Until the power fails, connected to the power line.
 - b. At failure, battery powered inverter will be turned on
2. Ferroresonant UPS (hybrid UPS)
 - a. In normal operations, line power is present
 - b. Supply power is conditioned by ferroresonant transformer
 - i. Transformer maintains constant voltage at
 1. Varying input voltage
 2. Even at outage at the primary (supply side)
3. Line Interactive UPS
 - a. Interacts with the ac side
 - b. Smoothens the fluctuations of power line
4. Online UPS
 - a. Most advanced out of all
 - b. Inverter continuously provides clean power from the battery

[21] further explains that SPS and line-interactive modules are single conversion modules which can be synchronized only to their own input power sources whereas online UPS class can be known as a true UPS module with double conversion. Double conversion, which is ac to dc and then dc to ac power conversion, and mean time before failure (MTBF) over one million hours ensure the reliability and functionality of a UPS system which are two of the four fundamental elements of UPS as discussed in the previous section [21].

3.2.2 Redundancy

Redundant and parallel UPS systems allow the micro grid with high expandability and maintainability and thereby reliability. [25] specifies online and line-interactive UPS configurations as the two major distributed UPS systems that allow high reliability with higher degree of redundancy.

Systems with redundancy are generally known as $N + 1$ or $N + X$ UPS systems. Simple idea behind redundancy is that when N number of UPS is in active operation, 1 or X number of units will remain standby as reserves.

[26] classifies UPS into mainly two classes as follows;

1. Serial redundancy (hot standby)
2. Parallel redundancy (active connection)

The note further recommends the first over the second option due to the following reasons;

- In the parallel redundancy topology
 - Failure of one UPS unit may cause disturbance of the AC output load
 - Failure of one may *drag* the other unit too down

In general, the tabulated UPS system configurations in Table 1 are available in the industry.

In the system of interest, parallel operation of AR is a mandatory case [15]. This demands parallel operation of UPS systems. For successful parallel operation of UPS, following requirements need to be met [27];

1. Same output voltage amplitude, frequency and phase
2. Equal current sharing between the units
3. Flexibility to increase the number of units
4. Plug and play operation at any time, known as *hot-swap* operation [21], [26] & various industrial data sheets.

Advantages of Parallel Operation could be outlined as thermal management, reliability, redundancy, modularity, maintainability and size reduction.

Table 1: UPS system configurations [21]

| System Configuration | Concurrent Maintenance | | | Fault Tolerance | | Maximum Availability |
|---------------------------|------------------------|--------|--------------|-----------------|--------------|----------------------|
| | Module | System | Distribution | Module | Distribution | |
| Single Module | No | No | No | Minimal | No | 99.95% |
| Parallel Redundant | Yes | No | No | Yes | No | 99.99% |
| Small Isolated Redundant | Yes | No | No | Yes | No | 99.99% |
| Large Isolated Redundant | Yes | No | No | Yes | No | 99.99% |
| Distributed Redundant | Yes | Yes | Yes | Yes | Yes | Continuous |
| Selective Redundant | Yes | Some | Selectively | Some | Selectively | Continuous |
| Power-Tie™ | Yes | Yes | Yes | Yes | Yes | Continuous |
| Hybrid AC/DC Power System | Yes | Yes | Yes | Yes | Yes | Continuous |

3.3 Paralleling UPS

Following discussion is based on [17, 22] looking at the fundamentals of paralleling of UPS systems.

3.3.1 Active Load Sharing

This is one method of paralleling the UPS however with the usage of *communication channels*.

1. Centralized control
2. Master-slave control
3. Current chain control
4. Average load sharing

Advantages: good output voltage regulation schemes, equal current sharing

Disadvantage: constraints in reliability & expandability due to the intercommunication

3.3.2 Droop Control Methods

This is the classical/conventional droop method which is also known as independent, autonomous or wireless control strategy.

- Adjusts the output voltage amplitude & frequency in function of active power and reactive power
- Uses only local power measurements; this ensures higher reliability & flexibility
- Drawbacks of conventional droop control schemes
 - Slow transient responses
 - Trade-offs between the power-sharing accuracy & the frequency and voltage deviations
 - Unbalanced harmonic current sharing
 - Higher dependence on inverter output impedance
 - If the line impedance is unknown, reactance power imbalances can occur

A. Active & Reactive Power Droop Control

This refers to the classical droop control governed by the theoretical reviews found in [4, 28, 29]. The studies show that the classical droop control depends on the impedance level of the micro grid which is a disadvantage as outlined above under the drawbacks.

B. Virtual Output Impedance (VOI): Multi-loop Approach

As a remedy to the dependence of classical droop control approach on the line impedance, a technique known as virtual output impedance has been proposed in [30] and [31] which enables to decouple this undesirable dependency on the nature of the impedance in the lines of the grid.

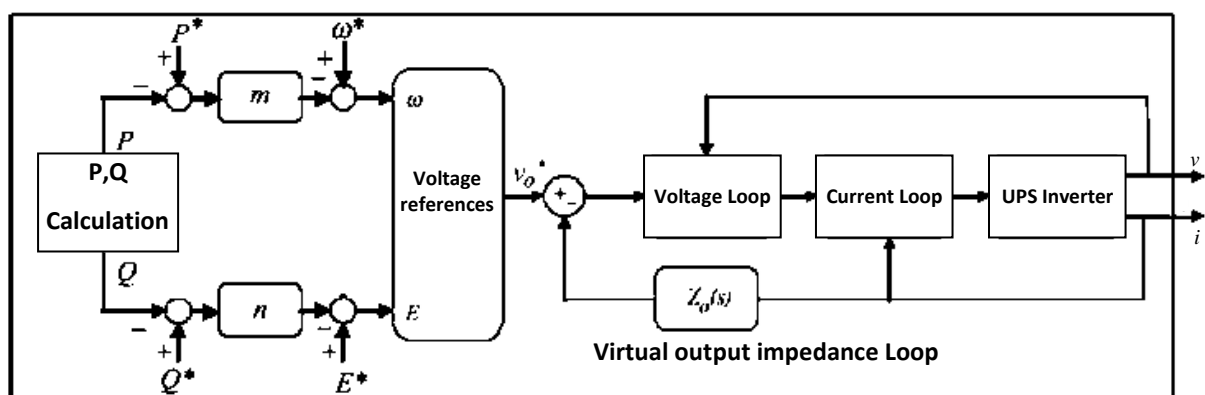


Figure 3-2: Block diagram for UPS control with virtual output impedance loop

As in the above figure, there is an extra loop with virtual impedance in addition to the known cascading loop structure extensively discussed under the section 5.3 of the thesis. The idea behind the approach is to fix the inverter output impedance with virtual output impedance (VOI) such that VOI is much larger than the combined value of VOI plus maximum line impedance

As in the figure shows, now the impedance has become a control variable instead of controlling parameter.

3.4 Battery Management

There could be several energy storage system options to facilitate UPS technology as back up supplies. Following are some of those as proposed in [17];

1. Battery energy storage system
2. Flywheels
3. Superconducting magnetic energy storage
4. Super-capacitor
5. Fuel cells
6. Compressed air energy storage

Each of the above has its own advantage and disadvantage. Under the scope of the master thesis, battery energy storage system seems to be the most viable option to be used as a back-up supply for UPS systems.

Based on the literature on battery management on [32, 33], it can be stated that key to effective battery design and management would be;

1. High MTBF
2. High redundancy
3. Economic design

3.5 Harmonic Filtering

Discussion of harmonics and the filtering configurations are based on the technical report from the General Electric [20].

3.5.1 Theoretical Review

To take the harmonic power (H) in to account, a new term known as *Total Apparent Power* (A) is introduced in addition to the known apparent power (S).

Eq. 3:1

$$S = \sqrt{P^2 + Q^2}$$

Eq. 3:2

$$A = \sqrt{S^2 + H^2}$$

Harmonic power describes the distortions due to the harmonic content. Power cube illustrates the relationship much better.

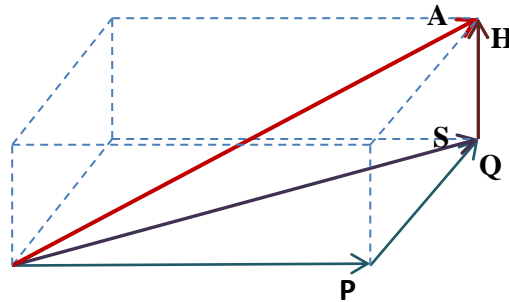


Figure 3-3: Power cube with harmonic power

3.5.2 Effects of Harmonics

Harmonics are superimposed to the fundamentals which then create a distorted wave from a sinusoidal wave. Non-linear loads cause current harmonics as a result cause voltage harmonics.

Effects can be identified as short-term and long term effects as described in [20]. Short term effects can be highlighted as;

1. Interference with telecommunication lines
2. Variations of motor torque with relative speed variations
3. Acoustical noise

The more adverse effects will be in the long run as follows;

1. Cables over heating due to
 - a. Skin effect
 - b. r.m.s current increase
2. Additional losses in the rotating machines
3. Losses in power transformers

3.6 Summary of Chapter

Technology of UPS has been well-established over the decades while it is still advancing with novel control strategies. Reliability, Functionality, Maintainability and Fault tolerance can be outlines as the performance criteria of the UPS systems whereas redundancy and expandability will be the properties that are found to be inspiring for the master thesis.

It can be concluded that the better performance of a UPS is always a trade-off between inertia and the cost of frequency response.

4 Virtual Synchronous Machine Concept & Control Strategies

4.1 Synchronous Generator Operation

Based on the text books [9] and [34], a concise theoretical explanation is presented here on the synchronous generator in relation to its inherent mechanical and electrical aspects beneficial for the concept of designing a virtual synchronous machine.

Figure 4-1 presents a schematic view of a basic 2-pole, single phase synchronous generator extracted from [34]. The figure illustrates how the field winding of the machine is wound on the rotor whereas the armature windings are wound on the stator of the machine. In addition to those two windings, synchronous generator rotor contains damper windings which come into the effect in the machine's transient state of operation.

Under the scope of the master thesis, there are mainly three inherent features of a synchronous generator that are identified to be very crucial in the stable and reliable operation of a power system hence will be discussed succinctly.

The three main inherent features of a synchronous generator are;

1. Inertia in the synchronous generator due to the rotating masses
2. Damping effect due to the damper windings in the rotor
3. Speed-droop characteristics of a synchronous generator for load sharing

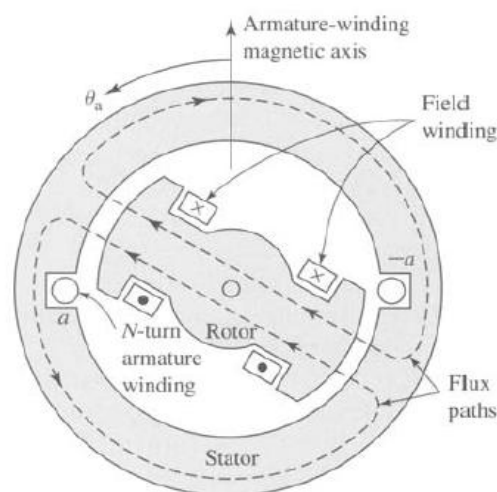


Figure 4-1: Schematic view of a 2-pole, single phase synchronous generator, Source: [34]

Having explained the synchronous generator machine, it is worth to have a quick glimpse at how the entire generator unit operates for the understanding of control and autonomous behaviour of a complete generator unit. Figure 4-2 presents a general block diagram of a generation unit.

Key control units of such a generator unit are;

1. Governor

SG is driven by the *prime mover*, which could be a turbine or a diesel engine is equipped with a speed control unit known as governor. Purpose of the governor is to control either the speed of the machine (i.e. frequency of the generator voltage) or the output mechanical power adhering to the pre-specified power-frequency characteristics [9].

2. Automatic Voltage Regulator (AVR)

The dc excitation current of the field windings consequently the terminal voltage of SG is controlled by the AVR.

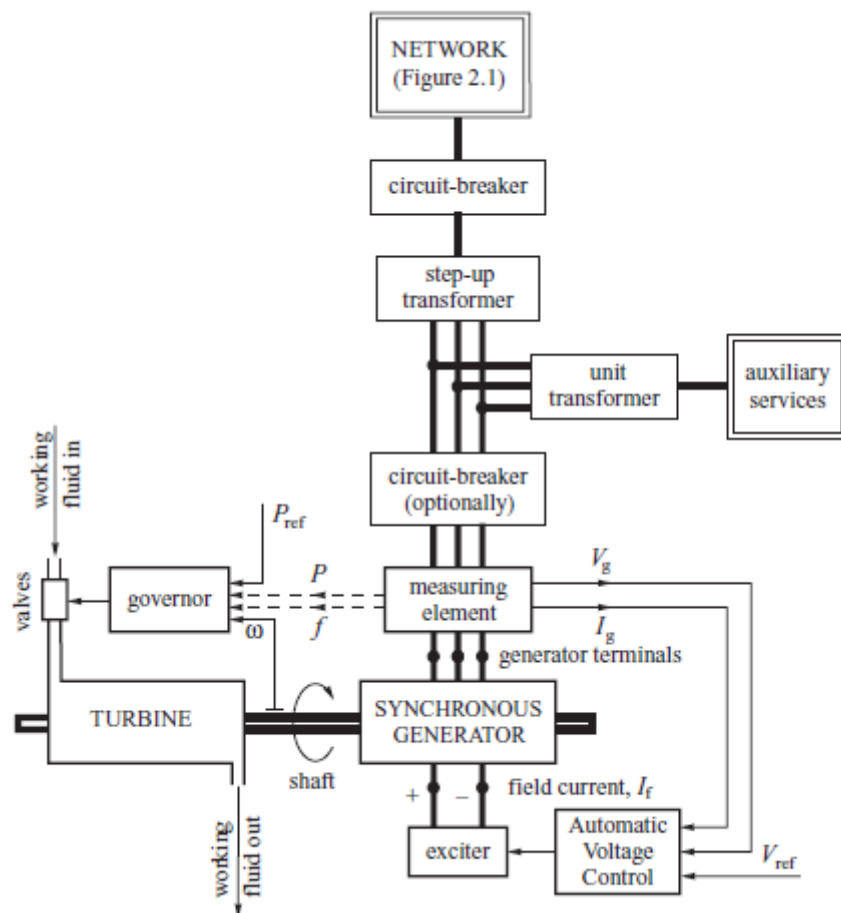


Figure 4-2: Generation unit block diagram, Source: [9]

4.1.1 Inertia in the Synchronous Generator due to the Rotating Masses

Rotor with the field and damper windings of the synchronous generator, as it rotates, creates a sinusoidal rotating flux in the air gap which eventually results in the electromotive force in the armature terminals.

If we may look at the swing equation of the synchronous generator dynamics,

Eq. 4:1

$$J \frac{d\omega}{dt} = \tau_m - \tau_e - D \cdot \Delta\omega$$

$$\text{where } \Delta\omega = \omega - \omega_{syn}$$

J = moment of inertia of the rotating masses

ω = angular speed of the rotor shaft

τ_m = mechanical torque

τ_e = counteracting electromagnetic torque neglecting damper effect

D = damping torque coefficient

ω_{syn} = synchronous speed or speed at steady state

At steady state of operation, $\omega = \omega_{syn} = \text{constant}$, $\therefore D \cdot \Delta\omega = 0$ & $\tau_m = \tau_e$

τ_m , the mechanical torque has higher time constants due to the slow torque response in the prime mover hence its changes are relatively slow. Upon an imbalance in the electrical network, τ_e , electromagnetic torque can be varied almost instantaneous [9]. Therefore, due to some disturbances, if $\tau_e < \tau_m$, the rotor will accelerate and if $\tau_e > \tau_m$, the rotor will decelerate.

The rate of change of speed of the rotor is dependent on J which is the moment of inertia of the rotating mass. There is a portion of kinetic energy in this rotating mass stored during the steady operation of generator which is extremely beneficial at an imbalance of torques. At an imbalance, this kinetic energy will be absorbed by the system to alleviate the speed deviations from synchronous speed.

4.1.2 Damping effect due to the damper windings in the rotor

Damper winding which introduces the damping effect in the synchronous generators plays an important role to regain synchronism when the generator rotor experiences rotor speed deviations due to *small disturbances*.

In physical nature, damper winding is no much difference from the rotor of a squirrel cage induction machine with short circuited windings. Damper windings can be wound either

only in rotor d-axis or both d-q axes [9]. The latter gives improved damping and the former leads to sub-transient saliency of the machine [9].

Depending on the resistance to reactance ratio, the damping response may vary. Higher resistance in the winding will offer a lower torque/slip ratio as for induction machines with large rotor resistance. Lower resistance gives higher damping torque for small $\Delta\omega$.

To understand the damping effect introduced by the damper winding, it is worth to first briefly look at the electromagnetic phenomena of a synchronous generator upon a small disturbance.

When a short circuit occurs in the grid, to retain the flux linkage in the armature and rotor windings constant as per the constant flux linkage theory [9], short circuit current is induced in the armature windings.

However, this induced armature current results in the armature reaction phenomena which drive armature reaction flux across the air gap which links with rotor windings. To compensate this armature reaction flux linkages in the rotor, additional current is induced in the rotor windings, in detail, field winding and damper winding wound in the rotor. This additional current is induced in the damper winding.

The generator response upon such a fault is analysed breaking the total fault time frame into three states known as *sub-transient*, *transient* and *steady state* which is the stable condition. The damper current will come into play only during the transient state as it has a screening effect against the induced flux during sub-transient state.

Again looking back at the swing equation Eq. 4:1 it can be deduced to express as a power equation as follows;

Eq. 4:2

$$J \frac{d\omega}{dt} = P_m - P_e - P_D$$

$$\text{where } P_D = D \cdot \Delta\omega$$

P_D = Damping Power

Rotor and power oscillations under the effect of damping upon a small disturbance are illustrated in the Figure 4-3 from [9].

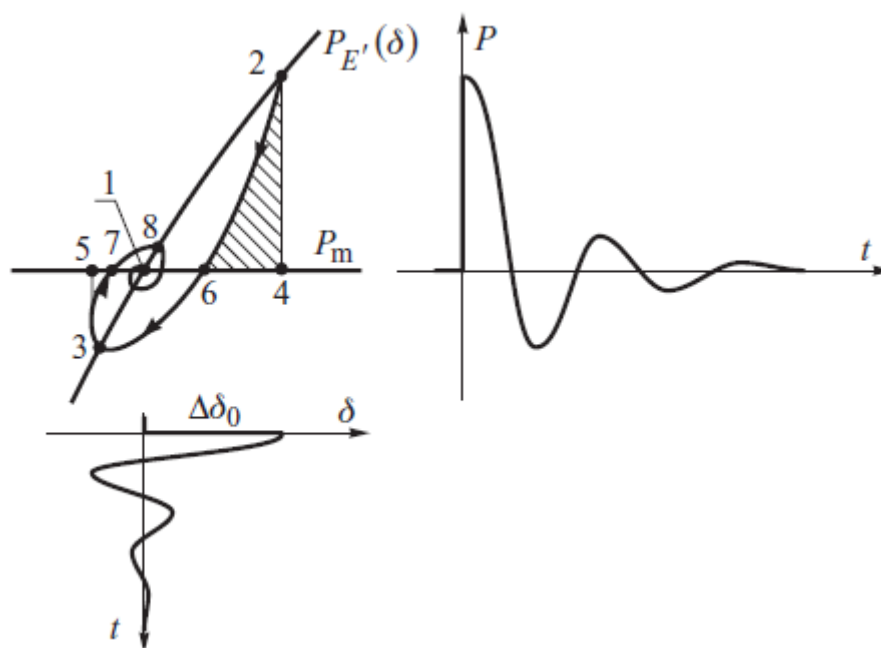


Figure 4-3: Rotor and power oscillations with damping included, Source: [9]

When the rotor is disturbed from its initial equilibrium point, it could be either accelerated or decelerated. If $\Delta\omega > 0$, damping power will be negative i.e. effectively opposing the acceleration and if the $\Delta\omega < 0$, damping power will be positive and supporting the airgap power P_e in opposing the deceleration. The rotor will eventually follow a modified trajectory and reach synchronism without infinite oscillations also known as *hunting* [7] which would be the case at the absence of damping effect.

4.1.3 Droop Characteristics of a Synchronous Generator in Load Sharing

This discussion is an extended explanation of the advantage of inherent inertia present in SG due to its rotating masses examined in the section 4.2.1 Inertia in the SG. The discussed advantage will be viewed in the active power or load sharing perspective between two generator sets in an *islanded system*.

Synchronous generator rotor speed, under steady state conditions, is proportional to the frequency of the armature current and as a result the frequency of the terminal voltage [34]. This is governed by the following equation;

Eq. 4:3

$$f_e = \left(\frac{\text{poles}}{2}\right) \cdot \frac{n}{60}$$

f_e = electrical frequency of the voltage generated in the synchronous generator

n = rotor mechanical speed in revolutions per minute

Again, if the swing equation is considered, it is apparent that when a mismatch occurs between the input mechanical power from the *prime mover* to the generator and output electrical power from the generator to the network, the rotor speed will vary. This speed-load dependence of two parallel synchronous generators can be characterized by the curves as given in the Figure 4-4.

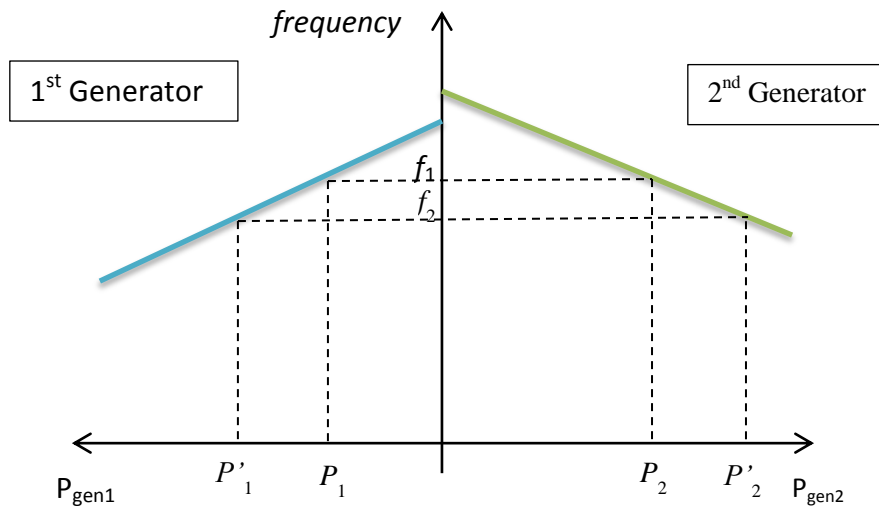


Figure 4-4: Speed-droop characteristics of a synchronous generator

In an islanded system, when two generator sets operate in parallel, they will share the same frequency. If the load in the system increases substantially, the additional load will be shared by the two generator sets according to their droop settings. However, if the frequency drops in this case below a certain threshold values below which the operation is detrimental to the system components, the speed reference of the *governors* of two SGs needs to be adjusted.

4.2 Virtual Synchronous Machine

Advantages of a synchronous generator due to its inherent features were discussed in the previous section. These benefits which contribute to the system stability and reliability have been the true motivation to emulate the synchronous generator behaviour in the active rectifiers by virtual means for its autonomous operation in the islanded mode.

Concept of virtual synchronous machine (VSM) has been evolved from the concept of Uninterruptible Power Supplies (UPS) which are already in successful use for supplying critical loads. Therefore VSM implementation incorporates several UPS techniques as such as energy storage for back up supply [18] which will be discussed in the following section 4.2.1 Virtual Inertia.

VSM implementation in active rectifiers has been discussed in [7], [3], [6], [35], [36], [37] and [38] fundamentally looking at the following properties for emulation;

1. Virtual inertia in the active rectifier
2. Virtual damping in the active rectifier

In addition to those two virtual properties, for the successful implementation of droop control techniques in active rectifiers in parallel without communication media between the active rectifiers, following mimic property is suggested in [31] and [39];

3. Virtual impedance

It is also worth to note that there are also some *additional advantages* of a virtual synchronous machine design in comparison to an actual synchronous generator which can be realized due its non-physical but virtual existence owed to modelling and control algorithms. As outlined in [7], key extra benefits would be;

1. **System parameters can be varied. For an example, inertia, damping coefficient, machine impedances of a VSM can be varied upon the application and system response whereas these values are fixed and frozen in SG once manufactured.**
2. **System parameters can be chosen upon the application which are impossible with SG**
3. **In VSM, typical challenges of SG like magnetic saturation and eddy current losses will be absent**

However the biggest challenge of realization of successful VSM in active rectifiers arises when a fault occurs in the grid. Despite it is not a direct drawback of a VSM concept, since the total model is realized with power electronics, the question arises whether the semiconductor components will provide sufficient current to blow the fuses and protect the system components from potential threat.

4.2.1 Virtual Inertia

Importance of virtual inertia is viewed at an instance where the primary reserve of the converter fails. In the system of interest, this will be the dc power input to the active rectifier. Under such adverse circumstances, to avoid system failure and eventual *black out*, a fast-acting back up storage unit as such as flow batteries, fuel cells, flywheels, superconductor inductors or compressed air devices [40] can be used. However as [41] suggests, the selection of storage unit depends on various grid and VSM parameters like loads of the grid and VSM action time.

Different techniques of virtual inertia implementation are proposed in numerous literatures. [42] and [43] propose virtual inertia implementation using phase locked loop (PLL) and dynamic frequency support techniques respectively.

However, in the master thesis, it is assumed a constant and uninterrupted dc input to the active rectifier hence inertia is emulated using only virtual moment of inertia value in the VSM dynamics. This is extensively discussed in the specialization project report [15].

4.2.2 Virtual Damping

Damping emulation is also carried out by simply incorporating the damping effect to the machine model. More details can be again found in the modelling chapter of [15].

4.2.3 Virtual Impedance

An equivalent circuit diagram of a synchronous generator will be analysed to understand the theory behind the physical phenomena.

Without losing the generality, a salient pole synchronous generator is considered and can be represented by the following equivalent diagram for its *steady state*.

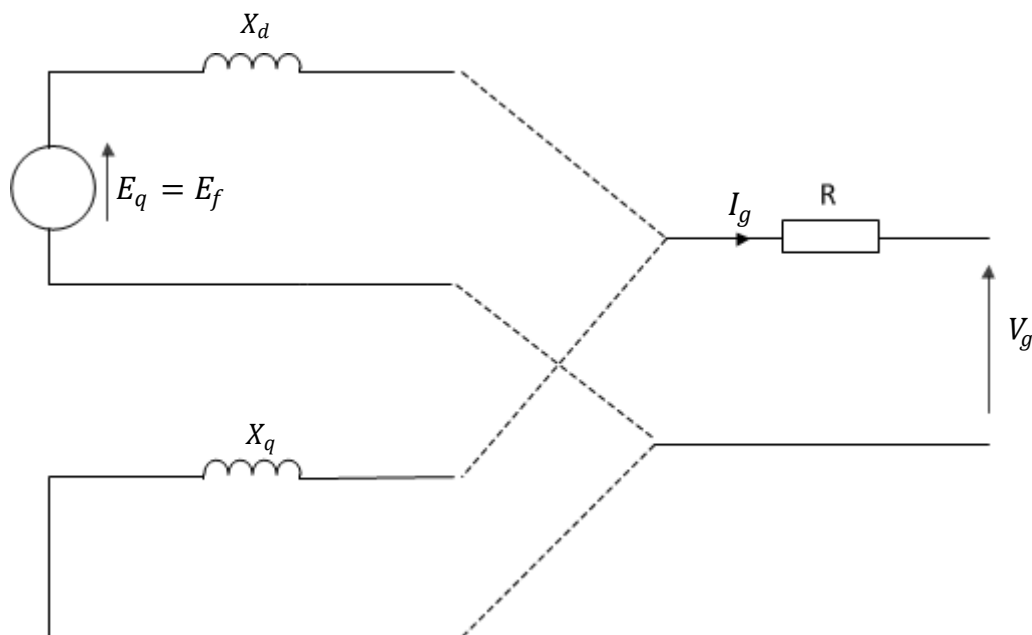


Figure 4-5: Equivalent steady state circuit diagram of a salient pole synchronous generator

E_q = q-axis induced electro motive force (emf)

E_f = resultant induced emf

V_g = generator terminal voltage

I_g = generator current

X_d = d-axis synchronous reactance

X_q = q-axis synchronous reactance

It can be proven that in a round rotor generator where rotor saliency is neglected for simplicity (\therefore reactance will be denoted by X_{eq}), the relationship between active power (P), reactive power (Q) and internal power angle (δ_g) will be as follows;

Eq. 4:4

$$P = \frac{E_q V_g}{X_{eq}} \sin \delta_g$$

Eq. 4:5

$$Q = \frac{E_q V_g}{X_{eq}} \cos \delta_g - \frac{V_g^2}{X_{eq}}$$

Now extending the scenario including the network, following discussion attempts to explain the importance of grid impedance in the droop control techniques.

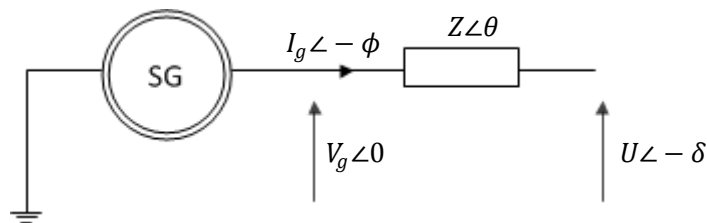


Figure 4-6: Basic power flow diagram between a generator and grid across line impedance

$V_g \angle 0$ = Generator voltage taken as the reference phase

$U \angle - \delta$ = Grid voltage

$Z \angle \theta$ = Line impedance where $|Z| = \sqrt{R^2 + X^2}$

$I_g \angle - \phi$ = Generator current with lagging power factor angle

[29], [44] and [45] provide a similar relationship of voltages and powers to the following after basic circuit analysis of the power flow diagram;

Eq. 4:6

$$U \sin \delta = \frac{XP - RQ}{V_g}$$

Eq. 4:7

$$V_g - U \cos \delta = \frac{RP + XQ}{V_g}$$

When $X \gg R$ in the line, following approximations can be made which lead to the *conventional/classical droop* characteristics;

Eq. 4:8

$$\delta \cong \frac{XP}{V_g U}$$

Eq. 4:9

$$V_g - U \cong \frac{XQ}{V_g}$$

Under this circumstance, P will be a function of frequency, f (as f is proportional to the differential of δ) whereas Q will be function of voltage difference.

When $R \gg X$, the above relationships will be swapped as now as given in the following equations;

Eq. 4:10

$$V_g - U \cong \frac{XP}{V_g U}$$

Eq. 4:11

$$\delta \cong \frac{XQ}{V_g}$$

This is known as the *inverted droop* or *opposite droop* in different literature whichever it is gives the idea behind its twist from the classical droop.

At this point, it is worth to look back at the nature of micro grids in terms of their line impedances. Keeping in mind that our system of interest is a low voltage micro grid, [29] explains, low voltage micro grid lines are more resistive. However, there could be some instances where the low voltage micro grids may have negligible line impedance. For an example, a micro grid in an aero plane, due to its less power line lengths and improved technology, may exhibit such properties. Likewise it can be discussed two line impedance cases in low voltage micro grids;

1. Significant impedance and higher R:X ratio
2. Insignificant impedance and negligible R:X ratio

In the first case, the analysis of the micro grid can be carried out according to the Figure 4-6 and explanation corresponding to the inverted droop techniques.

If the micro grid falls in the second category, then Z in Figure 4-6 will be negligible and V_g and U will be almost equal. Under this context, the impedance analysis can be carried out with reference to Figure 4-5 and its explanation where the internal impedance of the SG (or VSM) is extracted out and considered as the line impedance. Then the interested voltages will be internal voltage, E_q and U , for example.

However, enormous number of literature on droop control proposes assorted methods for droop control techniques in a *decentralized* and *communication-less* architecture. Decoupling of active and reactive power has been main subject in [44] and [46].

Another promising approach for active and reactive power decoupling enhancement is to modify the characteristics of the grid by adding *virtual impedance* in series to the converter. This approach comes with important benefits as such as better control on the output impedance and avoidance of power loss had real resistors and reactors been used. The main drawback in virtual impedance is the voltage drop across the impedance hence reduction of the output voltage range of the converter. Virtual impedance could be either inductive or resistive where [40] and [47] proposes the earlier type while [48] suggests a resistive impedance.

4.3 Summary of Chapter

Physical nature of the synchronous generator has been studied to understand the inertia, damping and load sharing properties which are found to be relevant for the master thesis. The governor and AVR performance has also been presented to understand the frequency and voltage control principles.

The idea of virtual impedance is carefully analysed. The advantages as well as the challenges of a virtual synchronous machine model over a physical synchronous machine have also been presented.

5 Active Rectifier Control Strategies

Distributed generation, particularly with renewable energy sources, encounters unique challenges those would have been avoided with conventional power generation. They are the lower efficiency and poorer controllability [49], [50] mainly due to the intermittent and unpredictable nature of solar and wind energies in specific.

As a result, direct connection of DG to the grid leaves the power network precarious which may lead to grid instability or even failure [50]. This is the very reason why the control strategies hold high interest in both the input-side and grid-side power electronic converters.

Under the scope of the master thesis, an analytical study of controls of grid-side converter, also known as the active rectifier in this context, is presented in this chapter focussing the following controls;

1. Control of converter output current
2. Control of converter output voltage
3. Control of active power input to the grid
4. Control of reactive power transfer between MG and the grid/load
5. Grid synchronization

At the event of two or more techniques are available for each control, a comparison is carried out to choose the most compatible alternative under the context of the master thesis.

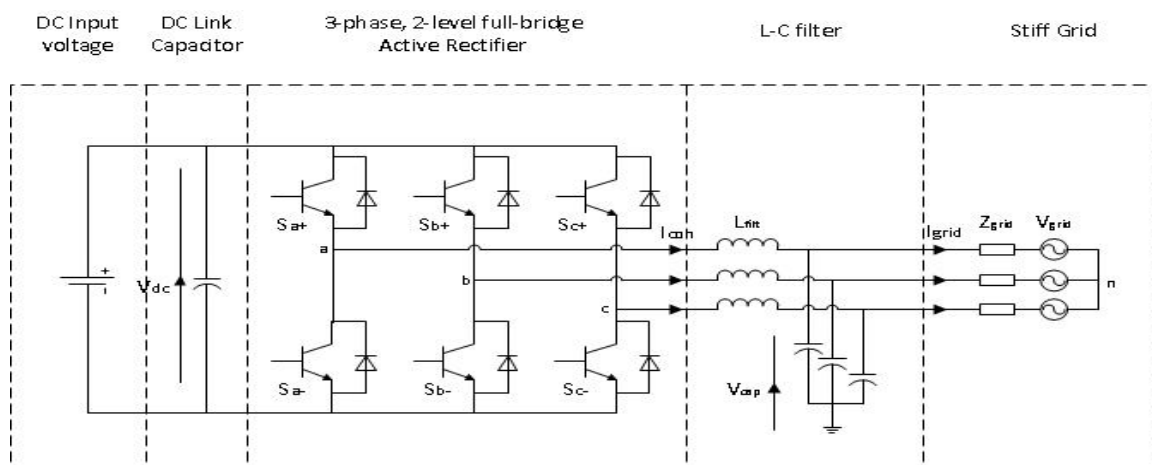


Figure 5-1: Grid Connected Three-Phase, Two-Level Active Rectifier with LC filter

Figure 5-1 presents a generic configuration of the active rectifier with its LC filter in connection to the grid with the line impedance. The voltage balance equations for the configuration can be presented as follows based on [51] and [52];

Eq. 5:1

$$V_{dc} \left[S_a - \frac{1}{3} \sum_{i=a,b,c} S_i \right] = L_{filt} \frac{dI_{con,a}}{dt} + V_{cap} + R_{grid} I_{grid,a} + V_{grid}$$

$$V_{dc} \left[S_b - \frac{1}{3} \sum_{i=a,b,c} S_i \right] = L_{filt} \frac{dI_{con,b}}{dt} + V_{cap} + R_{grid} I_{grid,b} + V_{grid}$$

$$V_{dc} \left[S_c - \frac{1}{3} \sum_{i=a,b,c} S_i \right] = L_{filt} \frac{dI_{con,c}}{dt} + V_{cap} + R_{grid} I_{grid,c} + V_{grid}$$

Meanwhile, a simplified control scheme for the active rectifier can be illustrated as in Figure 5-2. A more detailed and complex control architecture is unveiled in the next section.

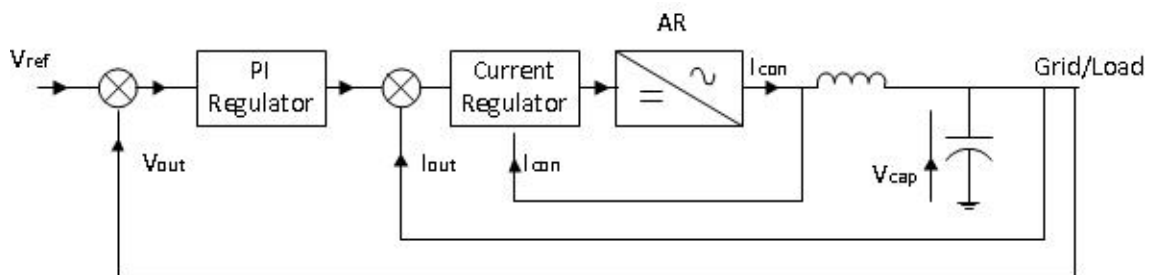


Figure 5-2: Generic control loop configuration of active rectifier

5.1 Single Control Loop vs. Multiple Control Loop

To ensure the generality of the discussion, single and multiple control-loop structures are presented here. As [24] outlines, closed loop control techniques can be primarily broken into two classes as;

1. Single voltage control loop strategy

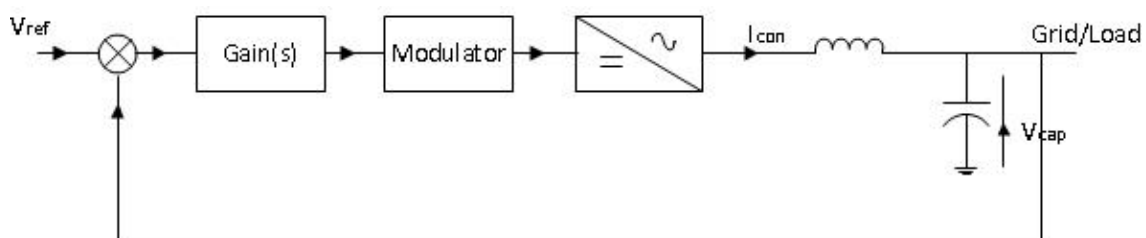


Figure 5-3: Block diagram of single feedback loop

This strategy, as shown in the Figure 5-3, is with single feedback loop for the converter output voltage regulation. The feedback control can be either continuous or discrete as explained in [53] and [54]. SPWM has been the most common feedback control technique used in continuous form which can be implemented in as natural sampling type, average type or instantaneous type as described in [55]. First two types are found to be promising at high frequencies while the instantaneous type offers more robust and dynamic performance in comparison for UPS applications [56].

2. Multiple control loop strategy

Figure 5-2 in the chapter 0 introduction is a typical multiple control-loop block diagram. Multiple control loop strategies for converters utilize primarily an outer voltage loop and inner current loop for controlling the dynamic and non-linear behaviour of the system [24], [57] in spite of other options discussed in [31] as an example where innermost loop controls the voltage.

Figure 5-4 is an expansion of the Figure 5-2 including the aforementioned control loops in the introduction of this chapter. Phase-locked Loop (PLL) is used to estimate the phase of the grid voltage. Estimated phase is then fed for converter output voltage and current controlling modules.

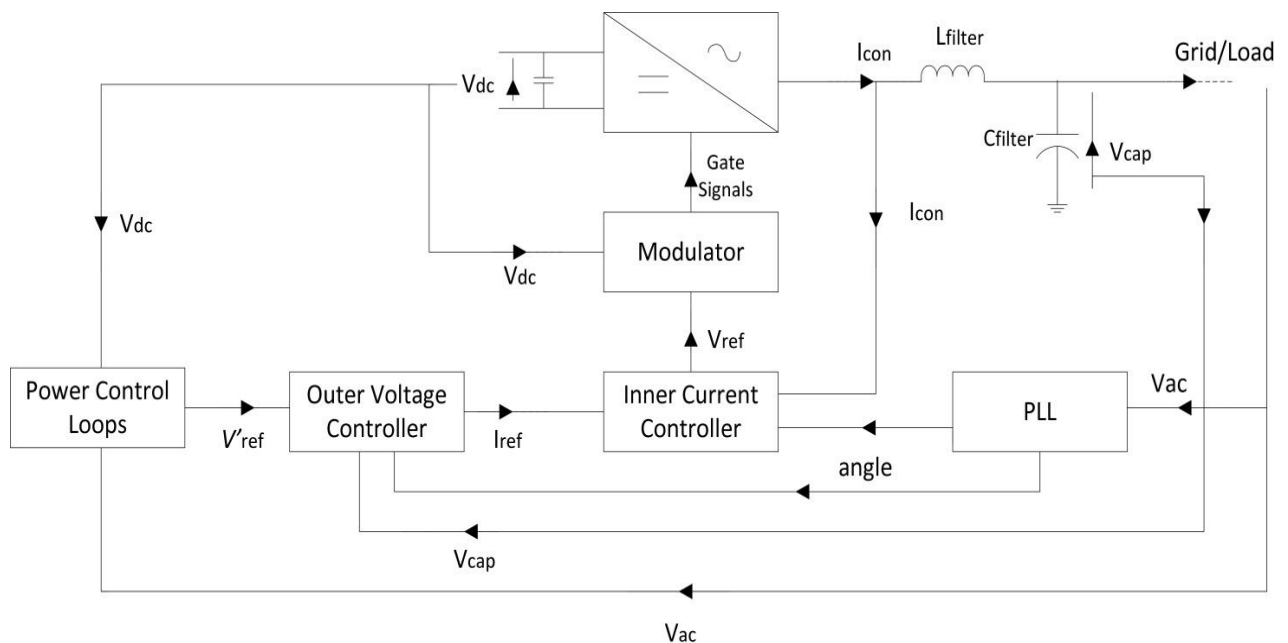


Figure 5-4: Detailed multiple control loop configuration of an active rectifier

Inner current control loop feeds back either ac-side filter inductor current [58] or ac-side filter capacitor current [59] to compare with its reference signal. Here, the reference signal will be the error-compensated signal from the outer voltage control loop. The inner current control loop plays a pivotal role in the overall dynamic responsiveness of the control structure hence its optimal performance is indispensable in the present control schemes. A detailed explanation is provided in the section 5.3.1

The outer voltage control loop uses the converter output voltage, precisely the voltage across the filter capacitor, as the feedback signal. This feedback signal will be compared with the reference voltage generated by the power control loops. The voltage error is subsequently compensated by a PI or PR module which is discussed further in this chapter.

Different control structures for multiple control loops were also proposed with an inner power loop instead of a current loop and in another case, outer power loop with an inner current loop [60], [61].

In the master thesis, the technique of multiple control loop strategies is employed with inner current loop and outer voltage loop which is the classical cascading structure, due to its proven dynamic performance despite the non-linearity of the loads. It should also be noted that the active rectifier control strategies for the master thesis were carried out based on the architecture given in the Figure 5-4.

5.2 Stationary Reference Frame Control vs. Synchronous Reference Frame Control

Active rectifier control architectures could also be classified based on different reference frames of which synchronous reference frame (SRF) and Stationary Reference Frame are the most prevalent.

Figure below demonstrates the orientations of the α - β and d - q reference frames with respect to the natural abc reference frame. In fact, the original control strategy is based on the abc natural reference frame on which number of literature are available [50], [58]. However, due to the availability of much more advanced control strategies based on the other two, natural reference frame control is neglected in the discussion.

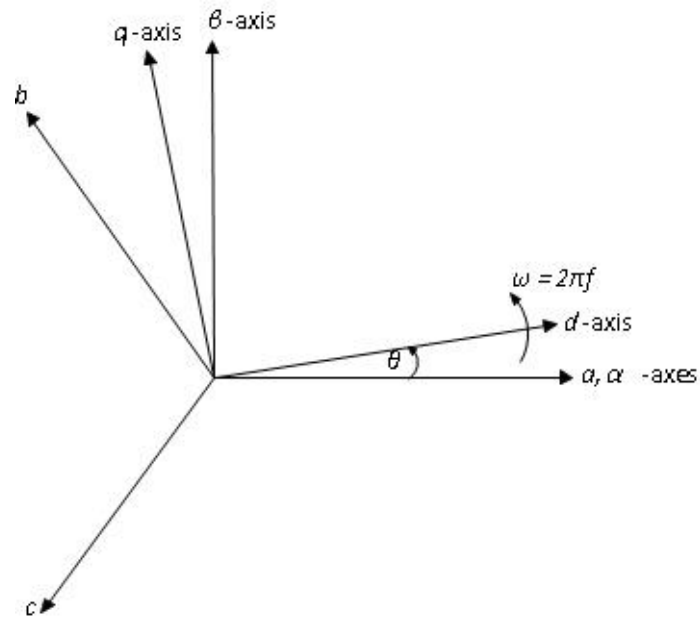


Figure 5-5: Orientation of the natural abc-reference frame, stationary $\alpha\beta$ -reference frame and synchronously rotating dq-reference frame

1. Stationary Reference Frame based Control Strategy

This strategy uses $\alpha\beta$ -reference frame which is a set of hypothetical orthogonal axes affixed to the stator of an induction machine where α is aligned with stator a-axis and β leads by 90° [62] as shown in the Figure 5-5.

Under this control strategy, measured grid currents are transformed into stationary reference frame using the $abc \rightarrow \alpha\beta$ module. Since the reference frame here is stationary but the grid quantities are sinusoidal, the control variables will also be sinusoidal. Due to the inherent shortcoming of PI controllers in failing to remove the steady-state error when controlling sinusoidal waveforms [50], [63], other means of controlling have been proposed of which PR controllers have been the most promising for grid-tied systems.

Based on [63] and [64], PR controllers are able to achieve a very high gain around the resonance frequency which results in eliminating the steady state error.

2. Synchronous Reference Frame based Control Strategy

Synchronous Reference Frame (SRF) control, also known as Rotating Frame Control, transforms measured grid quantities to a reference frame which rotates synchronously with the grid voltage [50]. The SRF illustration is shown in the Figure 5-5 where now the referred set of axes is orthogonal d - q axes which rotate synchronously at the grid frequency. Thereby, the control variables will be dc values (in steady state) hence the inherent shortcoming of PI controller is avoided thus filtering and controlling can be easily achieved [50].

Schematic in Figure 5-6 shows typical d - q control architecture. Inner current controller controls active (I_d) and reactive (I_q) currents. Reactive current control could be made zero if reactive power control is not allowed [49]. The reference to active current control is fed in by the output of the outer voltage (dc link voltage) control.

From the figure it is evident that the $abc \rightarrow dq$ transformation module for current utilizes the grid voltage angle. The purpose of this angle extraction is to have the controlled current in phase with the grid voltages. Phase-Locked Loop (PLL) has been the state-of-the-art technique in determining the phase angle of the grid voltages in the case of DG systems [65],[66],[67]. The detailed design and tuning criteria of PLL are featured in the later sections.

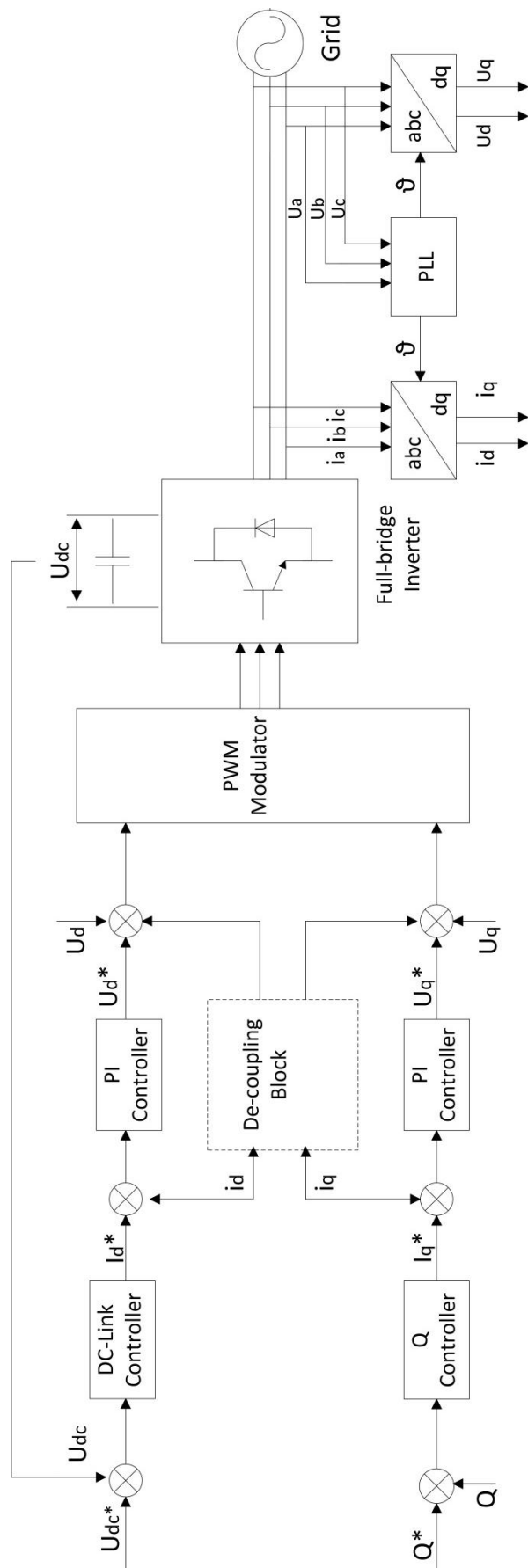


Figure 5-6: Generic control architecture for SRF based control strategy

5.3 Control Loops

Following discussion focuses the details of the inner current control loop and outer voltage control loop.

5.3.1 Inner Current Control Loop

As the foregoing section stated, inner current control loop is a control module with major significance in determining the high performance and responsiveness of the power electronic converters. Important contributions from the current controller will be power quality improvement with harmonic compensation and current protection [50]. [58] expands predominant advantages of having a fast current controller in comparison to conventional open-loop voltage PWM controlled converter;

1. Control of instantaneous current waveform and high accuracy
2. Peak current protection
3. Overload rejection
4. Dynamic response
5. Compensation of
 - a. the effects due to load parameter changes
 - b. the semiconductor voltage drop and dead times of the converter
 - c. the dc-link and ac-side voltage changes

In a classical viewpoint, the inner current control loop controls the current in the filter inductor, L_{filter} [58], [66], [68] as in Figure 5-4. Further to that, [69] discloses a method for designing inner current control loops to directly control the active and reactive power outputs of the converter adhering to the concept known as Direct Power Control.

Output of the inner current control loop may directly provide the switching signals to the bridge gates depending on the type of current modulation technique or current controller implemented in the system. Survey on different implementation of current controllers is performed in the section 5.4 below.

5.3.2 Outer Voltage Control Loop

The purpose of the outer voltage control loop is to control the output voltage and thereby balance the power flow of the active rectifier [50]. Usually it designed with slow dynamics aiming system stability. Referring back to the Figure 5-4, it is illustrated that the voltage control loop gets its reference from the outermost power loops while it generates the references to the innermost current loop.

5.4 Controllers

In the AR control scheme there are several controllers in operation for current, voltage and active and reactive powers control in separation. Under this section, the emphasis is given to the options for controllers for tracking the references. The analysis briefly presents each of their significances and drawbacks thereby a deduction is made in the choice of controller for the AR implementation.

5.4.1 Linear PI Controller

Linear PI controller is an established reference tracking technique associated with the d - q control structure due their satisfactory combinational performance. Equation Eq. 5:2 states the transfer function on the d - q coordinate structure.

Eq. 5:2

$$G_{PI}^{(dq)}(s) = \begin{bmatrix} K_p + \frac{K_i}{s} & 0 \\ 0 & K_p + \frac{K_i}{s} \end{bmatrix}$$

Harmonic compensation of such controllers is based on the low pass and high pass filters as stated in the [70] and it is worth to note that the complexity of harmonic compensation is considerably high with respect to the PR controllers.

5.4.2 PR Controller

Classical PI controllers are prone for a number of drawbacks, mainly the aforementioned steady state error in the stationary reference frame control and the need of decoupling the phase dependency. Despite the avoidance of the above drawback in the stationary reference frame control structure, performance of multiple reference frame transformation is found to be difficult with the low-cost, fixed-point digital signal processors (DSP) [63].

Proportional-Resonant (PR) Controller is an alternative reference tracking control technique which inherently eliminates the steady state error in the stationary reference frame control scheme. As a result the computation burden in the DSP is alleviated while offering similar frequency response to that of a PI controller.

Below equation provides the transfer function of PR controller in the abc reference frame. It is seen that it gives a similar shape to the Eq. 5:2 with off-diagonal terms being zero.

Eq. 5:3

$$G_{PR}^{(abc)}(s) = \begin{bmatrix} K_p + \frac{K_i}{s} & 0 & 0 \\ 0 & K_p + \frac{K_i}{s} & 0 \\ 0 & 0 & K_p + \frac{K_i}{s} \end{bmatrix}$$

Further to that, PR controller offers selective harmonic elimination feature [5], [64] , [61] therefore provide better performance in terms of power quality enhancement.

5.4.3 Hysteresis Controller

Hysteresis controllers are mainly used for controlling of current mainly due to the following advantages over the foregoing controllers;

1. Simplicity of implementation
2. Faster control loops
3. Negligence of load parameters for controller design

This type of controllers derives the bridge inverter switching signals by calculating the error by comparing the reference and actual current values. The error is then compared through a hysteresis comparator to generate the switching signals.

The main drawback of this scheme is that the switching frequency may vary widely during the fundamental period, resulting in irregular inverter operation [71].

After weighing off the prevalence, performance and ease of design, PI control scheme was chosen and implemented under the scope of the master thesis.

5.5 Decoupling Control of d and q Components

As the foregoing discussion on the controllers, a decoupled pair of active current (I_d) and reactive current (I_q) is essential in effective and independent current regulation for SRF control. However, due to the filter inductance, cross-coupled terms of d , q components are found in the mathematical derivations. In the same time, the dependency of control parameters on the grid voltage is also identified.

Fundamentally two different approaches are proven for decoupling of the components known as;

1. Feed-forward approach
2. Feedback approach

Based on [52], [72], [73], [74] and [75], it can be concluded that in the feed-forward method, value of the line inductance is not necessary to be known when the line resistance is taking negligible values. This is an advantage of the feed-forward method over the feedback method. However, a slightly higher oscillatory behaviour is the trade-off of feed-forward approach which needs to be addressed in the tuning process of the control loops.

Under the master thesis, due to its proven performance, the feed-forward method is adopted for decouple of d, q components.

5.5.1 Decoupling Control of PI Current Controller

To analyse the presence of crossed-coupling and the feed-forward techniques for decoupling d and q terms, the schematic of the LCL filter of the active rectifier is disclosed in the Figure 5-7.

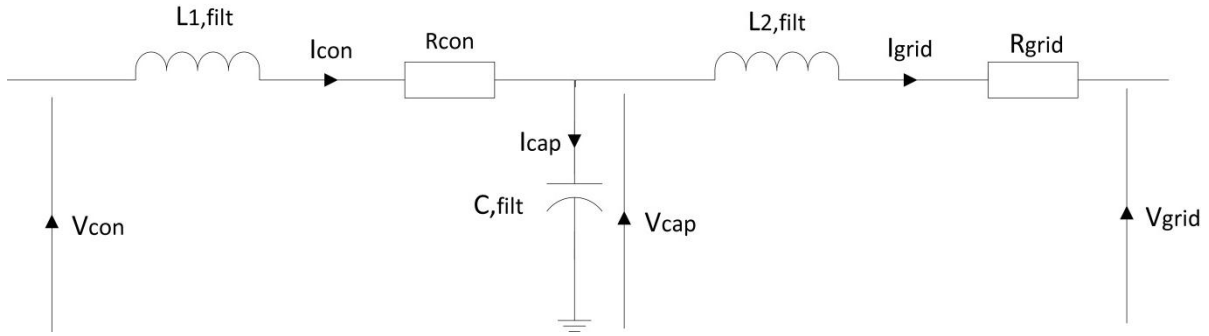


Figure 5-7: LCL filter of the grid side of the active rectifier

Based on [52] and [76], following expressions can be derived for the filter from the first principles;

Eq. 5:4

$$L_{1,filter} \cdot \frac{di_{con}}{dt} = V_{con} - V_{cap} - R_{con} \cdot I_{con}$$

$$L_{2,filter} \cdot \frac{di_{grid}}{dt} = V_{cap} - V_{grid} - R_{grid} \cdot I_{grid}$$

In the steady state, the voltage and current vectors rotate at the same speed, ω_{syn} , the synchronous speed. Taking that into account and transforming the above expressions from natural frame to dq SRF, following expressions can be obtained;

Eq. 5:5

$$L_{1,filter} \cdot \frac{dI_{con,d}}{dt} = V_{con,d} - V_{cap,d} - R_{con} \cdot I_{con,d} + \omega_{syn} \cdot L_{1,filter} \cdot I_{con,q}$$

Eq. 5:6

$$L_{1,filtr} \cdot \frac{dI_{con,q}}{dt} = V_{con,q} - V_{cap,q} - R_{con} \cdot I_{con,q} - \omega_{syn} \cdot L_{1,filtr} \cdot I_{con,d}$$

Eq. 5:7

$$L_{2,filtr} \cdot \frac{dI_{grid,d}}{dt} = V_{cap,d} - V_{grid,d} - R_{grid} \cdot I_{grid,d} + \omega_{syn} \cdot L_{2,filtr} \cdot I_{grid,q}$$

Eq. 5:8

$$L_{2,filtr} \cdot \frac{dI_{grid,q}}{dt} = V_{cap,q} - V_{grid,q} - R_{grid} \cdot I_{grid,q} - \omega_{syn} \cdot L_{2,filtr} \cdot I_{grid,d}$$

Eq. 5:9

$$C_{filtr} \cdot \frac{dV_{cap,d}}{dt} = I_{grid,d} - I_{con,d} + \omega_{syn} \cdot C_{filtr} \cdot V_{cap,q}$$

Eq. 5:10

$$C_{filtr} \cdot \frac{dV_{cap,q}}{dt} = I_{grid,q} - I_{con,q} + \omega_{syn} \cdot C_{filtr} \cdot V_{cap,d}$$

Careful observation of Eq. 5:5 and Eq. 5:6 shows the fact that d and q components are cross-coupled in each expression. Further to that, the expressions bare an undesirable dependency on the filter capacitor voltage components.

The cross-coupling terms can be eliminated using the feed-forward compensation collecting all feed-forward terms into newly defined single term as shown as follows;

Eq. 5:11

$$\text{Let } V_{ff,d} = V_{cap,d} - \omega_{syn} \cdot L_{1,filtr} \cdot I_{con,q} \quad \& \quad V_{ff,q} = V_{cap,q} + \omega_{syn} \cdot L_{1,filtr} \cdot I_{con,d}$$

Eq. 5:12

$$\begin{aligned} \text{Then } V_{con,d} &= R_{con} \cdot I_{con,d} + L_{1,filtr} \cdot \frac{dI_{con,d}}{dt} + V_{ff,d} \\ \& \quad V_{con,q} &= R_{con} \cdot I_{con,q} + L_{1,filtr} \cdot \frac{dI_{con,q}}{dt} + V_{ff,q} \end{aligned}$$

Now the feed-forward compensation has removed the cross-coupled terms in SRF control structure. Transforming the system into the per-unit values based on the Appendix A: Definition of per-unit system, the inner current controller can be designed on the following plant transfer function and structure.

Eq. 5:13

$$h(s) = \frac{1}{\left(r_{con} + s \cdot \frac{l_{1,filtr}}{\omega_b}\right)} = \frac{\frac{1}{r_{con}}}{1 + T_{con} \cdot s}$$

$$\text{where } T_{con} = \frac{l_{1,filtr}}{\omega_b \cdot r_{con}} = \frac{L_{1,filtr}}{R_{con}}$$

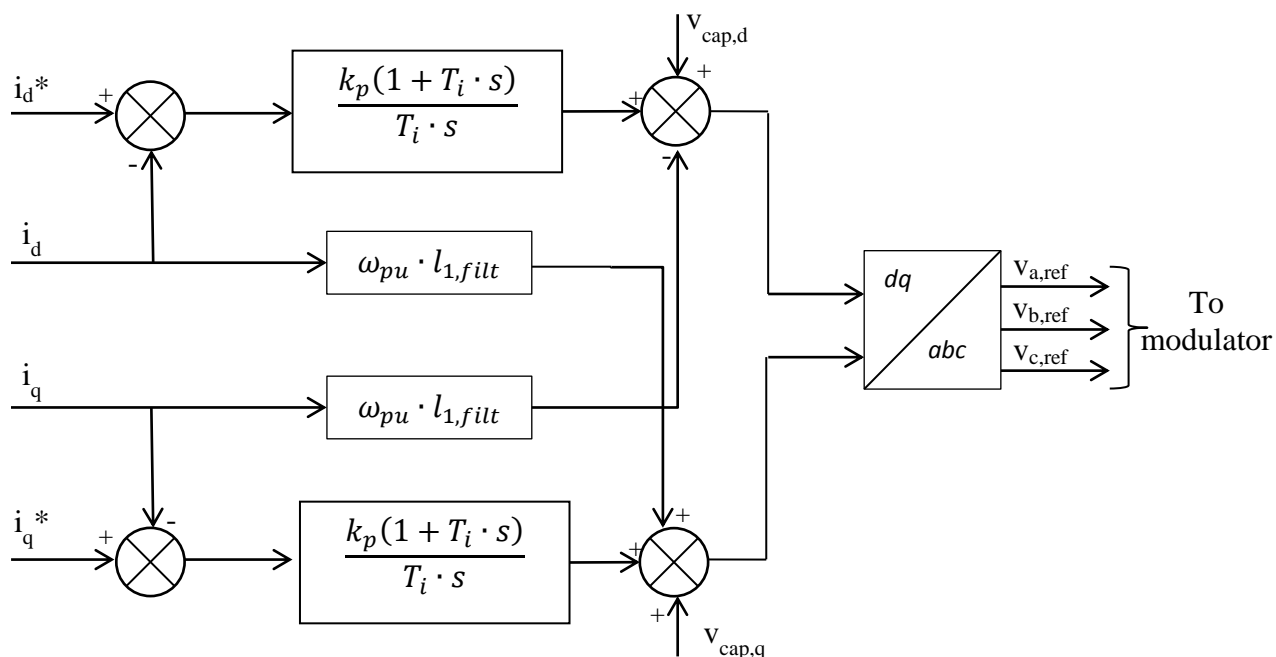


Figure 5-8: Feed-forward compensation in SRF for the PI current controller

5.5.2 Decoupling Control of PI Voltage Controller

With reference to the Figure 5-7, following relationship can be expressed in the stationary reference frame.

Eq. 5:14

$$I_{con} = C_{filt} \frac{dV_{cap,\alpha}}{dt} = I_{con} - I_{grid}$$

Taking per-unit system into effect, above equation (written for 3 phases) can be transformed into *dq*-frame and expressed as follows;

Eq. 5:15

$$i_{con,d} - i_{grid,d} = \frac{c_{filt}}{\omega_b} \frac{dv_{cap,d}}{dt} - \omega_{pu} \cdot c_{cap} \cdot v_{cap,q}$$

$$i_{con,q} - i_{grid,q} = \frac{c_{filt}}{\omega_b} \frac{dv_{cap,q}}{dt} - \omega_{pu} \cdot c_{cap} \cdot v_{cap,d}$$

Above equations show a similar problem of cross-coupling as it was experienced in Eq. 5:5 and Eq. 5:6 in the process of designing the current controller.

Using a similar approach of de-coupling as previous, following expressions can be derived for the output of the PI voltage control loop;

$$i_{con,d}^* = \underbrace{i_{grid,d}}_{\text{Feed-forward}} - \underbrace{\omega_{pu} c_{filt} v_{cap,q}}_{\text{de-coupling}} + \underbrace{i_{d,PI}}_{\text{PI - output}}$$

$$i_{con,q}^* = \underbrace{i_{grid,q}}_{\text{Feed-forward}} + \underbrace{\omega_{pu} c_{filt} v_{cap,d}}_{\text{de-coupling}} + \underbrace{i_{q,PI}}_{\text{PI - output}}$$

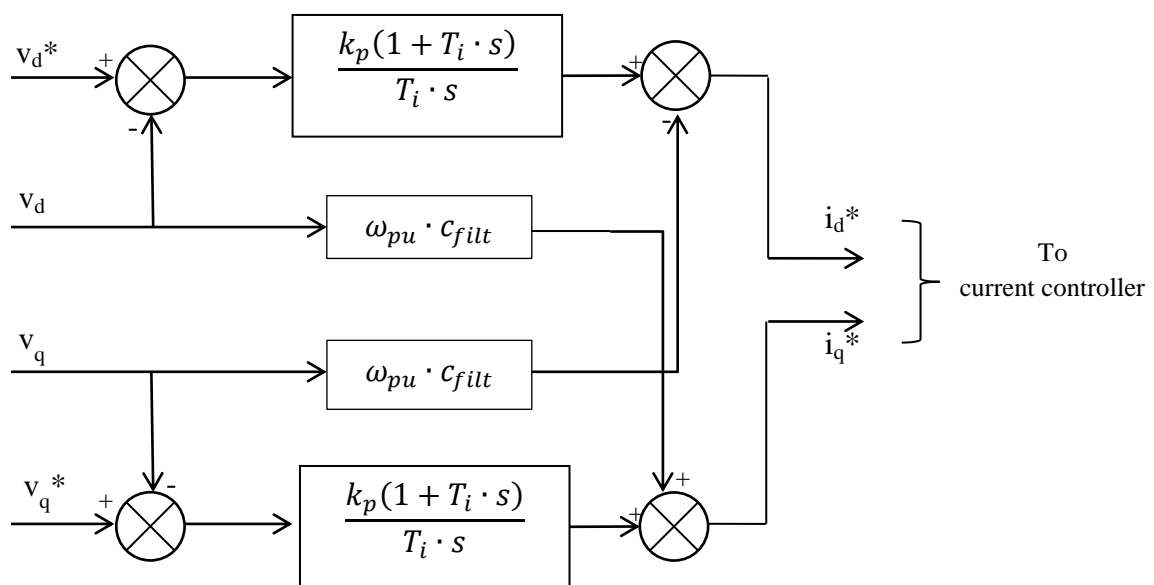


Figure 5-9: Feed-forward compensation in SRF for the PI voltage controller

5.6 P-Q vs. VSI Control

For the reasons described in the introduction, micro sources need to be interfaced through active rectifiers. There are mainly two types of active rectifier control models proposed in [13] and [14]. They will be discussed in this section.

1. PQ Model

The philosophy of control of this model is based on active power (P) and reactive power (Q) values hence it is known as PQ model. This model, however, requires external voltage and frequency references hence having SGs in the network is essential for PQ model utilization. This gives rise to the fact that PQ model is not possible for island operation.

As [13] describes, PQ inverter control corresponds to a combined control of both inverter and primary energy source, when this becomes physically possible. This means that the inverter only injects into the grid the power available at its input. The reactive power injected corresponds to a pre-set value defined locally or from the Micro Grid Central Control (MGCC). The P and Q control of an inverter can be performed using a current control technique: the inverter current is controlled in amplitude and phase to meet the desired set-points of active and reactive power.

2. VSI Model

A classical voltage source inverter (VSI) with special control strategies are used to model a VSI type active rectifier model. In this case, the inverter will emulate the behaviour of a synchronous generator in terms of load sharing. Frequency and voltage of the active rectifier will be controlled by droop control techniques.

When VSI connected to the stiff network, reference values for P and Q will be obtained from the stiff grid.

Complete modelling of VSI is well explained in [11].

In conclusion, it must be stated that under the master thesis, VSI model is chosen mainly because PQ model does not support island operation. However, there is also space to adopt a hybrid system with a mix of communication and droop control. Power, voltage and frequency reference values may be communicated through low bandwidth communication channels whereas load control can be performed locally to act upon fast transients.

5.7 Droop Control

Classical and novel droop control techniques have been discussed under the UPS chapter section 3.3.2.

A classical droop control technique for active power sharing has been employed in the master thesis. Direct control of reactive power has been proposed for future scope of work.

5.8 Phase-Locked Loop

Phase-Locked Loop (PLL) has been a well-established technique to extract the phase angel from grid voltages [77]. The main purpose of the PLL in this circumstance is to track the grid voltage frequency and filter out noise and short term disturbances without introducing a phase lag [52]. PLL is mainly used at the event of grid synchronization where the phase of the inverter output voltage must be in-phase with the grid voltage phase. However, there are other novel techniques like dual second order generalized integrator (DSOGI) based approaches for grid synchronization which can be found in [66] and [78].

In the master thesis, the synchronous reference frame (SRF) PLL has been chosen to achieve the above purpose as it has been the most widely accepted method [77], [79].

Figure 5-10 illustrates the general structure of a synchronous reference frame PLL. The grid voltage vectors which are in the natural $a-b-c$ frame are transformed in the $d-q$ frame. Then the d, q quantities are filtered and from which the angle between them is calculated using the inverse tangent ($\arctan2$) function.

Phase angle error (ϑ_{error}) is then treated through a PI controller. Nominal frequency (f_n) has been the feed-forward term in the structure to make the frequency tracking more precise and faster [79]. A pure integrator functions as the voltage controlled oscillator (VCO) to calculate the estimated phase (ϑ^{est}) from the frequency.

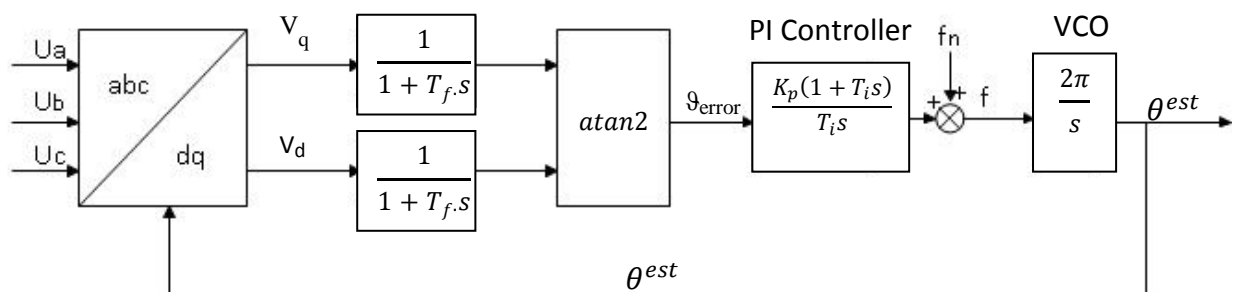


Figure 5-10: General structure of SRF PLL

In the ideal case, the orientation of the d -axis must align with the grid voltage vector. Any deviation between the orientation of SRF d -axis and the phase angle of the instantaneous voltage vector results in a non-zero V_q component and non-zero ϑ_{error} . Hence, the PLL will attempt to keep the V_q component zero and thereby ϑ_{error} zero by adjusting the calculated grid frequency. Eventually, the PLL will be in lock when the estimated frequency is equal to the phase angle of the grid voltage vector.

5.9 Summary of Chapter

Different control strategies inspired by modern UPS systems have been reviewed, compared and have chosen the strategy that suits the thesis giving valid reasons.

SRF based multiple cascading control structure has been proposed for the active rectifier control. PI controllers and its essential decoupling techniques are also chosen over PR controllers and hysteresis controllers. The thesis work will follow VSI model over the PQ model due to the possibility of grid-tied and island modes of operation.

6 Modeling of Active Rectifier

The chosen control strategies for current, voltage and power control in the previous chapters have been modelled and implemented. This chapter presents the graphical performance analysis of each control module.

The modelling has been carried out adhering a module-by-module approach testing and optimizing one module at a time. The chapter discloses modelling and designing of the following system modules;

1. Phased-Lock Loop (PLL)
2. Inner Current Control Loop
3. Outer Voltage Control Loop
4. Virtual Synchronous Machine Module

The modelling and simulation was carried out in the Matlab/Simulink® environment in aid of SymPowerSystems® toolbox for electrical components. In the following explanation, all the time values are in seconds and other parameters will be in SI units if not stated otherwise.

6.1 Proposed Active Rectifier Model

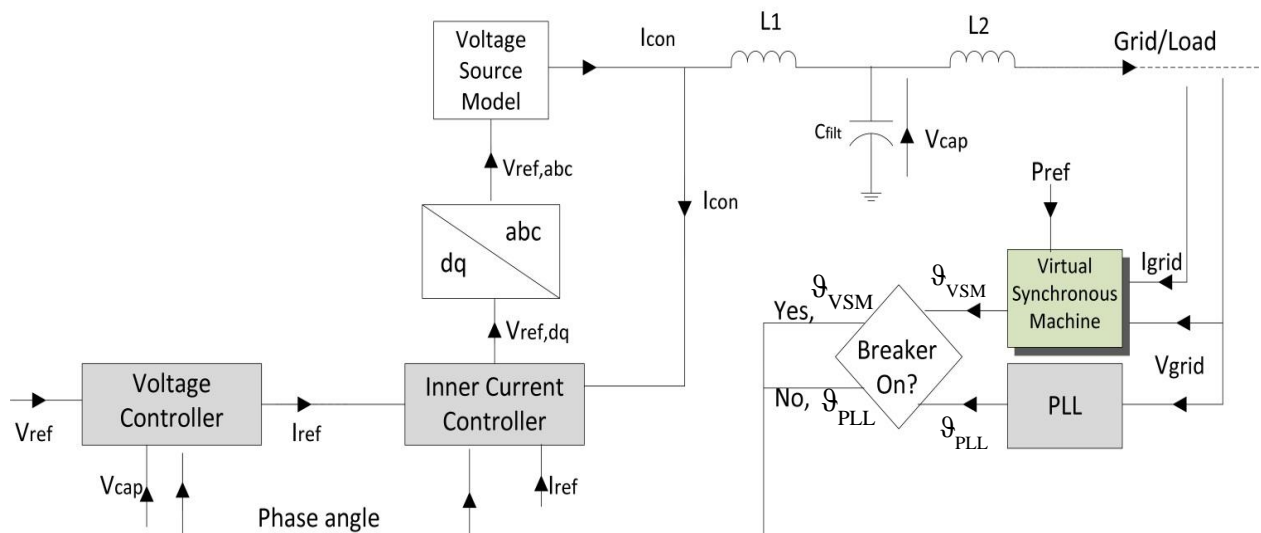


Figure 6-1: Proposed total system architecture with virtual synchronous machine model

The proposed control strategy for the active rectifier can be expressed as in the Figure 6-1. The figure bears resemblance of the Figure 5-4 to a greater extent. The structure is based on the SRF control scheme where d - q components in per-unit used for controllers.

The paramount addition of the proposed solution is the virtual synchronous machine (VSM) module. This module adds the virtual damping, virtual inertia and droop control properties for power controlling purposes.

The most significant simplification of the model is the usage of voltage source models instead of the power electronic inverter bridge. Avoidance of it enables to drop out the use of a modulation block. However, if hysteresis current control technique (section 5.4.3) were used, modulation block would have not come into play in the first place.

The output of the active rectifier is interfaced with an LCL filter to the stiff grid/local load. Adhering to the theoretical analysis in the previous chapter, the output current is the current passes through the first inductor (L_1) whereas the output voltage is measured across the filter capacitor (C_{filt}).

The performance of each major block is described in the following sections.

6.2 Phase-Locked Loop (PLL)

The PLL module has been developed based on the fundamentals and tuning explained in the section 5.8 and Appendix C: Tuning of control loops, despite the availability of a couple of PLL models in the SymPowerSystems® library. This extra effort was taken to have the full understanding and control of the PLL structure.

Figure 6-2 provides the PLL mask and its internal structure. And also to verify its functionality, a step change of the grid frequency has been simulated to observe the behaviour of the PLL output (Figure 6 1 (c)). It was observed from the plot given in Figure 6-3, with PLL frequency satisfactorily follows the grid frequency with an acceptable rise time and overshoot.

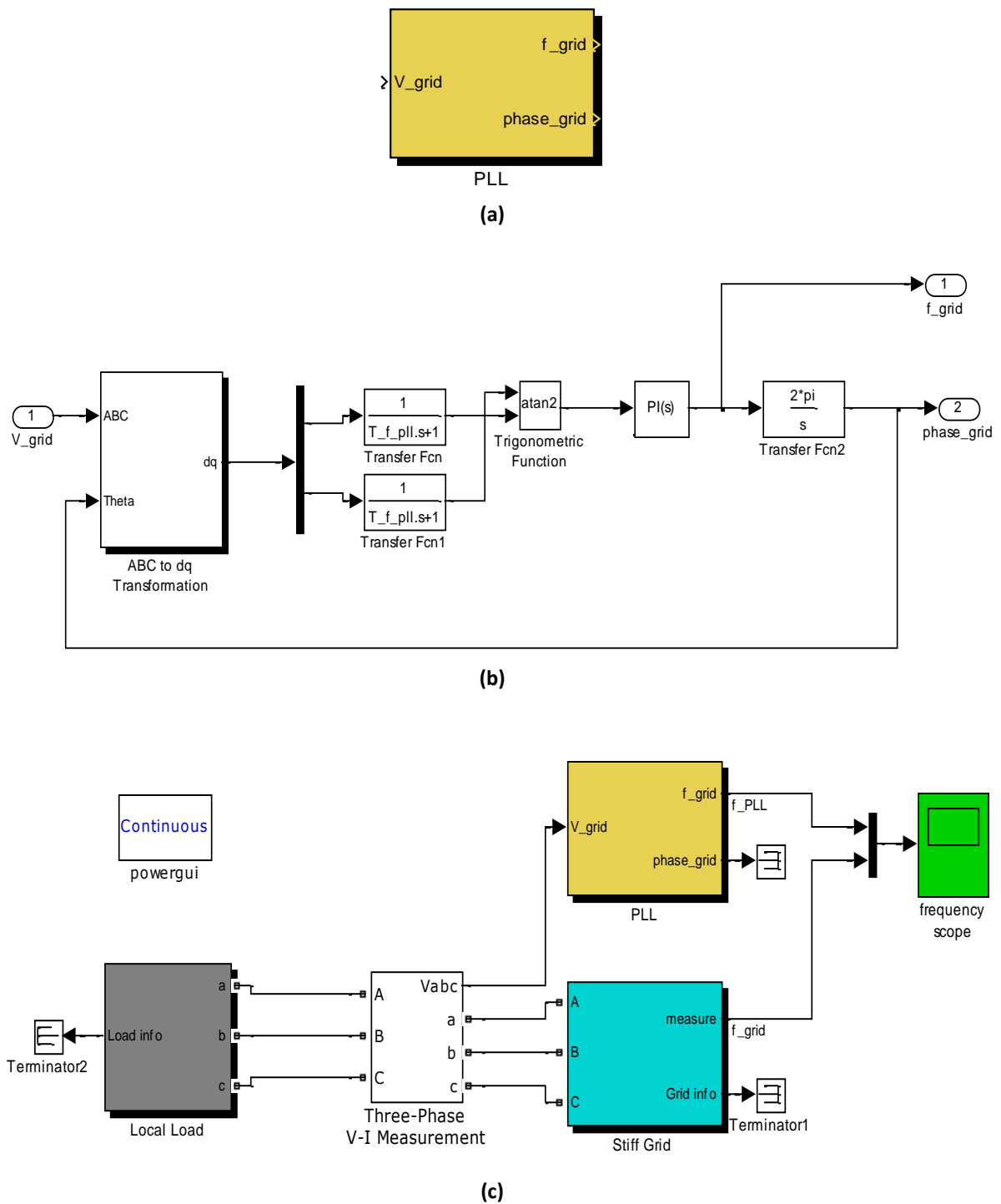


Figure 6-2: PLL (a) model mask (b) internal structure (c) simulation against a frequency step change in the grid

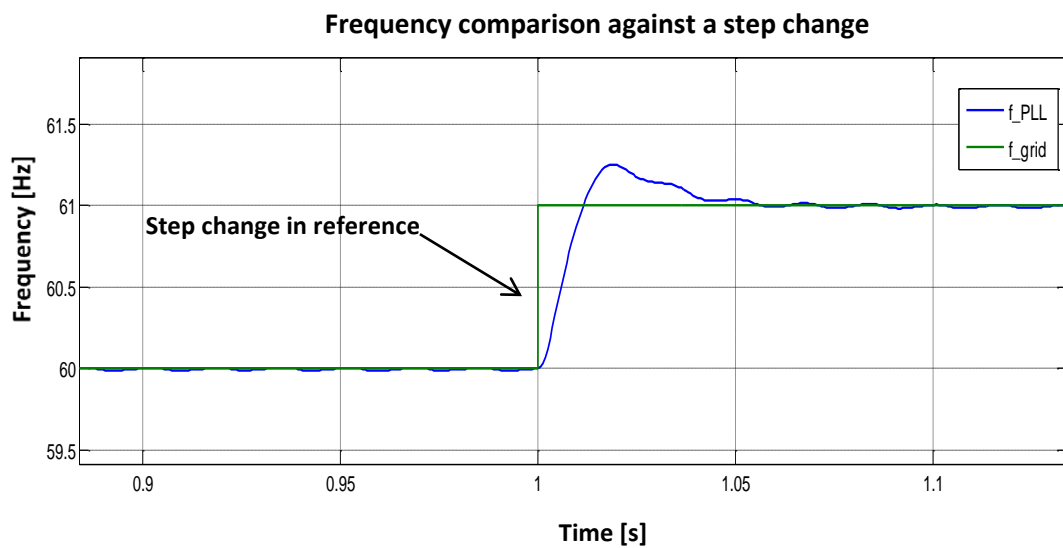


Figure 6-3: Frequency plot of PLL against a step change in grid frequency

The Figure 6-3 shows the functionality of the modelled SRF PLL. The purpose of the PLL is to extract the grid frequency from the grid voltage. The figure shows how the output frequency from the PLL quickly follows the grid frequency which is its reference, upon a step change. The overshoot and time for steady state are controllable parameters with appropriate tuning procedures.

6.3 Inner Current Control Loop

Inner current controller functionality upon a step reference change is demonstrated in the Figure 6-5. Both I_d and I_q show satisfactory response to the step change in the reference at times 2 s and 4 s respectively.

The tuning of the control loop has been executed in accordance with the modulus optimum criteria based on [80] and [81]. The details are found in the Appendix C: Tuning of control loops.

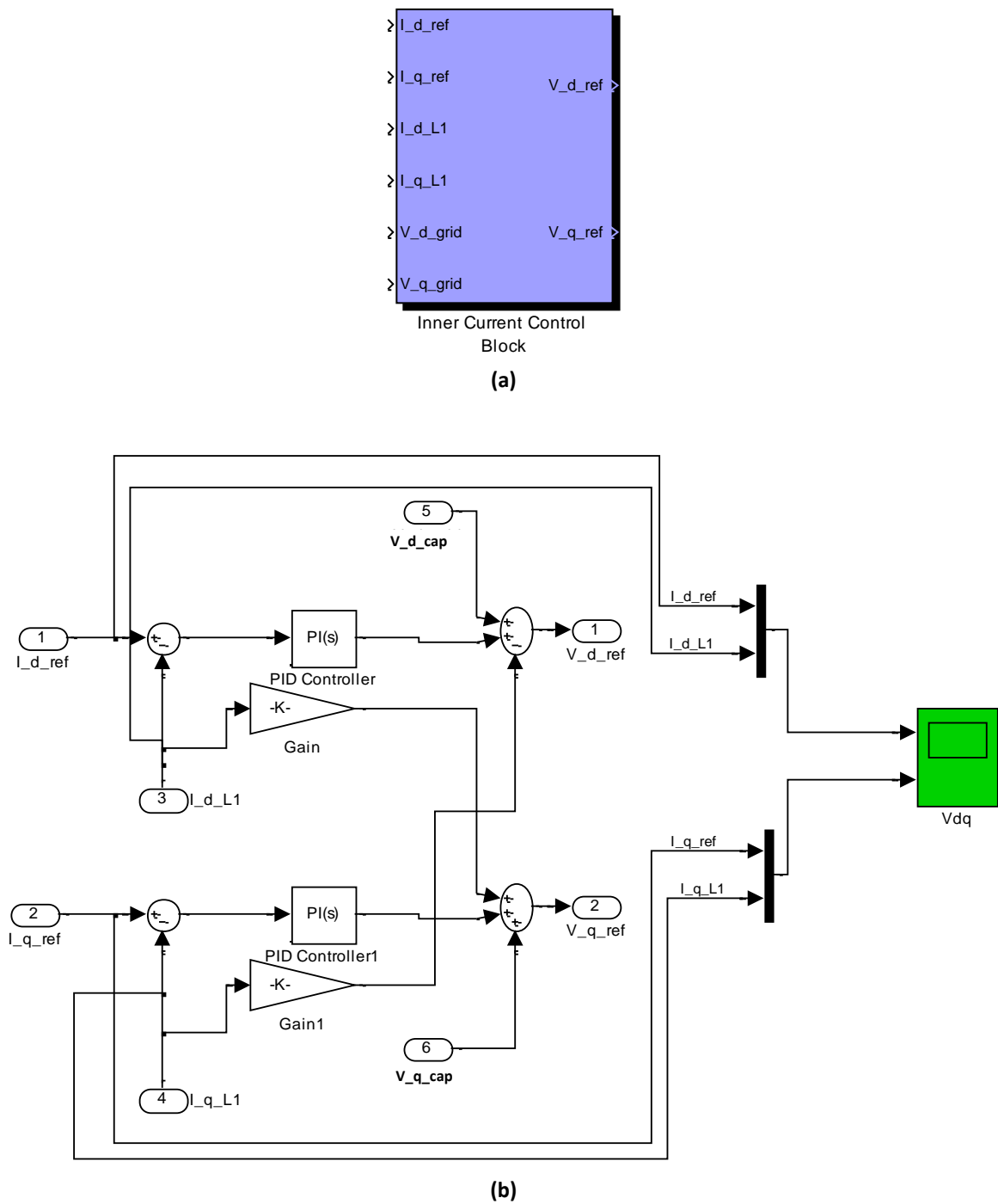


Figure 6-4: Inner Current Controller (a) mask (b) internal structure

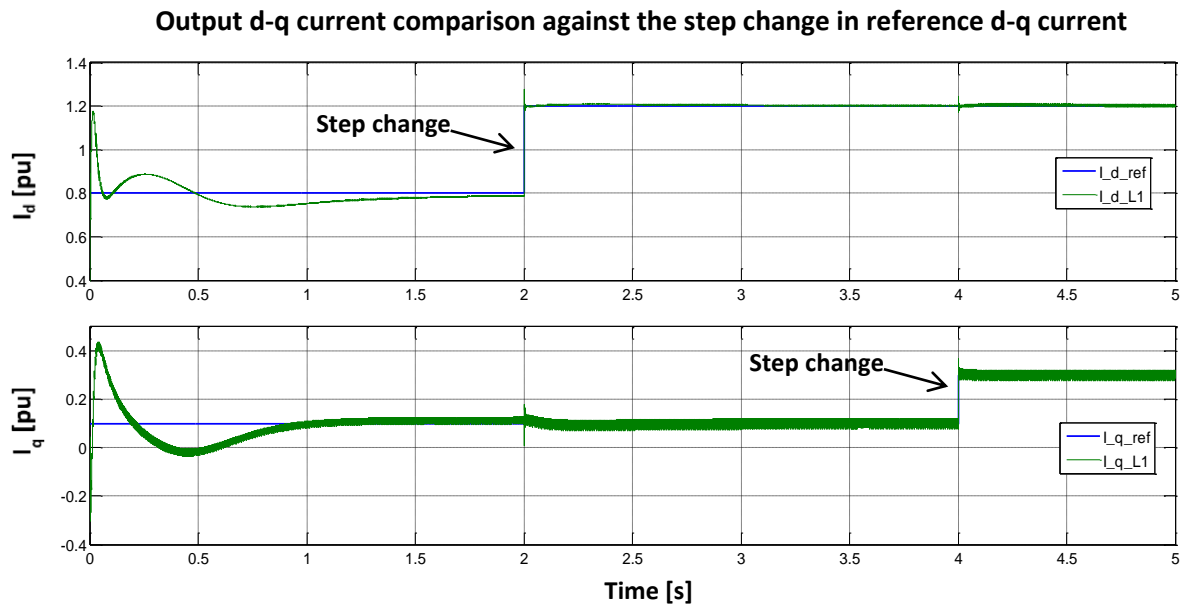


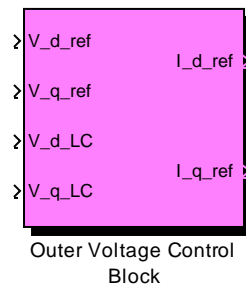
Figure 6-5: Inner current controller output d-q current plot against step changes in I_d and I_q reference currents at $t = 2$ and $t = 4$ respectively

6.4 Outer Voltage Control Loop

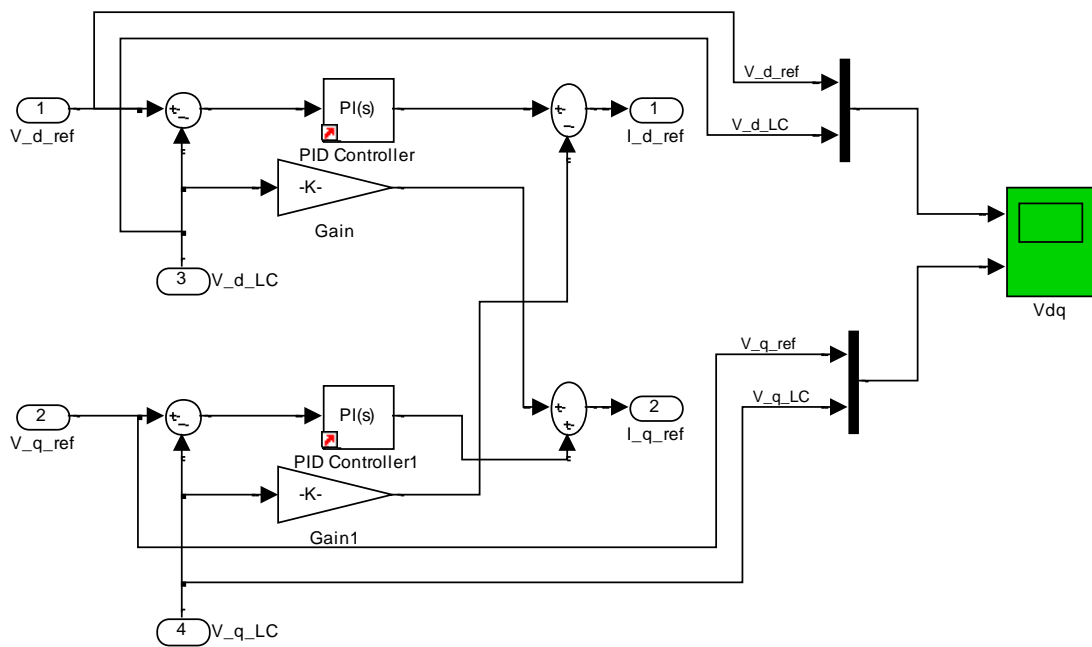
Outer voltage controller block performance upon a step reference change is demonstrated in the Figure 6-6. Both I_d and I_q show satisfactory response to the step change in the reference at times 2 s and 4 s respectively.

In spite of decoupling the cross-coupled effects of d - q terms against each other, short term oscillations could be noticed in each graph due to the step change of the other. This could be due to the feed-forwarding of grid voltage which may contain noise. On the other hand, feed-forwarding has been found to be inherently more oscillation-prone as described in the section 5.5. However, this also suggests the model has more space for tuning optimization.

The tuning of the control loop has been executed in accordance with the symmetric optimum criteria based on [81] and [82]. The details are found in the Appendix C: Tuning of control loops



(a)



(b)

Figure 6-6: Outer voltage controller (a) mask (b) internal structure

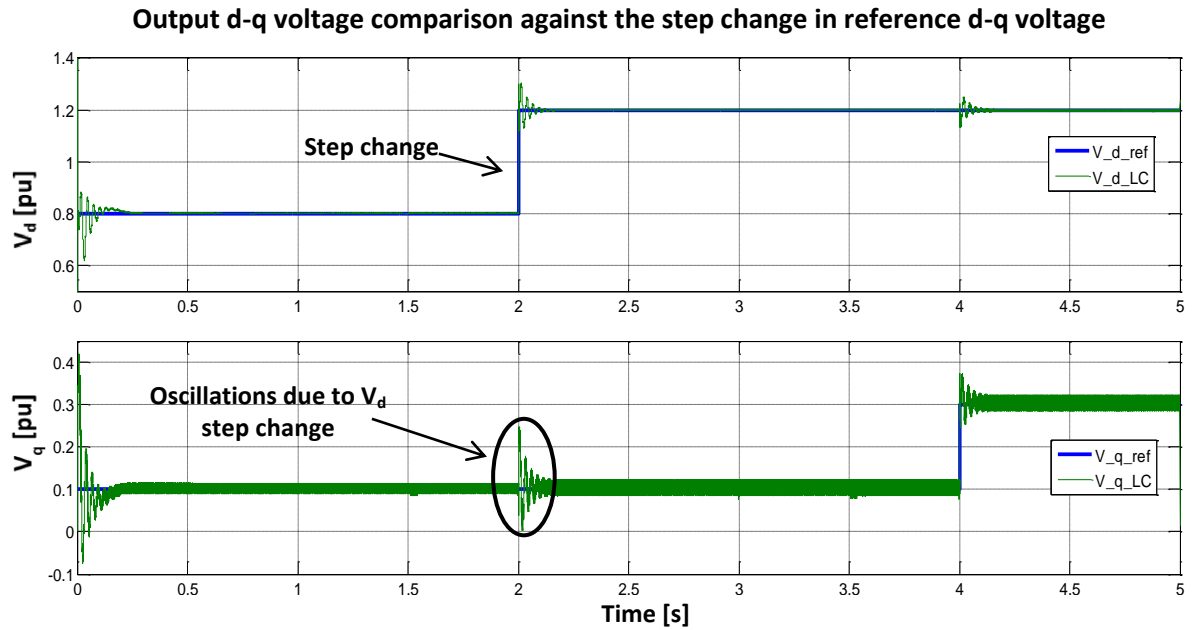


Figure 6-7: Outer voltage controller output d-q current plot against step changes in V_d and V_q reference currents at $t = 2$ and $t = 4$ respectively

6.5 Virtual Synchronous Machine Model

The virtual synchronous machine (VSM) model has been developed based on the swing equation given in Eq. 4:1. This module, shown in the Figure 6-8, calculates the swing equation-based phase angle for the other control modules. Based on the swing equation, following deduction can be expressed to elaborate how VSM module calculates the phase angle.

$$P_M - P_E - P_D = J \cdot \omega_{vsm} \frac{d\omega_{vsm}}{dt}$$

$$\int \frac{2(P_M - P_E - P_D)}{J} dt = \int 2 \omega_{vsm} \cdot \frac{d\omega_{vsm}}{dt} dt$$

$$RHS = \int 2 \omega_{vsm} \cdot \frac{d\omega_{vsm}}{dt} dt$$

Integrating by parts,

$$2 \int \omega_{vsm} \frac{d\omega_{vsm}}{dt} dt = \omega_{vsm}^2$$

therefore,

$$\frac{2}{J} \int (P_M - P_E - P_D) dt = \omega_{vsm}^2$$

by further intergrating,

$$\int_{\omega_{PLL}} \sqrt{\omega_{vsm}^2} dt = \theta_{vsm}$$

The active power droop control has also been executed in this module based on the following relationship;

Eq. 6:1

$$P_m = P_{ref} + \frac{f_{ref} - f_{vsm}}{droop}$$

note: droop > 0

The virtual damping has been implemented based on the following relationship to replicate the round rotor (non-salient) synchronous machine behaviour;

Eq. 6:2

$$P_D = k_{damping}(\omega_{vsm} - \omega_{grid})$$

More detailed explanation has been presented in the master specialization project report [15].

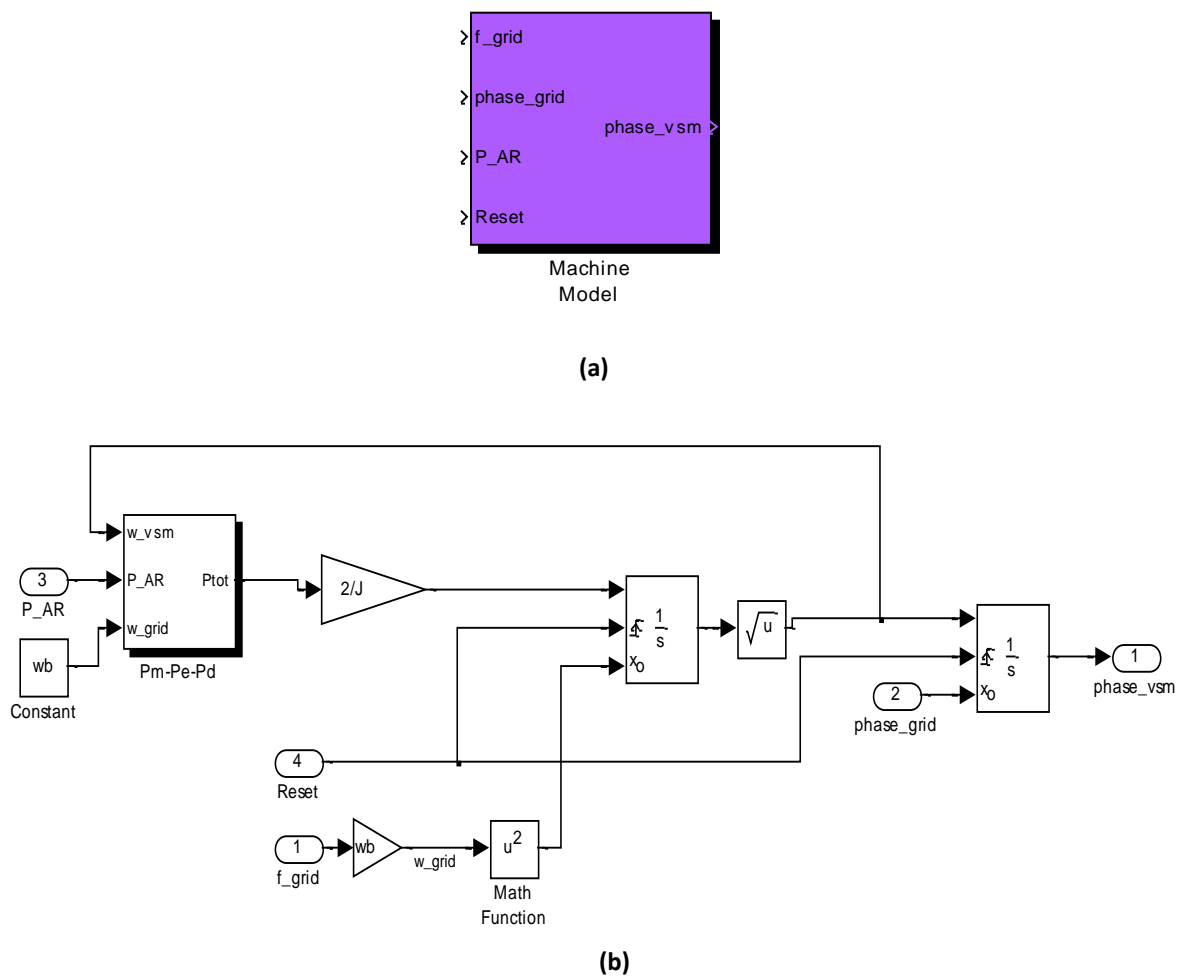


Figure 6-8: Virtual synchronous machine model (a) mask (b) internal structure with mechanical dynamics

6.6 Active Rectifier Simulation Model

The modules discussed so far and some other auxiliary blocks have been put together to create the complete active rectifier model. Figure 6-1 in section 6.1 provides an outlook of the total model. The internal simulation schematic is found in the Figure 6-9.

The main challenge encountered in this phase of modelling was the vulnerability for failure. As a result, the expansion of the system was narrowed down and some of the control loops like reactive power control and virtual impedance feedback loop control could not be implemented. The challenge was found to be lying in the tuning procedures which require advance and demanding techniques which were out of the initial scope of the thesis.

The fragility of the system has been largely reduced by resetting the continuous time-integrators in the VSM module at every breaker switching on event which allows the synchronism.

The active rectifier with the LCL filter and breaker connected to a local load in a micro grid is shown in the Figure 6-10. The micro grid is connected to a stiff grid in the figure which can be tripped for island operation.

The default settings of the active rectifier and LCL filter are given in the Table 2 (notation is based on Figure 5-7). The values are approximated to real system values obtained from the industry.

Table 2: Default values for LCL filter parameters

| Filter Parameters | SI unit | Per unit |
|--------------------------|-------------------|-----------------|
| $L_{1, \text{filt}}$ | 57 μH | 0.8e-1 pu |
| R_{con} | 0.7 m Ω | 0.285e-2 pu |
| C_{filt} | 800 μC | 0.74e-1 pu |
| R_{cap} | 0.2 m Ω | 0.8e-3 pu |
| $L_{2, \text{filt}}$ | 57 μH | 0.8e-1 pu |
| R_{grid} | 0.7 m Ω | 0.285e-2 pu |

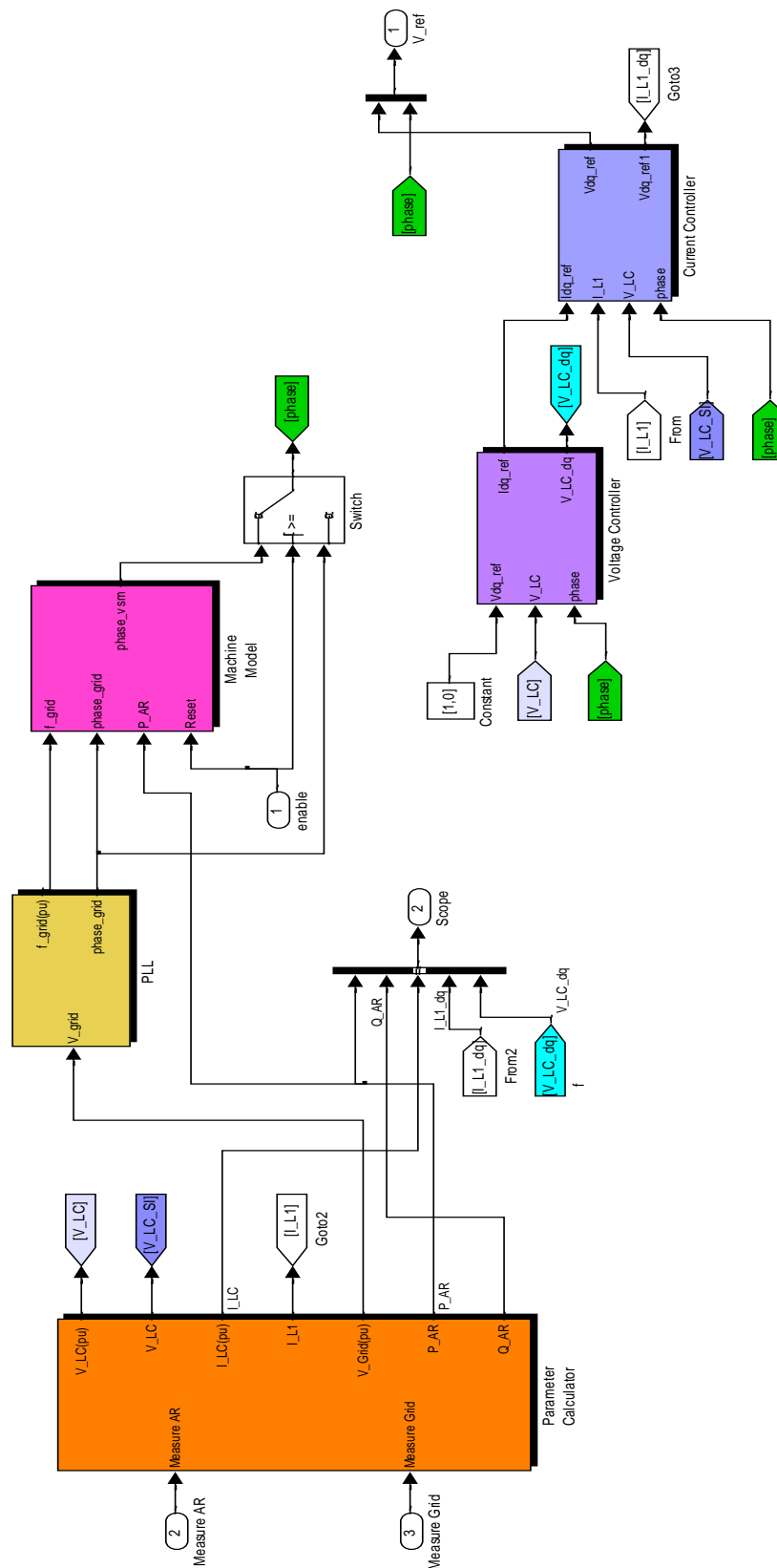


Figure 6-9: Integrated architecture of PLL, inner current controller, outer voltage controller and machine model

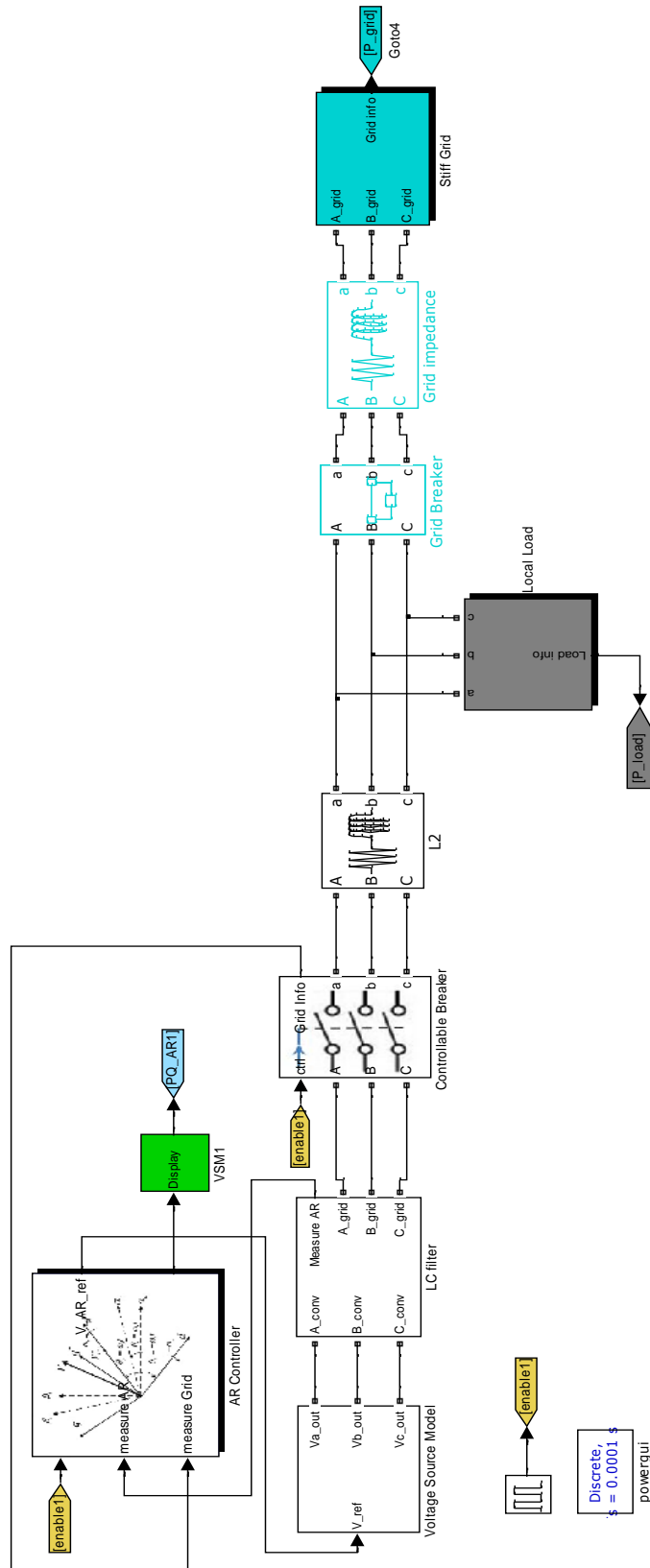


Figure 6-10: Active rectifier connected along with the LCL filter and controllable breaker to a local load and stiff grid

6.7 Summary of Chapter

Based on the theoretical review in chapter 5, the PLL, inner current controller, outer voltage controller and the machine model have been modelled. Each model has been tested and verified individually.

Subsequently, by integrating the modules, the total system for VSM-base active rectifier prototype has been developed. The LCL filter has also been developed based on closely approximated values in real life micro grid.

7 Simulation Results & Discussion

The modelled active rectifier along with the LCL filter has been simulated for different cases and discussed the performance in this chapter. The simulation cases can be categorized as given below;

1. Active rectifier – Stand-alone operation
 - a. In grid-tied mode
 - b. In Island mode
 - c. For different scenarios as such as
 - i. virtual inertia response variations
 - ii. virtual damping co-efficient variations
 - iii. step change in load
2. Active rectifier – Parallel operation
 - a. In grid-tied mode
 - b. In Island mode
 - c. For different scenarios as such as
 - i. Step change in load
 - ii. Paralleling of multiple units

In a general note, in every simulation case, the active rectifier (AR) is enabled at least after 0.2 s dead time from the simulation initialization. This is to avoid the high level of overshoot (approximately 1.5 pu at rated voltage) that occur in the output current if the AR is enabled immediately. The overshoot has been improved vastly by varying the tuning parameters. However, the dead time has been still implemented to avoid an undesired tripping event due to the high initial current which might have otherwise resulted in considerable power excursions during this critical 0.2 s period.

As section 5.2 explains, the reactive power control has not been enabled by making reference voltage for q -component of SRF structure (V_q) making zero. Reactive power control has been indirectly executed with the output voltage control. As a result, quite acceptable reactive power regulation can be observed in the simulation graphs.

In the discussion the system comprised of active rectifier(s), LCL filter(s) and local load(s) has been known as the micro grid. The controllers in the AR have been modelled in the per-unit whereas all the times indicated in the graph are in seconds.

7.1 Single Active Rectifier Simulation

The active rectifier model in stand-alone operation has been demonstrated in this section. The default parameter values are tabulated below.

Table 3: Default values for active rectifier and system parameters

| System Parameters | SI Unit |
|------------------------------------|-------------------------|
| Voltage (phase to phase, rms) | 690 V |
| Current (phase) | 2300 A |
| Nominal frequency | 60 Hz |
| Active Rectifier Parameters | |
| Reference Power | 2e6 W |
| Virtual inertia | 50 kg·m ² |
| Virtual damping co-efficient | 8e5 N·s·m ⁻¹ |
| Load Parameters | |
| Active power demand | 1e6 W |
| Reactive power demand | + 100 var |

7.1.1 Grid-tied Mode

Here, a single active rectifier (AR) has been simulated when it is connected to the stiff grid (Figure 7-1). Stiff grid can be thought of as an ocean of power which has enormous resilience in terms of stability. Here, the AR has output its full reference active power of 2 MW of which only 1 MW is consumed by the load. The balance power is consumed by the stiff grid.

It has taken approximately 0.1 s for the AR to provide full load from no-load state. It is observed that power consumption of the stiff grid follows almost the mirror image of the AR power supply curve. This implies the fact that stiff grid adds a 'power cushion' to a micro grid and absorbs the transients which in return adds stability to the micro grid.

7.1.2 Island Mode

Here, the AR has been run in grid-tied mode for 0.4 s and subsequently the stiff grid has been tripped off and then tripped off from the micro grid to island the micro grid at 0.6 s. The

Figure 7-2 shows the active and reactive power transients.

When the micro grid has been islanded at 0.6 s, the stiff grid has not been there anymore to consume the additional power output from the AR. As a result, the output power of AR has been dropped to 1 MW that is precisely sufficient to source the local power demand.

It is also evident the stiff control of active power mainly because of the virtual synchronous machine-based control directly acts upon the active power control coupled with the swing equation and phase angle deduction based on the swing equation (refer section 6.5). On the other hand, at the tripping event, reactive power of AR and a result of the stiff grid have shown an abrupt spike but eventual steady state. The absence of active control of reactive power can be thought as the reason for such undesirable spikes in the reactive power figures.

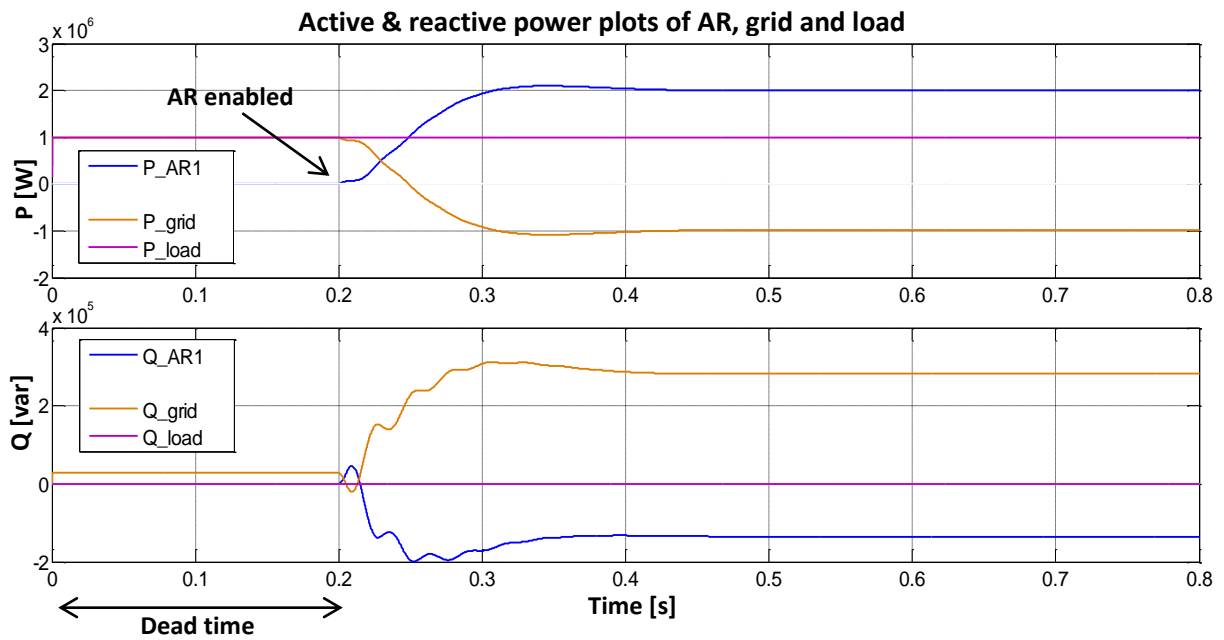


Figure 7-1: Active and reactive power plots of AR, grid and load in grid-tied mode. AR is connected to the grid at $t = 0.2$ s

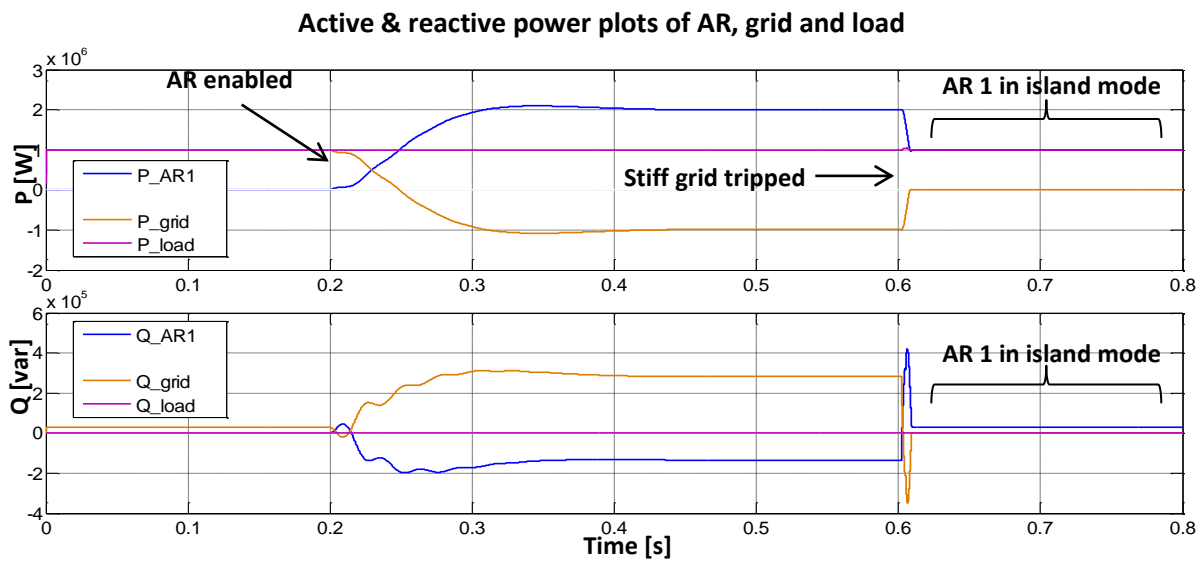


Figure 7-2: Active and reactive power plots of AR, grid and load in grid-tied and island modes. AR is connected to the grid at $t = 0.2$ s, stiff grid is tripped at $t = 0.6$ s

7.1.3 Simulation for different cases

1. Virtual inertia response variations

Active & reactive power plots on low and high virtual inertia values

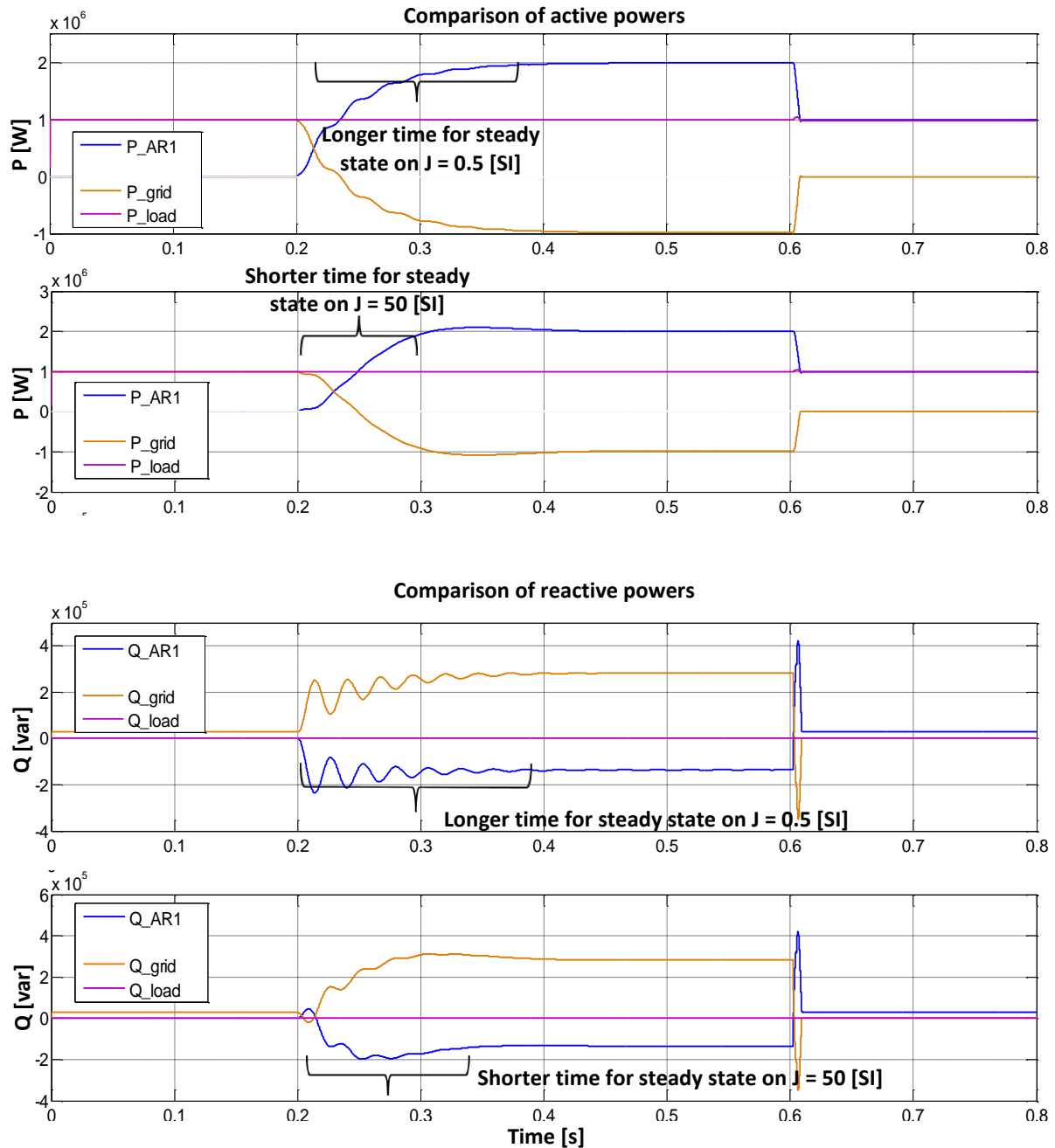


Figure 7-3: Comparison of active and reactive powers when virtual inertia, $J = 0.5$ [SI] and $J = 50$ [SI] respectively

Under this section, the essence of the impact of virtual inertia response is illustrated. In the Figure 7-3, two case one with different virtual inertia values have been compared and contrasted.

Looking at the top 2 graphs of the figure which presents the active power plots of each case, it is manifest that in the second plot, AR output power achieves faster steady state after the grid connection at 0.2 s. This is true to the reactive power curves in the bottom two graphs as well. This clearly indicates that the inertia value of the virtual synchronous machine can play a significant role in deciding how quickly the AR output power can achieve steady state upon a disturbance.

However, it is too early to infer that higher the inertia, faster the steady state. The Figure 7-4 provides evidence against that fact. The figure presents the AR output power variations upon the grid connection against different virtual inertia values. The inertia response seems to be optimal at $J=50$ [SI] which is not the highest value out of the compared values. The physical reason behind this observation is when J increases, the (virtual) kinetic energy increases in proportion. As a result, it may take a longer time for the (virtually) rotating system to come to rest or synchronism. When the J is too low, the system is prone for oscillations as seen in the plot with lower J values.

Therefore this plot gives a strong message that the inertia value demands an optimization and this optimality may differ from case to case. The beauty of the virtual synchronous machine concept is that optimization from case to case is quite possible unlike in a real machine where inertia response is based on the physical presence of rotating masses.

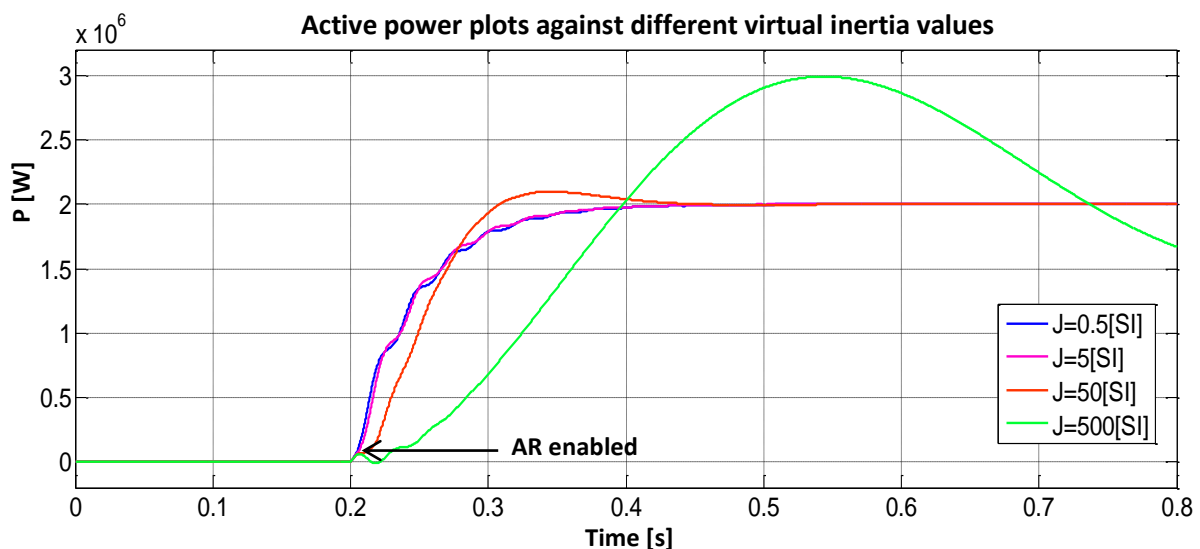


Figure 7-4: Active power steady state time variations against different virtual inertia values

2. Virtual damping co-efficient variations

Virtual damping co-efficient has been varied and simulated two cases to plot the graphs in the Figure 7-5. The changes of the damping co-efficient proportionately vary the damping power as given in Eq. 6:2. Again, it is clearly evident that the damping power is strongly influential in achieving synchronism.

Active & reactive power plots on low and high virtual damping values

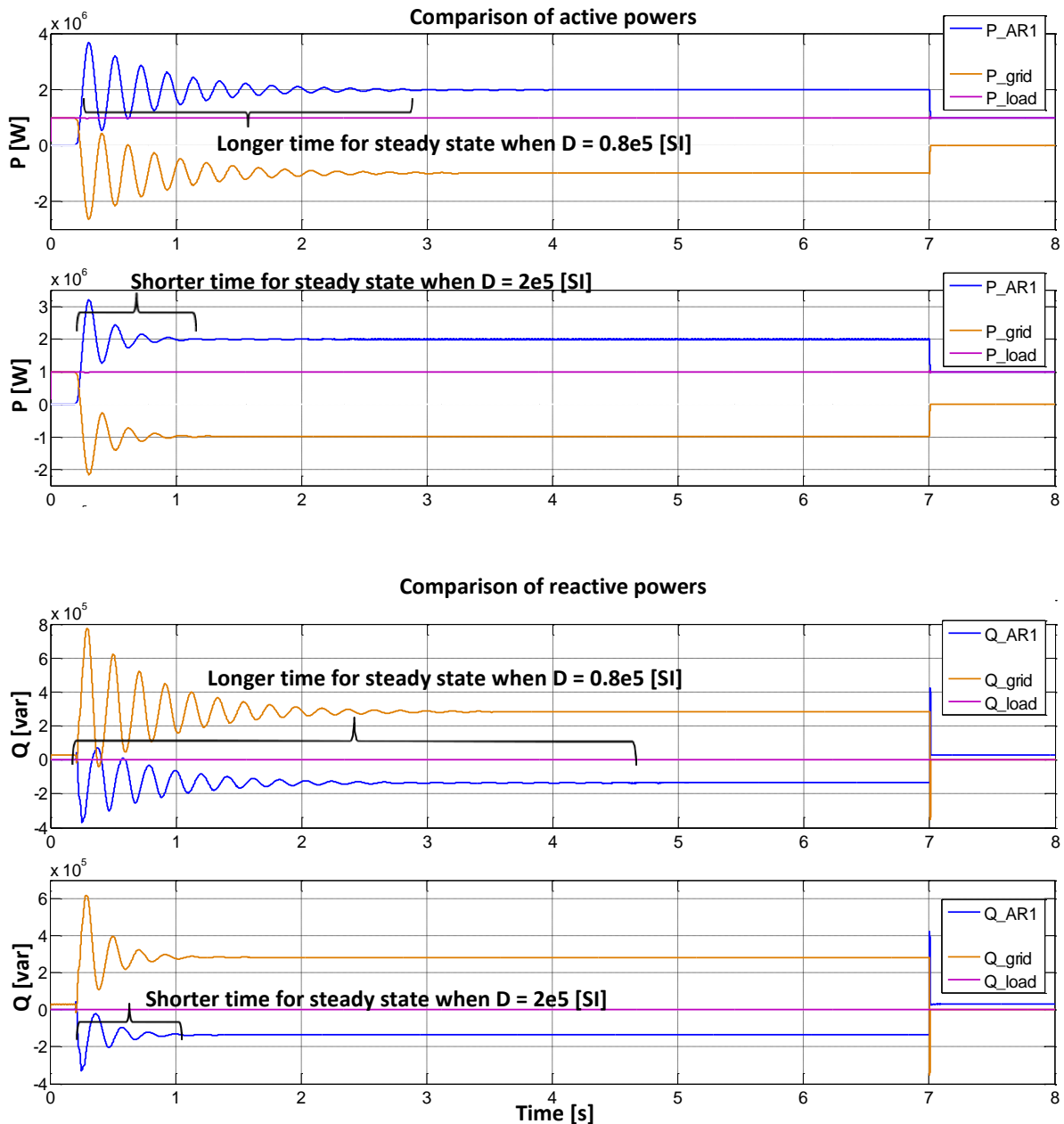


Figure 7-5: Comparison of active and reactive powers when virtual damping, $D = 0.8e5$ [SI] and $D = 2e5$ [SI] respectively

In both active power response comparisons (top two graphs) and the reactive power comparisons (bottom two graphs), it can be seen that higher the damping coefficient, faster the AR output powers reach steady state. Unlike in the previous case of inertia response, here there is a positive correlation of the damping coefficient (or damping power) with the time to achieve steady state. Swing equation: $J \frac{d\omega}{dt} = P_m - P_e - P_D$ shows that higher the P_D , faster it dampens the acceleration or deceleration to bring the total power in to steady state (or to rest).

The Figure 7-6 illustrates this correlation more emphatically. With respect to the default damping coefficient value ($=8e5$ [SI]), when the damping co-efficient is lowered 20 times ($=0.4e5$ [SI]), the time to dampen the output power will be incomparably long. When it is 10 times smaller ($=0.8e5$), the damping time increases in more than 3 seconds.

Also it is noticeable that higher the damping co-efficient, lower the power over shoot therefore lower the output current overshoot. This implies the protective measures and the current ratings of the power cables and lines can be extensively relaxed when having higher damping properties of the AR.

Again, it is worthy to note that the damping effect of virtual synchronous machine-based active rectifier is flexible and can be optimized according to the demand unlike in an actual synchronous generator which generates damping power with fixed, physical damper windings.

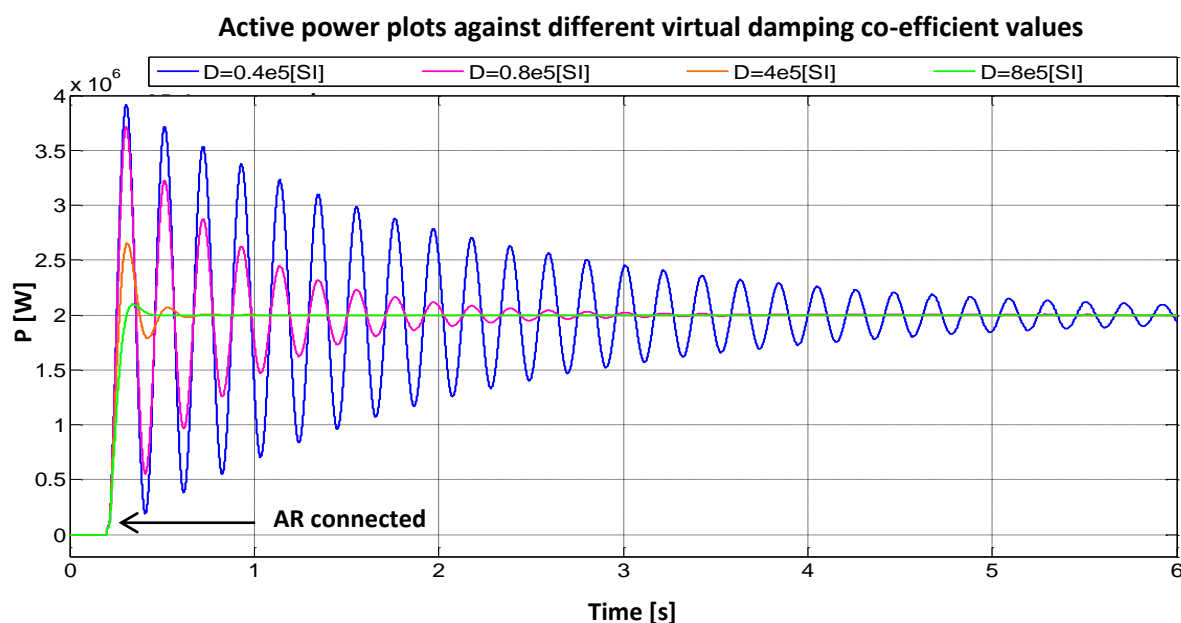


Figure 7-6: Active power damping time variations against different virtual damping co-efficient values

3. Active rectifier response to a step load in grid-tied mode

Step load 0.5 MW connected at 0.6 s

A step load has been introduced to the micro grid at 0.6 s in addition to the default load of 1 MW. The active rectifier has shown acceptable response upon the step load as shown in the Figure 7-7. It must be noted that as soon as the additional active power of 0.5 MW has been started to be consumed by the step load, the stiff grid power consumption has decreases by the same amount. This is because the AR power supply is constant at its reference value of 2 MW.

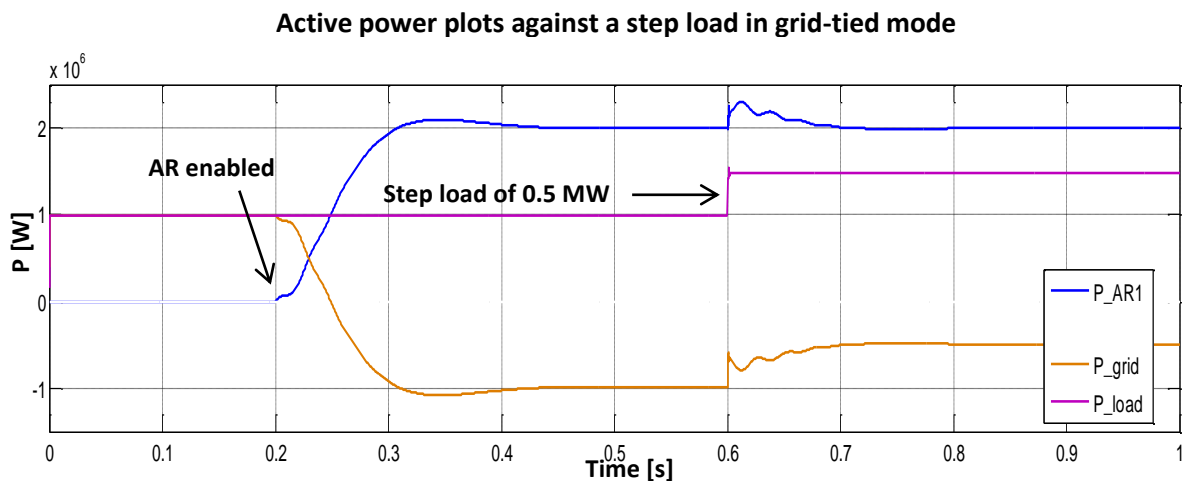


Figure 7-7: Active power plots against a step load change of 0.5 MW in grid-tied mode

4. Active rectifier response to a step load in island mode

Step load 0.5 MW connected at 0.6 s

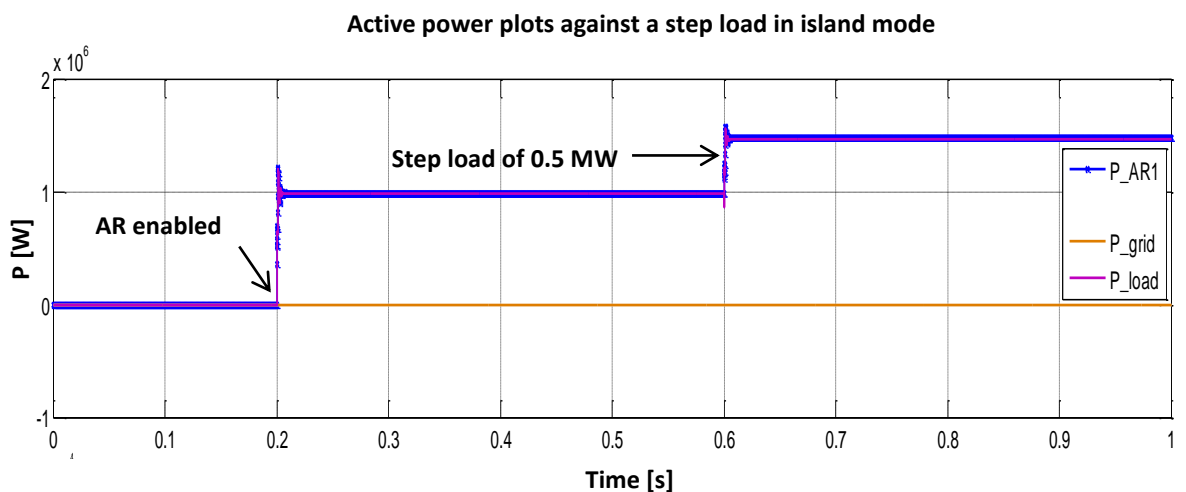


Figure 7-8: Active power plots against a step load change of 0.5 MW in island mode

Figure 7-8 presents the active rectifier (AR) power profile against a step load at 0.6 s in the island mode. The power profiles of AR and combined load have been almost identical and therefore overlapped.

This suggests that the AR controllers have fast response to the load changes in the micro grid. Also ideal overlapping indicates the robustness of the AR controller with strong resilience against load changes.

7.2 Parallel Active Rectifier Simulation

Two active rectifiers have been paralleled in the micro grid to investigate the parallel operation thereby the redundancy and load sharing features. At the end of the section, simulation results of paralleling of three ARs have been presented.

A schematic of the micro grid with the paralleled system is illustrated under the Figure 7-9. Table 4 presents the parameter values of each active rectifier in parallel and the system values. The parallel active rectifiers have identical features except the highlighted items, the reference powers and the droop percentages. It must be noted that the LCL filter parameters are identical in each active rectifier

Table 4: Default parameters for each AR in parallel operation and system parameters

| System parameters | Units |
|---|-------------------------|
| Voltage (phase to phase, rms) | 690 V |
| Current (phase) | 2300 A |
| Nominal frequency | 60 Hz |
| Active Rectifier 1 (AR 1) parameters | |
| Reference Power | 2e6 W |
| Active power droop | 0.02 [%] |
| Virtual inertia | 50 kg·m ² |
| Virtual damping co-efficient | 8e5 N·s·m ⁻¹ |
| Active Rectifier 2 (AR 2) parameters | |
| Reference Power | 3e6 W |
| Active power droop | 0.06 [%] |
| Virtual inertia | 50 kg·m ² |
| Virtual damping co-efficient | 8e5 N·s·m ⁻¹ |
| Load parameters | |
| Active power demand | 5e6 W |
| Reactive power demand | + 200 var |

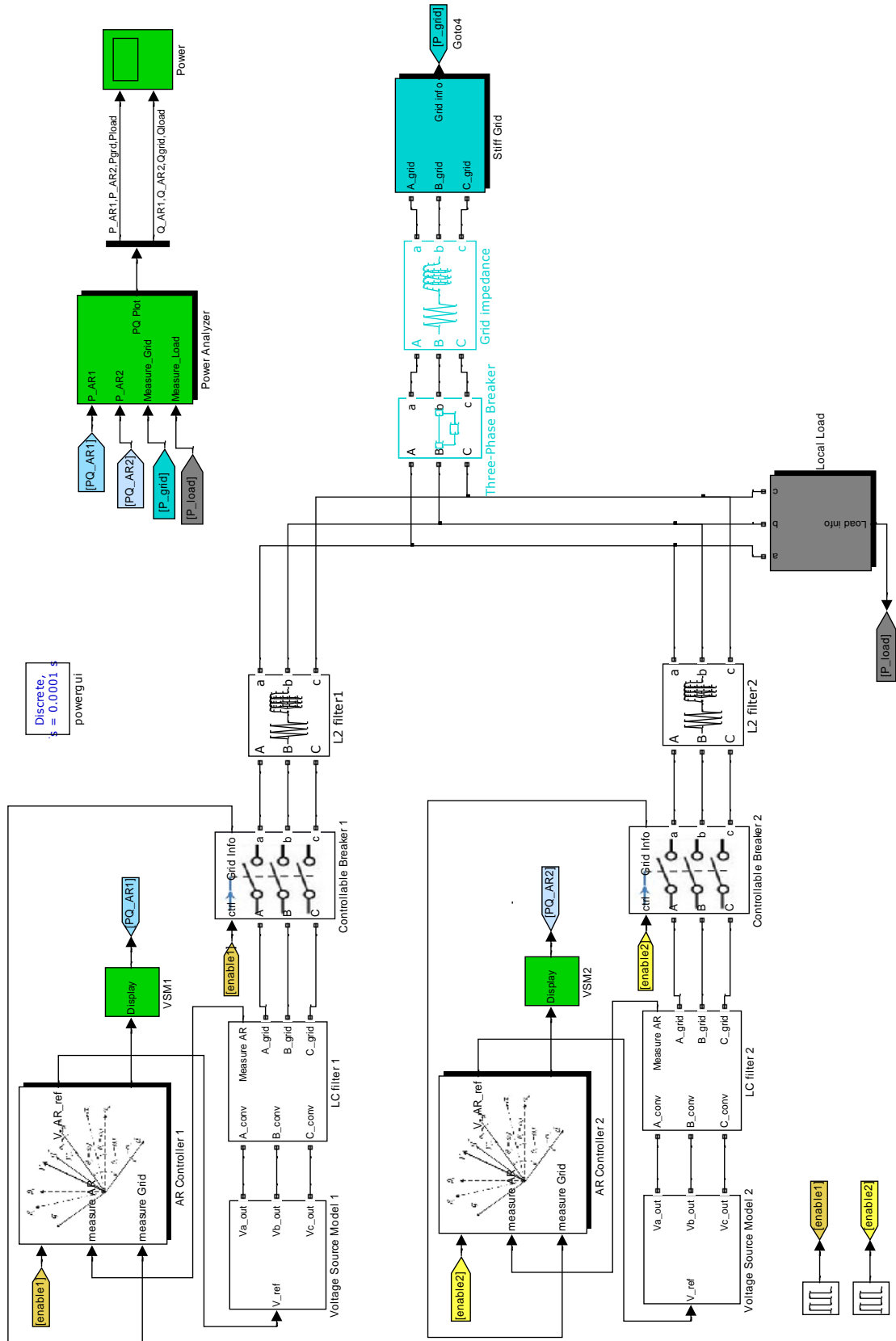


Figure 7-9: General simulation schematic with two active rectifiers connected in parallel with the stiff grid across their filters and impedances

7.2.1 Grid-tied Mode

Here the micro grid has been connected to the grid. The micro grid has contained two ARs connected in parallel. The power profiles are shown in the Figure 7-10.

Before ARs have been enabled, the entire active power load demand has been sourced by the stiff grid. At 0.2 s, when the ARs have been enabled, they have slowly built up to provide the fixed load. It is seen how the ARs have shared the load demand 2 MW and 3 MW respectively in the steady state. The grid power goes to zero at steady state as there is no excess power to be sourced or consumed by the grid to/from the micro grid.

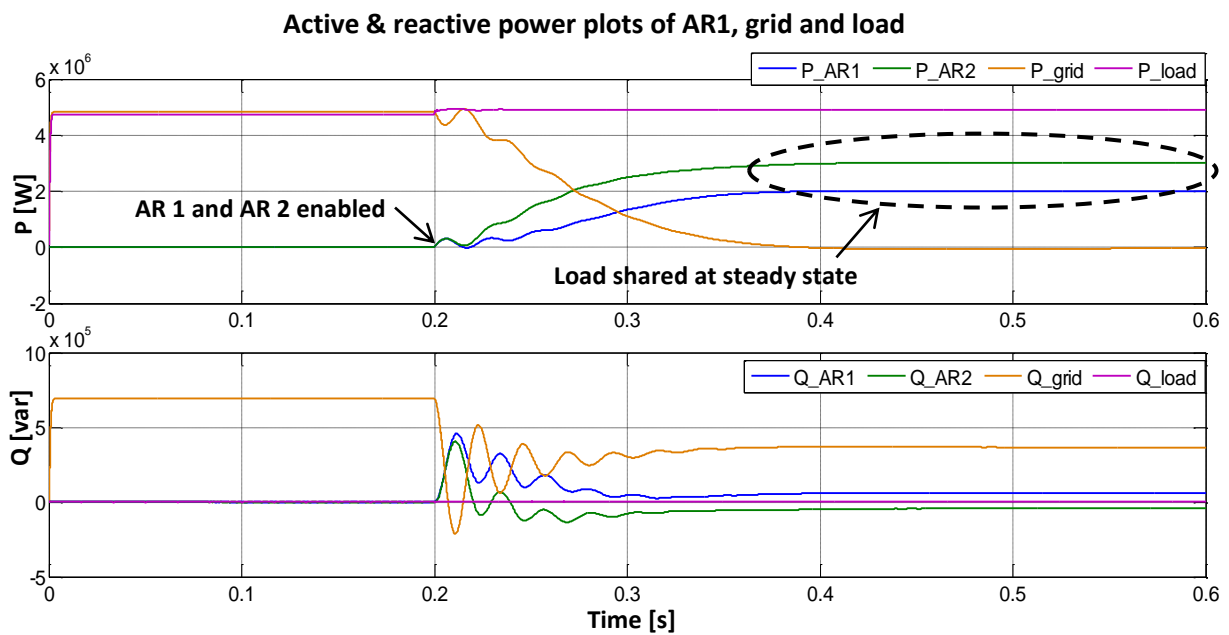


Figure 7-10: Active and reactive power plots of AR 1, AR 2, grid and load in grid-tied mode

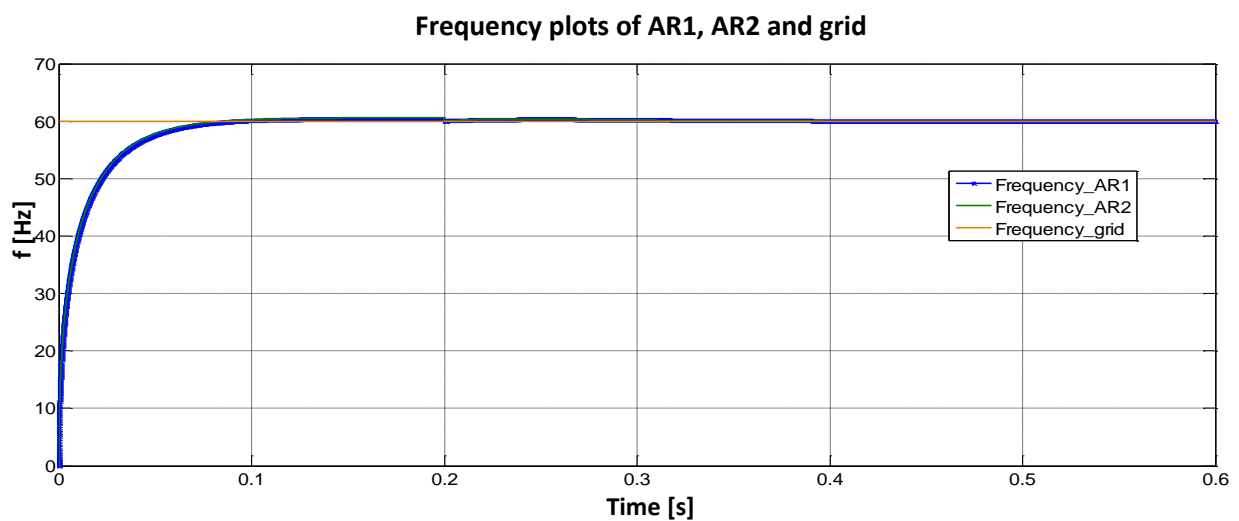


Figure 7-11: Frequency plots of AR1, AR2 and stiff grid in grid-tied mode

The frequency plots of Figure 7-11 shows steady curves of frequency affixed to the nominal frequency of 60 Hz. This steadiness is influenced by the stiff grid. It can be outlined that this one of the features and advantages of operating in grid-tied mode where the frequency excursions of the individual components will be negligible.

7.2.2 Island Mode

Here, the simulation has been carried out islanding the micro grid. Unlike in the previous case, here the load is also disabled until 0.2 s at which only the power has begun to flow with enabling of the ARs (Figure 7-12).

Similar to the grid-tied mode, in the island mode as well, the ARs shares the load in proportion to the respective reference powers in steady state.

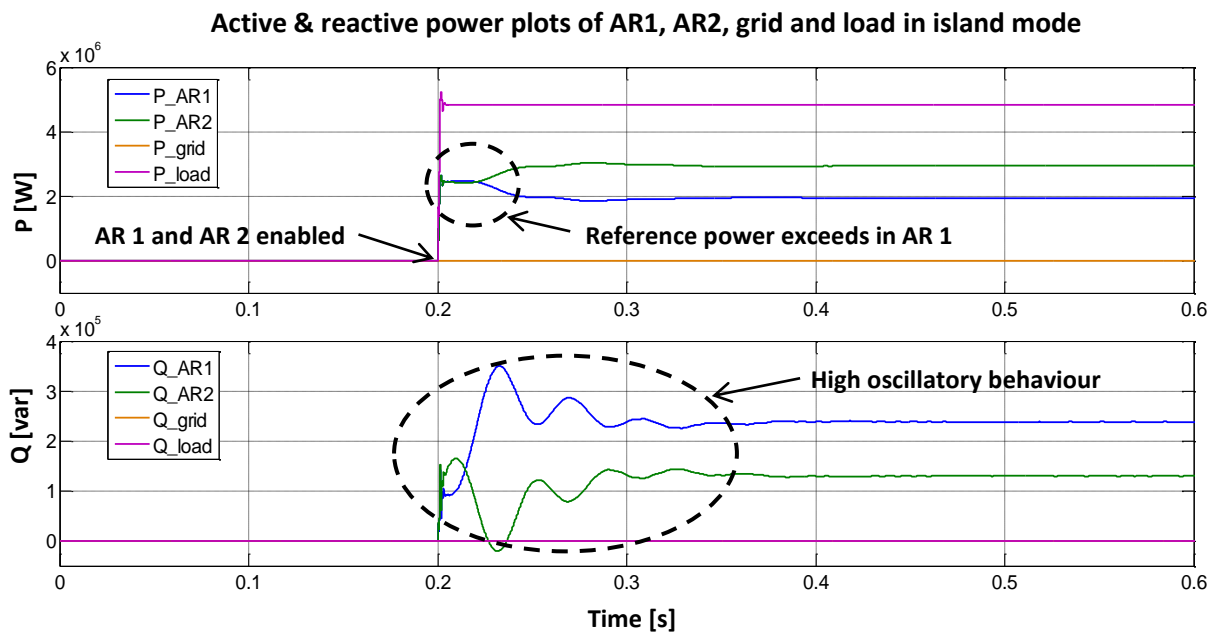


Figure 7-12: Active and reactive power plots of AR 1, AR 2, grid and load in island mode

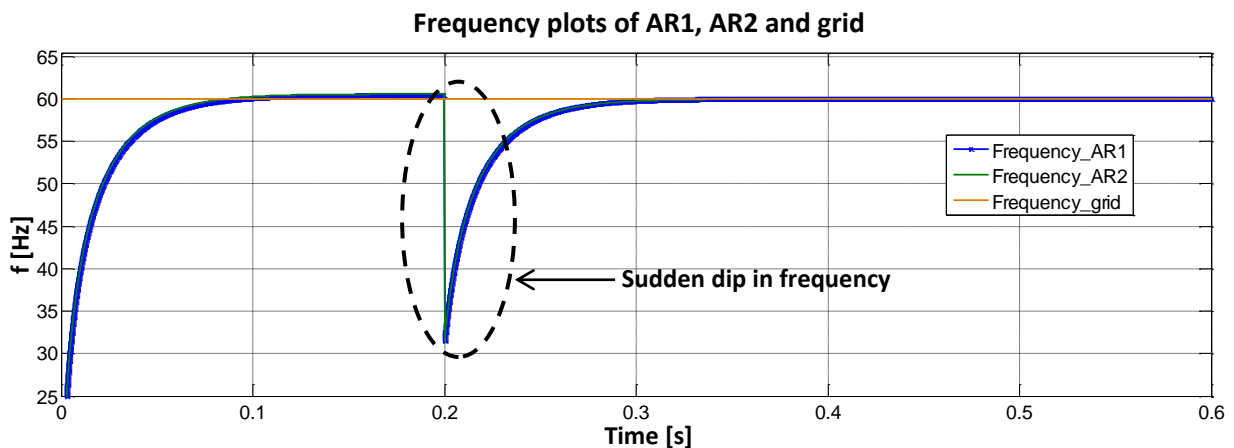


Figure 7-13: Frequency plots of AR1, AR2 and grid in island mode

In the same figure in active powers plot, it is noticeable that AR 1 initially shows an overshoot of power at the point of enabling. This is because the current limitation has not been implemented in the system. Therefore ARs do not understand its power rating. This is a notable absence that has to be carried out in the development in the project. The reactive power plots display more significant disturbance compared to that in the grid-tied mode. The reason for massive oscillation is because the direct control of reactive power has not been implemented. The reason for difference of oscillations in comparison is due again due to the absence resilience that would have been enjoyed in the grid-tied mode.

The Figure 7-13 highlights a significant behaviour in frequency of the island mode. Unlike in the, grid-tied mode, here the frequency has experienced a sudden dip at the connection of load to the ARs. When ARs move from no load condition to full load state, a frequency drop is expected according to the theoretical explanation in the chapter 3. However, here, the percentage of frequency drop has been alarming and would harm the micro grid components.

The dramatic frequency drop explains the value of *black start* of a micro grid. When a grid is energized from the zero power level, there is a standard procedure to follow before connecting the full load to the synchronous generators [13]. A similar procedure must be followed in real life when operating with active rectifiers as well.

7.2.3 Simulation for different cases

1. Step load in grid-tied mode

Initial load = 1 MW, Step load = 3 MW connected at 0.6 s;

Here, only the active power plots are considered as in the Figure 7-14. The most important information is provided in the

Figure 7-15 of frequencies. When the step load has been connected at $t=0.6$ s, the frequencies of AR 1 and AR 2 has dropped by about 0.2 Hz maximum for a very short period. However, the frequencies have regained the nominal frequency in quick time. This steadiness of the frequency can be attributed to the presence of the stiff grid in connection to the micro grid. The situation will be different in the island operation.

2. Step load in island mode

Reference Powers of AR1 & AR2 are equal, 3 MW each

Initial load = 1 MW, Step load = 3 MW connected at 0.6 s;

Under this case, power references of each AR have been made equal to show the behaviour of the micro grid. Figure 7-16 provides the active power plots of this case.



Figure 7-14: Active power plots of AR 1, AR 2, grid and load against a step load change of 3 MW in grid-tied mode

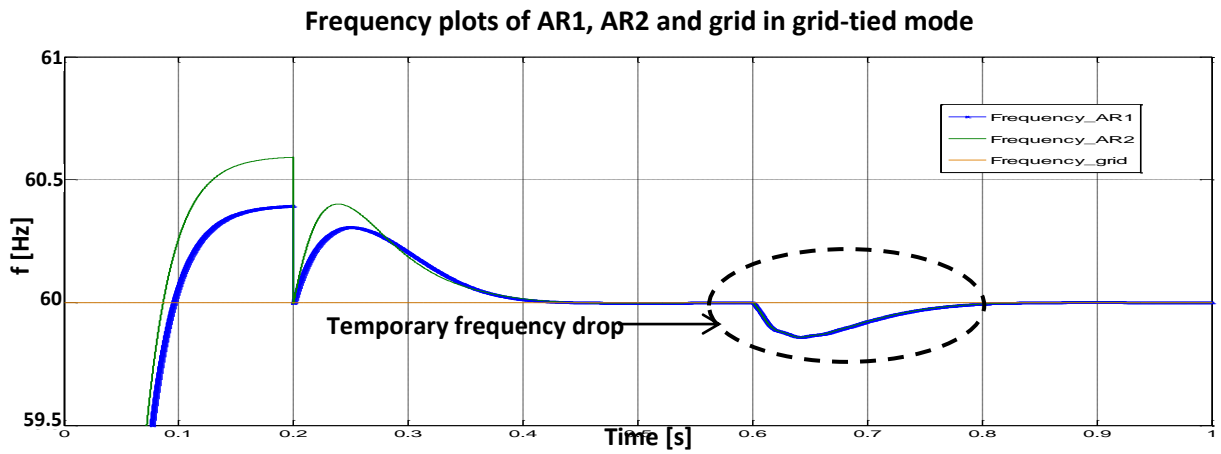


Figure 7-15: Frequency plots upon a step load change in grid-tied mode

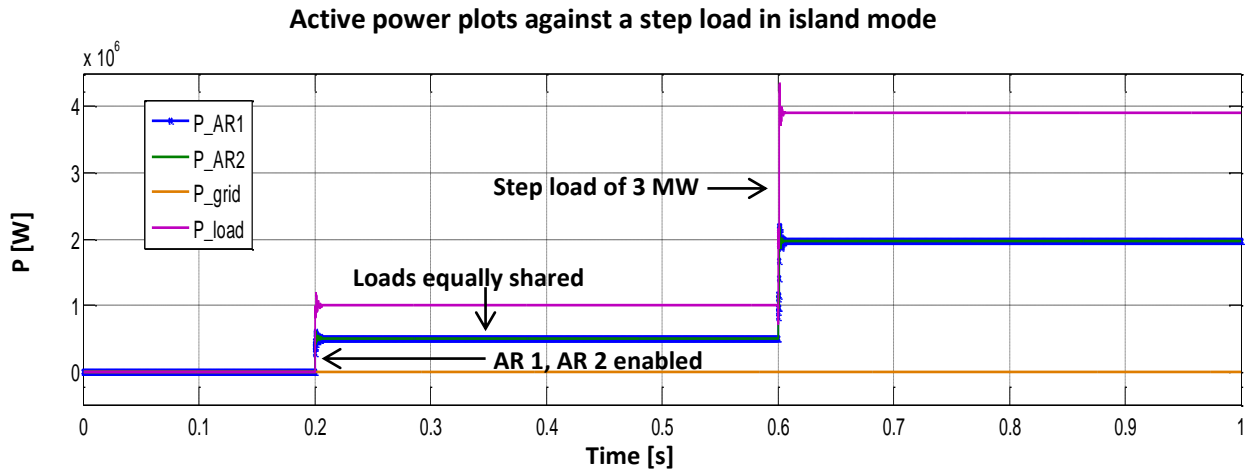


Figure 7-16: Active power plots of AR 1, AR 2, grid and load against a step load change of 3 MW in island mode. Reference Powers: AR 1=AR 2=3 MW

It is seen as expected, how the load has been equally shared by the two ARs. The most interesting aspect of this scenario is highlighted by the Figure 7-17 on frequency variations. Unlike in the grid-tied mode, here the frequency drop has remained in the steady state after the step increase in the load. This is because the extra load has been compensated only by the ARs without the stiff grid. As a result, the speed has been dropped in the virtual rotating masses as per the theoretical explanation in section 4.1.3. The speed references need to be readjusted to bring back the frequency in to original value.

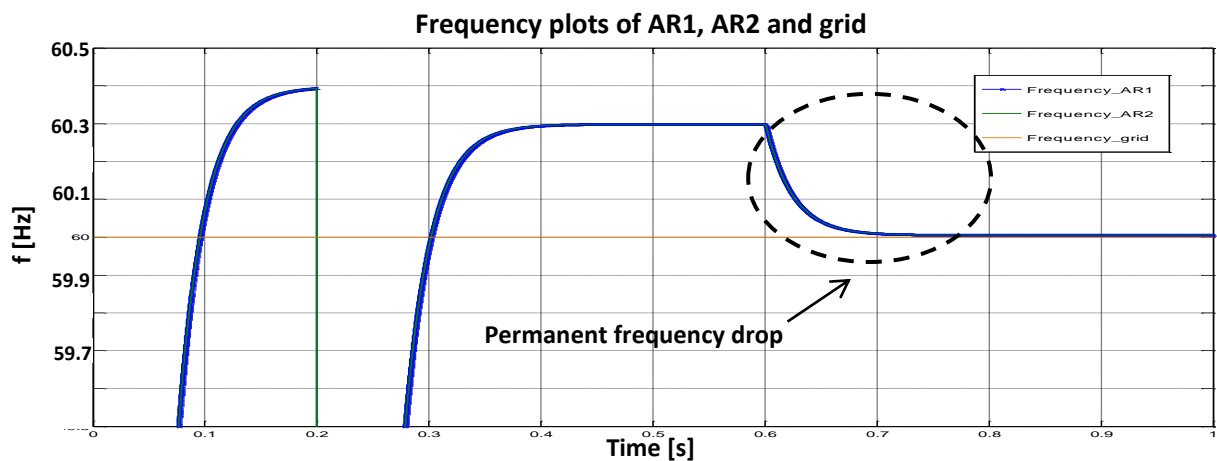


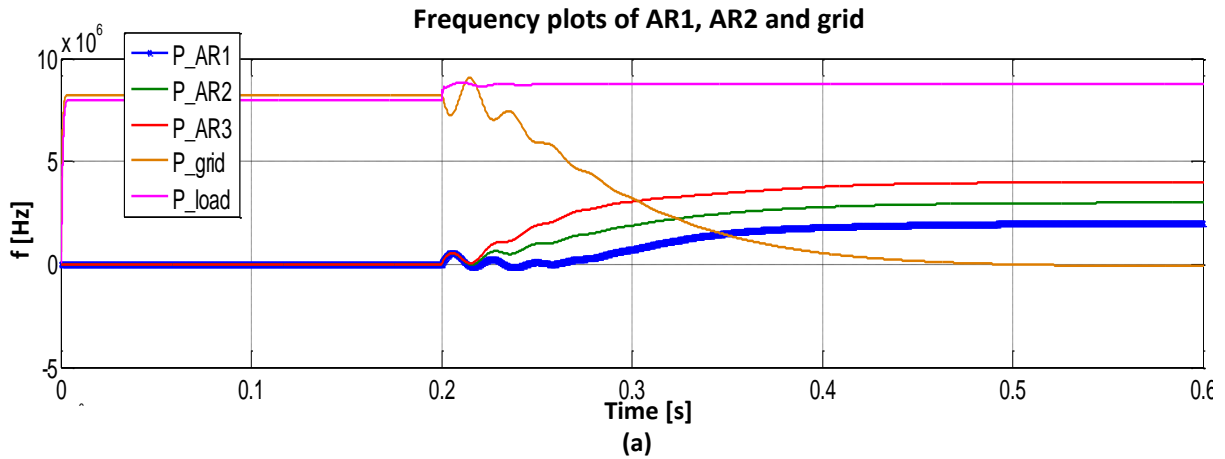
Figure 7-17: Frequency plots of AR 1, AR 2 and grid mode against a step load in island

3. Paralleling of 3 AR units

To demonstrate the possibility of paralleling many number of modelled ARs in the micro grid, the power plots of 3 active rectifier operation in both grid tied and island are presented

below. The power references have been 2 MW, 3 MW and 4 MW of AR 1, AR 2 and AR 3 respectively.

In grid-tied mode



In Island mode

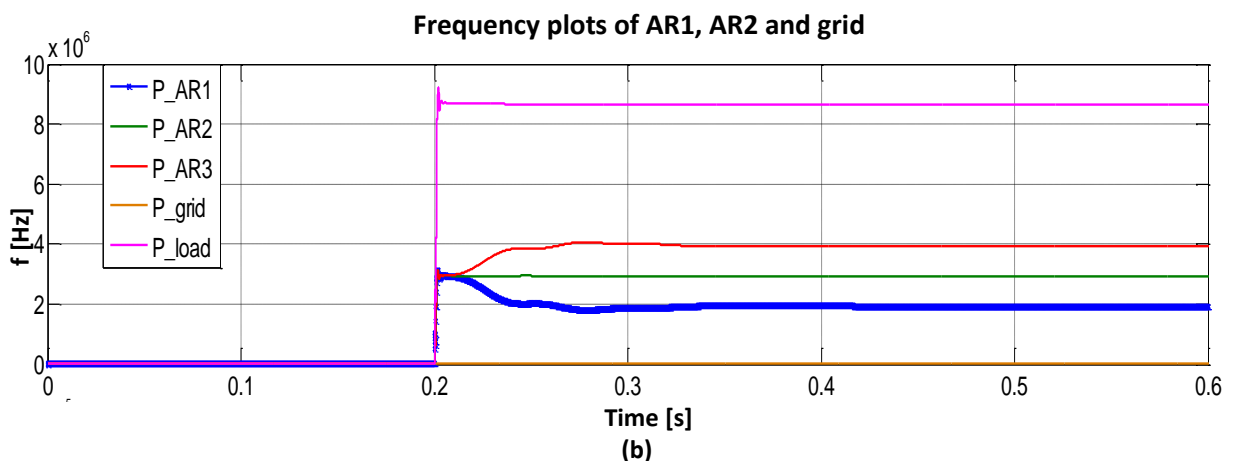


Figure 7-18: Paralleling of 3 ARs (a) in grid-tied mode (b) in island mode

This, on the other hand, shows the seamless *expandability* of the system, which is a valuable feature found in UPS systems.

7.2.4 Redundancy

To demonstrate the redundancy feature discussed in the chapter 3 on UPS, in island mode, one active rectifier has been suddenly tripped to observe the aftermaths.

It can be observed when AR 2 suddenly trips at 0.6 s, AR 1 has immediately compensated for the absent power share. This provides evidence to the feature of redundancy in the micro grid with active rectifiers to behave like UPS systems in parallel.

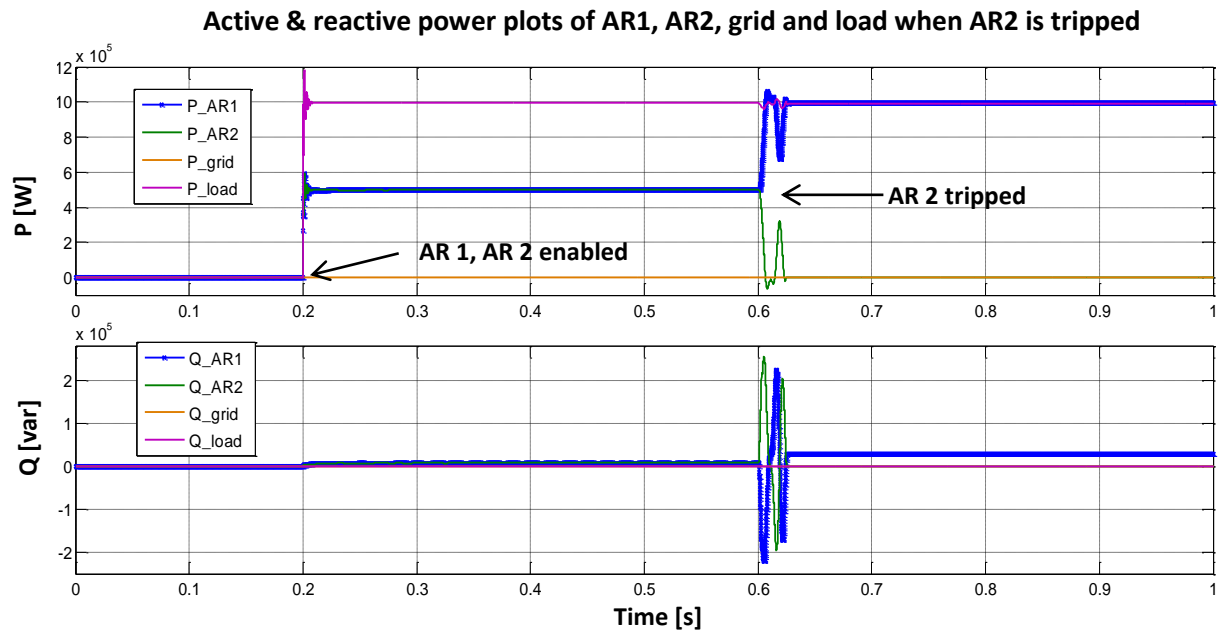


Figure 7-19: Active and reactive power plots of AR 1, AR 2, grid and load in island mode. AR 1 & AR 2 connected to the grid at $t = 0.2$. AR 1 tripped at $t = 0.6$

7.3 Summary of Chapter

The proposed model for virtual synchronous machine-based power control of active rectifiers for micro grids has been simulated in stand-alone, in parallel both in grid-tied mode and island mode.

The model has shown the behaviour of a synchronous machine by displaying damping, inertia responses and natural load sharing feature. Further to that, the model has emulated the synchronous machine performance in damping and virtual inertia responses due to its additional possibility of varying the virtual parameters to optimize the performance which is not the case of an actual synchronous machine. The feature of redundancy that is known for UPS has also been replicated by the active rectifiers.

The model needs to be improved in current limitation and reactive power control for better performance.

8 Conclusion

8.1 Conclusions

Under the scope of the master thesis, a simulation prototype of an active rectifier which controls power based on the virtual synchronous machine (VSM) approach has been developed. The control strategies of the proposed model have been inspired by the novel control techniques of well-established uninterruptible power supplies (UPS) and synchronous generator-sets. Therefore, the proposed system replicates the properties and performance of both synchronous generator and UPS system.

It is evident from the simulation results that the active rectifier model possesses the *damping*, *inertia response* and *load sharing* properties to behave as a synchronous generator and also *redundancy* and *expandability* to imitate UPS systems.

The designed active rectifier has displayed aforementioned properties in a micro grid with fixed loads as well as step loads. Active rectifier interfaced micro grid has shown equally promising results both in grid-tied and island modes. It has also been proven that the model can successful function in stand-alone as well as in parallel with theoretically infinite number of similar modules.

Highlight of the simulation results has been the flexibility of virtual machine parameters of the active rectifier. Unlike in an actual synchronous machine with physical presence of rotating masses and damper windings, the virtual damping and inertia response can be varied to achieve optimality. Further to that due to the software virtualization, no extra effort has to be taken in the proposed model to avoid magnetic saturation or eliminate eddy current losses.

The active rectifier has been modelled based on the synchronous reference frame control strategy. The current, voltage and phase-locked loops have shown satisfactory performance individually. However, a considerable degree of fragility has been experienced in the total system that has incapacitated the expansion of the control structure.

In conclusion it can be stated that the proposed virtual synchronous machine-based active rectifier has seemed to be very promising to interface micro grids because it enhances the system stability and reliability by emulating the behaviour of well-established synchronous machines and UPS.

8.2 Further Work

1. Direct control of reactive power needs to be implemented to ensure total power control.
2. Replacement of the voltage source model with the power electronic bridge inverter and PWM module
3. Further studies on harmonics need to be carried out and harmonic filtering needs to be implemented that will enhance the output power quality.
4. Current saturation limits need to be implemented to avoid overrated current flowing in steady state.
5. Supplementation of virtual inertia response with energy storage options;
In addition to the virtual inertia response with moment of inertia, by using a back-up storage system as in UPS, can improve the total effect of the inertia and thereby the frequency stability of the active rectifier.
6. Validating the simulation results with laboratory setup and experiments for optimal virtual machine parameters
7. To blow fuses upon a line fault, very high levels of current flow is required. It must be investigated how power electronic components would emulate this inherent feature easily available in a synchronous generator

8.3 Recommendations

1. It can be recommended to adopt more robust control architecture and tuning procedures which will allow more flexibility in control design.
2. Adoption of PR Controller instead of PI Controller can be useful in selective harmonic reduction as well as less costly hardware selection
3. It can be recommended to first replace the voltage source model with a hysteresis controller and inverter bridge and test the entire system. Subsequently, the hysteresis controller can be replaced by the PWM modulator which comes with inherent harmonic content.
4. Implementation of active damping to dampen out the oscillations that may occur between the LCL filter and the grid or active rectifier.

9 References

- [1] J. O. Lamell, T. Trumbo, and T. F. Nestli, "Offshore platform powered with new electrical motor drive system," in *Petroleum and Chemical Industry Conference, 2005. Industry Applications Society 52nd Annual*, 2005, pp. 259-266.
- [2] T. E. P. A. T. C. O. T. E. UNION, "DIRECTIVE 2009/28/EC OF THE EUROPEAN PARLIAMENT AND OF THE COUNCIL on the promotion of the use of energy from renewable sources and amending and subsequently repealing Directives 2001/77/EC and 2003/30/EC," ed, 2009.
- [3] H. P. Beck and R. Hesse, "Virtual synchronous machine," in *Electrical Power Quality and Utilisation, 2007. EPQU 2007. 9th International Conference on*, 2007, pp. 1-6.
- [4] D. Yan, S. Jianhui, M. Meiqin, and Y. Xiangzhen, "Autonomous controller based on synchronous generator dq0 model for micro grid inverters," in *Power Electronics and ECCE Asia (ICPE & ECCE), 2011 IEEE 8th International Conference on*, 2011, pp. 2645-2649.
- [5] J. M. Guerrero, "Microgrids Connecting Renewable Energy Sources into the Smartgrid," in *14th European Conference on Power Electronics and Applications*, Birmingham, UK, 2011.
- [6] J. Driesen and K. Visscher, "Virtual synchronous generators," in *Power and Energy Society General Meeting - Conversion and Delivery of Electrical Energy in the 21st Century, 2008 IEEE*, 2008, pp. 1-3.
- [7] Z. Qing-Chang and G. Weiss, "Synchronverters: Inverters That Mimic Synchronous Generators," *Industrial Electronics, IEEE Transactions on*, vol. 58, pp. 1259-1267, 2011.
- [8] D. Georgakis, S. Papathanassiou, N. Hatziargyriou, A. Engler, and C. Hardt, "Operation of a prototype microgrid system based on micro-sources quipped with fast-acting power electronics interfaces," in *Power Electronics Specialists Conference, 2004. PESC 04. 2004 IEEE 35th Annual*, 2004, pp. 2521-2526 Vol.4.
- [9] M. Jan, B. J. W., and B. J. R., *Power System Dynamics Stability and Control*: John Wiley & Sons Ltd., 2009.
- [10] P. Panagis, F. Stergiopoulos, P. Marabeas, and S. Manias, "Comparison of state of the art multilevel inverters," in *Power Electronics Specialists Conference, 2008. PESC 2008. IEEE*, 2008, pp. 4296-4301.
- [11] R. H. L. C. Hochgraf, D.M. Divan, T.A. Lipo, , "Comparison of multilevel Inverters for Static Var Compensation " Wisconsin Power Electronics Center, University of Wisconsin-Madison 1994.
- [12] C. L. Moreira, F. O. Resende, and J. A. P. Lopes, "Using Low Voltage MicroGrids for Service Restoration," *Power Systems, IEEE Transactions on*, vol. 22, pp. 395-403, 2007.
- [13] J. A. P. Lopes, C. L. Moreira, and F. O. Resende, "Microgrids black start and islanded operation," in *15th PSCC*, Liege, 2005.
- [14] J. A. P. Lopes, C. L. Moreira, and A. G. Madureira, "Defining control strategies for MicroGrids islanded operation," *Power Systems, IEEE Transactions on*, vol. 21, pp. 916-924, 2006.
- [15] A. Perera, "Virtual synchronous machine concept with active rectifiers for micro grids," Norwegian University of Science and Technology 2011.
- [16] RenewableUK. (2011, February 2012). *RenewableUK Position Paper on Inertia (V3-0)*. Available: http://www.bwea.com/pdf/publications/RenewableUK_Inertia_Position_Paper.pdf
- [17] J. M. Guerrero, L. G. De Vicuna, and J. Uceda, "Uninterruptible power supply systems provide protection," *Industrial Electronics Magazine, IEEE*, vol. 1, pp. 28-38, 2007.
- [18] T. M. U. Ned Mohan, William P. Robbins, *Power Electronics Converters, Applications and Design 3rd Edition*: John Wiley & Sons, Inc., 2006.

- [19] Z. Moussaoui, I. Batarseh, H. Lee, and C. Kennedy, "An overview of the control scheme for distributed power systems," in *Southcon/96. Conference Record*, 1996, pp. 584-591.
- [20] G. C. I. P. Protection. (2004, February 2012). *UPS technical note no. 4 Digital Energy™ Uninterruptible Power Supply*. Available: http://www.scanpocon.dk/Download/Scanpocon/Toolkit/content/Section%20III-Tech%20notes/Miscell-tech-notes/TCN_XXE_004_XXX_XXX_XGB_0411.pdf
- [21] J. Sears. (February 2012). *High-Availability Power Systems: Redundancy Options*. Available: <http://www.powerpulse.net/techPaper.php?paperID=90&print>
- [22] J. M. Guerrero, L. Hang, and J. Uceda, "Control of Distributed Uninterruptible Power Supply Systems," *Industrial Electronics, IEEE Transactions on*, vol. 55, pp. 2845-2859, 2008.
- [23] M. S. Racine, J. D. Parham, and M. H. Rashid, "An overview of uninterruptible power supplies," in *Power Symposium, 2005. Proceedings of the 37th Annual North American, 2005*, pp. 159-164.
- [24] S. B. Bekiarov and A. Emadi, "Uninterruptible power supplies: classification, operation, dynamics, and control," in *Applied Power Electronics Conference and Exposition, 2002. APEC 2002. Seventeenth Annual IEEE, 2002*, pp. 597-604 vol.1.
- [25] M. C. Chandorkar and D. M. Divan, "Decentralized operation of distributed UPS systems," in *Power Electronics, Drives and Energy Systems for Industrial Growth, 1996., Proceedings of the 1996 International Conference on, 1996*, pp. 565-571 vol.1.
- [26] N. ELECTRIC. (2002, February 2012). *Application note for three phase UPS systems in redundant configuration*. Available: <http://www.novaelectric.com/pdf/AN3PRS.PDF>
- [27] S. Duan, Y. Meng, J. Xiong, Y. Kang, and J. Chen, "Parallel operation control technique of voltage source inverters in UPS," in *Power Electronics and Drive Systems, 1999. PEDS '99. Proceedings of the IEEE 1999 International Conference on, 1999*, pp. 883-887 vol.2.
- [28] A. Tuladhar, H. Jin, T. Unger, and K. Mauch, "Parallel operation of single phase inverter modules with no control interconnections," in *Applied Power Electronics Conference and Exposition, 1997. APEC '97 Conference Proceedings 1997., Twelfth Annual, 1997*, pp. 94-100 vol.1.
- [29] A. Engler and N. Sultanis, "Droop control in LV-grids," in *Future Power Systems, 2005 International Conference on, 2005*, pp. 6 pp.-6.
- [30] J. M. Guerrero, L. Garcia de Vicuna, J. Matas, M. Castilla, and J. Miret, "Output Impedance Design of Parallel-Connected UPS Inverters With Wireless Load-Sharing Control," *Industrial Electronics, IEEE Transactions on*, vol. 52, pp. 1126-1135, 2005.
- [31] T. Skjellnes, "Digital Control of Grid Connected Converters for Distributed Power Generation," doktor ingeniør, Department of Electric Power Engineering Norwegian University of Science and Technology, Trondheim, March 2008.
- [32] G. C. I. P. Protection. (2004, February 2012). *UPS technical note no. 9 Digital Energy™ Uninterruptible Power Supply*. Available: http://www.scanpocon.dk/Download/Scanpocon/Toolkit/content/Section%20III-Tech%20notes/Miscell-tech-notes/TCN_XXE_009_XXX_XXX_XGB_0411.pdf
- [33] G. C. I. P. Protection. (2004, February 2012). *UPS technical note no. 8 Digital Energy™ Uninterruptible Power Supply*. Available: http://www.scanpocon.dk/Download/Scanpocon/Toolkit/content/Section%20III-Tech%20notes/Miscell-tech-notes/TCN_XXE_008_XXX_XXX_XGB_0411.pdf
- [34] C. K. A. E. Fitzgerald, Stephen D. Umans, *Electric Machinery, 6th Edition*: McGraw-Hill, 2003.
- [35] Q.-C. Zhong, "Four-quadrant operation of AC machines powered by inverters that mimic synchronous generators," in *Power Electronics, Machines and Drives (PEMD 2010), 5th IET International Conference on, 2010*, pp. 1-6.
- [36] K. Sakimoto, Y. Miura, and T. Ise, "Stabilization of a power system with a distributed generator by a Virtual Synchronous Generator function," in *Power Electronics and ECCE Asia (ICPE & ECCE), 2011 IEEE 8th International Conference on, 2011*, pp. 1498-1505.

- [37] K. Visscher and S. W. H. De Haan, "Virtual synchronous machines for frequency stabilisation in future grids with a significant share of decentralized generation," in *SmartGrids for Distribution, 2008. IET-CIRED. CIRED Seminar, 2008*, pp. 1-4.
- [38] V. Van Thong, A. Woyte, M. Albu, M. Van Hest, J. Bozelie, J. Diaz, T. Loix, D. Stanculescu, and K. Visscher, "Virtual synchronous generator: Laboratory scale results and field demonstration," in *PowerTech, 2009 IEEE Bucharest, 2009*, pp. 1-6.
- [39] T. Skjellnes, A. Skjellnes, and L. Norum, *Load sharing for parallel inverters without communication*. [S.l.]: [s.n.], 2002.
- [40] J. M. Guerrero, J. C. Vasquez, J. Matas, M. Castilla, and L. G. de Vicuna, "Control Strategy for Flexible Microgrid Based on Parallel Line-Interactive UPS Systems," *Industrial Electronics, IEEE Transactions on*, vol. 56, pp. 726-736, 2009.
- [41] M. Albu, K. Visscher, D. Creanga, A. Nechifor, and N. Golovanov, "Storage selection for DG applications containing virtual synchronous generators," in *PowerTech, 2009 IEEE Bucharest, 2009*, pp. 1-6.
- [42] M. P. N. van Wesenbeeck, S. W. H. de Haan, P. Varela, and K. Visscher, "Grid tied converter with virtual kinetic storage," in *PowerTech, 2009 IEEE Bucharest, 2009*, pp. 1-7.
- [43] G. Delille, Franc, x, B. ois, and G. Malarange, "Dynamic frequency control support: A virtual inertia provided by distributed energy storage to isolated power systems," in *Innovative Smart Grid Technologies Conference Europe (ISGT Europe), 2010 IEEE PES, 2010*, pp. 1-8.
- [44] K. De Brabandere, B. Bolsens, J. Van den Keybus, A. Woyte, J. Driesen, R. Belmans, and K. U. Leuven, "A voltage and frequency droop control method for parallel inverters," in *Power Electronics Specialists Conference, 2004. PESC 04. 2004 IEEE 35th Annual, 2004*, pp. 2501-2507 Vol.4.
- [45] A. Engler, "Applicability of droops in low voltage grids," *DER Journal*, vol. No. 1, p. 5, 2005.
- [46] J. C. Vasquez, J. M. Guerrero, A. Luna, P. Rodriguez, and R. Teodorescu, "Adaptive Droop Control Applied to Voltage-Source Inverters Operating in Grid-Connected and Islanded Modes," *Industrial Electronics, IEEE Transactions on*, vol. 56, pp. 4088-4096, 2009.
- [47] L. Yun Wei and K. Ching-Nan, "An Accurate Power Control Strategy for Power-Electronics-Interfaced Distributed Generation Units Operating in a Low-Voltage Multibus Microgrid," *Power Electronics, IEEE Transactions on*, vol. 24, pp. 2977-2988, 2009.
- [48] D. De and V. Ramanarayanan, "Decentralized Parallel Operation of Inverters Sharing Unbalanced and Nonlinear Loads," *Power Electronics, IEEE Transactions on*, vol. 25, pp. 3015-3025, 2010.
- [49] F. Blaabjerg, C. Zhe, and S. B. Kjaer, "Power electronics as efficient interface in dispersed power generation systems," *Power Electronics, IEEE Transactions on*, vol. 19, pp. 1184-1194, 2004.
- [50] F. Blaabjerg, R. Teodorescu, M. Liserre, and A. V. Timbus, "Overview of Control and Grid Synchronization for Distributed Power Generation Systems," *Industrial Electronics, IEEE Transactions on*, vol. 53, pp. 1398-1409, 2006.
- [51] V. Blasko and V. Kaura, "A new mathematical model and control of a three-phase AC-DC voltage source converter," *Power Electronics, IEEE Transactions on*, vol. 12, pp. 116-123, 1997.
- [52] W. Gullvik, "Modeling, Analysis and Control of Active Front End (AFE) Converter," Philosophiae doctor, Department of Electric Power Engineering, Norwegian University of Science and Technology, 2007.
- [53] N. M. Abdel-Rahim and J. E. Quicoe, "Analysis and design of a multiple feedback loop control strategy for single-phase voltage-source UPS inverters," *Power Electronics, IEEE Transactions on*, vol. 11, pp. 532-541, 1996.
- [54] A. Kawamura, R. Chuarayapratip, and T. Haneyoshi, "Deadbeat control of PWM inverter with modified pulse patterns for uninterruptible power supply," *Industrial Electronics, IEEE Transactions on*, vol. 35, pp. 295-300, 1988.

- [55] D. M. Divan, "Inverter topologies and control techniques for sinusoidal output power supplies," in *Applied Power Electronics Conference and Exposition, 1991. APEC '91. Conference Proceedings, 1991., Sixth Annual, 1991*, pp. 81-87.
- [56] T. Kagotani, K. Kuroki, J. Shinohara, and A. Misaizu, "A novel UPS using high-frequency switch-mode rectifier and high-frequency PWM inverter," in *Power Electronics Specialists Conference, 1989. PESC '89 Record., 20th Annual IEEE, 1989*, pp. 53-57 vol.1.
- [57] N. Mohan, *Electric Drives, An Integrative Approach*. Minneapolis, USA: MNPERE 2003.
- [58] M. P. Kazmierkowski and L. Malesani, "Current control techniques for three-phase voltage-source PWM converters: a survey," *Industrial Electronics, IEEE Transactions on*, vol. 45, pp. 691-703, 1998.
- [59] C. D. Manning, "Control of UPS inverters," in *Uninterruptible Power Supplies, IEE Colloquium on*, 1994, pp. 3/1-3/5.
- [60] C. J. Ramos, A. P. Martins, A. S. Araujo, and A. S. Carvalho, "Current control in the grid connection of the double-output induction generator linked to a variable speed wind turbine," in *IECON 02 [Industrial Electronics Society, IEEE 2002 28th Annual Conference of the]*, 2002, pp. 979-984 vol.2.
- [61] D. Candusso, L. Valero, A. Walter, S. Bacha, E. Rulliere, and B. Raison, "Modelling, control and simulation of a fuel cell based power supply system with energy management," in *IECON 02 [Industrial Electronics Society, IEEE 2002 28th Annual Conference of the]*, 2002, pp. 1294-1299 vol.2.
- [62] N. Mohan, *Advanced Electrical Drives, Analysis, Control and Modeling using Simulink*. Minneapolis, USA: MNPERE, 2001.
- [63] R. Teodorescu, F. Blaabjerg, M. Liserre, and P. C. Loh, "Proportional-resonant controllers and filters for grid-connected voltage-source converters," *Electric Power Applications, IEE Proceedings -*, vol. 153, pp. 750-762, 2006.
- [64] S. Fukuda and T. Yoda, "A novel current tracking method for active filters based on a sinusoidal internal model," in *Industry Applications Conference, 2000. Conference Record of the 2000 IEEE, 2000*, pp. 2108-2114 vol.4.
- [65] J. A. Suul, K. Ljokelsoy, and T. Undeland, "Design, tuning and testing of a flexible PLL for grid synchronization of three-phase power converters," in *Power Electronics and Applications, 2009. EPE '09. 13th European Conference on*, 2009, pp. 1-10.
- [66] J. A. Suul, "Control of Grid Integrated Voltage Source Converters under Unbalanced Conditions," Philosophiae Doctor, Department of Electric Power Engineering, Norwegian University of Science and Technology, Trondheim, 2012.
- [67] H. Guan-Chyun and J. C. Hung, "Phase-locked loop techniques. A survey," *Industrial Electronics, IEEE Transactions on*, vol. 43, pp. 609-615, 1996.
- [68] N. R. Zargari and G. Joos, "Performance investigation of a current-controlled voltage-regulated PWM rectifier in rotating and stationary frames," *Industrial Electronics, IEEE Transactions on*, vol. 42, pp. 396-401, 1995.
- [69] T. Noguchi, H. Tomiki, S. Kondo, and I. Takahashi, "Direct power control of PWM converter without power-source voltage sensors," *Industry Applications, IEEE Transactions on*, vol. 34, pp. 473-479, 1998.
- [70] M. J. Newman, D. N. Zmood, and D. G. Holmes, "Stationary frame harmonic reference generation for active filter systems," *Industry Applications, IEEE Transactions on*, vol. 38, pp. 1591-1599, 2002.
- [71] L. Malesani and P. Tenti, "A novel hysteresis control method for current-controlled voltage-source PWM inverters with constant modulation frequency," *Industry Applications, IEEE Transactions on*, vol. 26, pp. 88-92, 1990.
- [72] S. Buso, L. Malesani, and P. Mattavelli, "Comparison of current control techniques for active filter applications," *Industrial Electronics, IEEE Transactions on*, vol. 45, pp. 722-729, 1998.

- [73] Y. Sato, T. Ishizuka, K. Nezu, and T. Kataoka, "A new control strategy for voltage-type PWM rectifiers to realize zero steady-state control error in input current," *Industry Applications, IEEE Transactions on*, vol. 34, pp. 480-486, 1998.
- [74] C. Jong-Woo and S. Seung-Ki, "Fast current controller in three-phase AC/DC boost converter using d-q axis crosscoupling," *Power Electronics, IEEE Transactions on*, vol. 13, pp. 179-185, 1998.
- [75] D. N. Zmood and D. G. Holmes, "Stationary frame current regulation of PWM inverters with zero steady-state error," *Power Electronics, IEEE Transactions on*, vol. 18, pp. 814-822, 2003.
- [76] R. Nilsen, *Kompendium i elektriske motordrifter*: Norwegian University of Science and Technology, 2000.
- [77] C. Se-Kyo, "A phase tracking system for three phase utility interface inverters," *Power Electronics, IEEE Transactions on*, vol. 15, pp. 431-438, 2000.
- [78] P. Rodriguez, A. Luna, M. Ciobotaru, R. Teodorescu, and F. Blaabjerg, "Advanced Grid Synchronization System for Power Converters under Unbalanced and Distorted Operating Conditions," in *IEEE Industrial Electronics, IECON 2006 - 32nd Annual Conference on*, 2006, pp. 5173-5178.
- [79] L. N. Arruda, S. M. Silva, and B. J. C. Filho, "PLL structures for utility connected systems," in *Industry Applications Conference, 2001. Thirty-Sixth IAS Annual Meeting. Conference Record of the 2001 IEEE*, 2001, pp. 2655-2660 vol.4.
- [80] J. A. Suul, "Tuning of control loops for grid side voltage source converters," SINTEF Energy AS02-03 2012.
- [81] J. W. Umland and M. Safiuddin, "Magnitude and symmetric optimum criterion for the design of linear control systems: what is it and how does it compare with the others?," *Industry Applications, IEEE Transactions on*, vol. 26, pp. 489-497, 1990.
- [82] J. A. Suul, M. Molinas, L. Norum, and T. Undeland, "Tuning of control loops for grid connected voltage source converters," in *Power and Energy Conference, 2008. PECon 2008. IEEE 2nd International*, 2008, pp. 797-802.

Appendix A: Definition of per-unit system

Based on the accepted conventions for electrical machines and drives systems, the per-unit system can be presented as follows;

$$S_N = \sqrt{3} \cdot V_{LL,rms,N} \cdot I_{rms,N} = 3 \cdot V_{phase,rms,N} \cdot I_{rms,N} = \frac{3}{2} \cdot V_{phase,peak,N} \cdot I_{peak,N}$$

$$\omega_N = 2 \cdot \pi \cdot f_N$$

$$S_b = S_N = \frac{3}{2} \cdot V_b \cdot I_b$$

$$V_b = V_{phase,peak,N}$$

$$I_b = I_{peak,N}$$

$$f_b = f_N$$

$$Z_b = R_b = \frac{V_b}{I_b}$$

$$L_b = \frac{Z_b}{\omega_b}$$

$$C_b = \frac{1}{\omega_b \cdot Z_b}$$

Appendix B: Reference frame transformations

4. Amplitude-invariant Clarke transformation

$$\begin{bmatrix} x_\alpha \\ x_\beta \\ x_0 \end{bmatrix} = \begin{bmatrix} 1 & -\frac{1}{2} & -\frac{1}{2} \\ 0 & \frac{\sqrt{3}}{2} & -\frac{\sqrt{3}}{2} \\ \frac{1}{2} & \frac{1}{2} & \frac{1}{2} \end{bmatrix} \begin{bmatrix} x_a \\ x_b \\ x_c \end{bmatrix}$$

5. Park transformation

$$\begin{bmatrix} x_d \\ x_q \end{bmatrix} = \begin{bmatrix} \cos\theta & \sin\theta \\ -\sin\theta & \cos\theta \end{bmatrix} \begin{bmatrix} x_\alpha \\ x_\beta \end{bmatrix}$$

Appendix C: Tuning of control loops

Let $a = 2\zeta + 1$
 where $\zeta = \text{damping factor}$

1. Tuning of PLL by Symmetric Optimum Criteria

The signs are based on the Figure 5-10
 let $a_{pll} = 3$ and $T_f = 0.002$ s

$$T_i = a_{pll}^2 \cdot T_f$$

$$K_p = \frac{1}{a_{pll} \cdot 2\pi \cdot T_f}$$

2. Tuning of inner current control loop by Modulus Optimum Criteria

let $f_{sw} = 2500$
 where $f_{sw} = \text{switching frequency}$

$$T_{sw} = \frac{1}{f_{sw}}$$

$$T_l = \frac{l_{1, filt}}{r_{con} \cdot \omega_b}$$

$$T_i = T_l$$

$$K_p = \frac{T_l r_{con}}{2T_{sw}}$$

3. Tuning of outer voltage control loop by Symmetric Optimum Criteria

Let $a_{vc} = 0.6$

$$T_c = \frac{C_{filt}}{\omega_b}$$

$$T_{eq} = 2T_{sw}$$

$$T_i = a_{vc}^2 T_{eq}$$

$$K_p = \frac{T_c}{a_{vc} T_{eq}}$$